USGS
science for a changing world

Geologic and Mineralogic Controls on Acid and Metal-Rich Rock Drainage in an Alpine Watershed, Handcart Gulch, Colorado

Scientific Investigations Report 2012–5067

U.S. Department of the Interior
U.S. Geological Survey

Cover: Red Cone Mountain in the upper portion of Handcart Gulch, Colo.

Geologic and Mineralogic Controls on Acid and Metal-Rich Rock Drainage in an Alpine Watershed, Handcart Gulch, Colorado

By Dana J. Bove, Jonathan S. Caine, and Heather A. Lowers

Scientific Investigations Report 2012–5067

U.S. Department of the Interior
U.S. Geological Survey

U.S. Department of the Interior
KEN SALAZAR, Secretary

U.S. Geological Survey
Marcia K. McNutt, Director

U.S. Geological Survey, Reston, Virginia: 2012

Suggested citation:
Bove, D.J., Caine, J.S., and Lowers, H.A., 2012, Geologic and mineralogic controls on acid and metal-rich rock drainage in an alpine watershed, Handcart Gulch, Colorado: U.S. Geological Survey Scientific Investigations Report 2012–5067, 121 p.

Contents

Abstract....1
Introduction....1
Purpose and Scope....3
Previous Studies....3
Geologic Setting....3
Methodology....3
Study Results....6
Intrusions, Dikes, and Breccias....6
Hydrothermal Alteration and Mineralization....9
Alteration of Felsic Lithologies....9
Alteration of Mafic Lithologies....14
Late-Stage Argillic Alteration of Felsic Lithologies....15
Late-Stage Chlorite Alteration....17
Sulfide Oxidation....20
Mineralized Zones and Water Geochemical Data....20
Summary and Discussion....21
Acknowledgments....23
References Cited....23
Appendix A....26
Appendix B....29
Appendix C....86
Appendix D....96

Figures

1. Map showing location of Handcart Gulch, Colo., with physiographic provinces and the Colorado Mineral Belt and Montezuma Mining District. Also shown is a satellite image draped on a tilted digital elevation model....2
2. Photograph showing Red Cone Mountain in the upper portion of Handcart Gulch, Colo....2
3. Topographic maps showing *A*, Handcart Gulch, Colo. *B*, The area immediately north of Handcart Gulch showing drill holes and surface sampling sites....4
4. Core logs showing lithology, alteration assemblages, and quantitative mineralogy in drill holes *A*, WP1. *B*, WP2. *C*, WP3. *D*, WP4. *E*, HCBW1. *F*, HCBW3.... link
5. *A*, Photograph showing core sample from drill hole in Handcart Gulch, Colo., showing relatively fresh intrusion of porphyritic dacite with larger phenocrysts of potassium feldspar that range up to 2 centimeters across. *B*, Graph showing intercept value of fluorine-chloride in relation to intercept value of fluorine....7
6. Cross-section reconstruction from surface mapping and drill-core logs showing Tertiary dacite intrusions and related alteration in Handcart Gulch, Colo....8

7. Photographs showing cores from *A*, Drill hole showing coarse clast-supported breccia with monolithologic clasts of foliated felsite with cross-cutting pyrite veinlets. *B*, Drill hole showing clast-supported breccia with clasts derived from adjacent wall rock. *C*, Drill hole showing clast-supported breccia with light-gray kaolinite and smectite-altered matrix. *D*, Drill hole showing dark gray pyritic clay, likely of clastic origin that lines the sharp contact between breccia and wall rock, Handcart Gulch, Colo 10
8. Boxplot showing pyrite content in weight percent as ascertained by quantitative X-ray diffraction analyses from drill core and surface samples from Handcart Gulch, Colo 12
9. Boxplots showing statistical data for copper, lead, and zinc abundances in drill holes WP1-WP4, Handcart Gulch, Colo 12
10. Boxplots showing statistical data from LA-ICPMS analyses of pyrite from drill holes WP1-4, HCBW-1, and HCBW-3, Handcart Gulch, Colo 13
11. Graph showing variation of mineralogy in dacite and rhyolite intrusions in drill holes/cores in Handcart Gulch, Colo., reflecting the characteristics of the major alteration assemblages 13
12. Photographs showing cores from *A*, Drill hole showing quartz-sericite-pyrite alteration haloes centered around fractures filled by pyrite. *B*, Drill hole showing quartz and pyrite, Handcart Gulch, Colo 14
13. Scanning electron micrograph image showing late-stage kaolinite and smectite that formed after illite 15
14. *A*, Photograph showing Waxy kaolinite from fracture in a breccia zone with vertical slickensides. *B*, Scanning electron micrograph image showing kaolinite morphology of waxy kaolinite 16
15. Scanning electron micrograph image of samples from several study areas in Handcart Gulch, Colo., showing *A*, Neoformed smectite morphology. *B*, Smectite that formed from the dissolution of chlorite. *C*, Plagioclase 17
16. Photograph showing core from drill hole WP1, Handcart Gulch, Colo., showing strong late-stage clay alteration and jarosite localized at the site of a prominent fracture zone 18
17. Graph showing stable isotopes d^{18}O in relations to dD for clays from the Handcart Gulch area, Colo., and hydrothermal clays from a magmatic hydrothermal acid-sulfate system in the Red Mountain Pass area, near Silverton, Colorado 17
18. *A*, Photograph showing core from drill hole in Handcart Gulch, Colo., showing late-stage chlorite that formed along foliation planes in quartz-sericite-pyrite-altered gneiss and with fracture-filling pyrite. *B*, Scanning electron micrograph image showing late stage chlorite and intergrown pyrite 18
19. Photograph showing core from drill hole WP1 in Handcart Gulch, Colo., showing zone of localized oxidation surrounded by rock containing mostly unoxidized pyrite 20
20. Scanning electron micrograph image showing oxidized pyrite coated by chalcocite, copper sulfates, and clay 21

Tables

B1. Quantitative X-ray diffraction results from surface samples 29
B2. Quantitative X-ray diffraction results from drill hole WP-1 in weight percent 36
B3. Quantitative X-ray diffraction results from drill hole WP-2 in weight percent 44
B4. Quantitative X-ray diffraction results from drill hole WP-3 in weight percent 49
B5. Quantitative X-ray diffraction results from drill hole WP-4 in weight percent 68
B6. Quantitative X-ray diffraction results from drill hole HCBW1 in weight percent 81
B7. Quantitative X-ray diffraction results from drill hole HCBW3 in weight percent 82
C1. Quantitative mineralogy by XRD showing alteration progression in dacite intrusions 86
C2. Quantitative mineralogy by XRD showing alteration progression in biotite-feldspar-quartz gneiss 89
C3. Quantitative mineralogy by XRD showing alteration progression in biotite-sillimanite-quartz gneiss and augen gneiss from outcrop (JSC prefix) and drill hole WP3 91
C4. Quantitative mineralogy by XRD showing alteration progression in amphibolite in drill holes WP3 and HCBW1 93
C5. Quantitative mineralogy by XRD showing alteration progression in feldspar-biotite-quartz granofels and gneiss in drill hole HCBW3 93
D1. Feldspar compositions from footage intervals in from drill holes HCBW1, WP1, and WP3 in weight percent oxide determined by electron probe analyses 96
D2. Amphibole compositions from footage intervals in drill hole HCBW1 in weight percent oxide determined by electron probe analyses 97
D3. Compositional data for chorite that replaced biotite 99
D4. Compositional data for late-stage chlorite from footage intervals in drill hole WP1 106
D5. Biotite compositions in weight percent oxide determined by electron probe analyses 108
D6. Sericite (fine-grained muscovite) compositions from footage intervals in drill holes WP1 and WP2 in weight percent oxide determined by electron probe analyses 116
D7. Smectite compositions in weight percent oxide determined by electron probe analyses. Samples analyzed from drill holes WP1 and WP3 121

Conversion Factors

Inch/Pound to SI

Multiply	By	To obtain
	Length	
foot (ft)	0.3048	meter (m)
	Volume	
cubic foot (ft^3)	0.02832	cubic meter (m^3)

SI to Inch/Pound

Multiply	By	To obtain
	Length	
millimeter (mm)	0.03937	inch (in.)
meter (m)	3.281	foot (ft)
kilometer (km)	0.6214	mile (mi)
	Area	
square kilometer (km^2)	247.1	acre
square kilometer (km^2)	0.3861	square mile (mi^2)
	Volume	
milliliter (mL)	0.0338140227	fluid ounces (oz)
	Mass	
gram (g)	0.03527	ounce, avoirdupois (oz)

Temperature in degrees Celsius (°C) may be converted to degrees Fahrenheit (°F) as follows:
°F=(1.8×°C)+32

Temperature in degrees Fahrenheit (°F) may be converted to degrees Celsius (°C) as follows:
°C=(°F-32)/1.8

Concentrations of chemical constituents in water are given in milligrams per liter (mg/L).

Geologic and Mineralogic Controls on Acid and Metal-Rich Rock Drainage in an Alpine Watershed, Handcart Gulch, Colorado

By Dana J. Bove, Jonathan S. Caine, and Heather A. Lowers

Abstract

The surface and subsurface geology, hydrothermal alteration, and mineralogy of the Handcart Gulch area was studied using map and drill core data as part of a multidisciplinary approach to understand the hydrology and affects of geology on acid-rock drainage in a mineralized alpine watershed. Handcart Gulch was the locus of intense hydrothermal alteration that affected an area of nearly 3 square kilometers (km^2). Hydrothermal alteration and accompanied weak mineralization are spatially and genetically associated with small dacite to low-silica rhyolite stocks and plugs emplaced about 37-36 Ma. Felsic lithologies are commonly altered to a quartz-sericite-pyrite mineral assemblage at the surface, but alteration is more variable in the subsurface, ranging from qsp-dominant in upper core sections to a propylitic variant that is more typical in deeper drill core intervals. Late-stage, hydrothermal argillic alteration [kaolinite and(or) smectite] was superimposed over earlier-formed alteration assemblages in the felsic rocks. Smectite in this late stage assemblage is mostly neoformed resulting from dissolution of chlorite, plagioclase, and minor illite in more weakly altered rocks. Hydrothermally altered amphibolites are characterized by biotitic alteration of amphibole, and subsequent alteration of both primary and secondary biotite to chlorite. Whereas pyrite is present both as disseminations and in small veinlets in the felsic lithologies, it is mostly restricted to small veinlets in the amphibolites.

Base-metal sulfides including molybdenite, chalcopyrite, sphalerite, and galena are present in minor to trace amounts in the altered rocks. However, geologic data in conjunction with water geochemical studies indicate that copper mineralization may be present in unknown abundance in two distinct areas. The altered rocks contain an average of 8 weight percent fine pyrite that is largely devoid of metals in the crystal structure, which can be a significant source of trace metals in other areas with acid rock drainage. Thus, elevated base-metal concentrations in the trunk stream and discrete springs in the study area, as determined in previous studies, are likely derived from discrete metal-rich sources, rather than the abundant pyrite veins or disseminations. Pyrite is oxidized in nearly all outcrops examined. Drill core data show that zones of pyrite oxidation range in depth from 100 m below the surface at higher elevations to just a few meters depth at the lowest elevations in the study area. However, discrete pyrite oxidation zones are present in drill core to depths of several hundred meters below the pervasive near-surface oxidation zones. These deeper discrete oxidation zones, which are present where fresh pyrite predominates, are spatially associated with fractures, small faults, and breccias.

Quartz-sericite-pyrite-altered rocks containing unoxidized pyrite likely have the highest acid-generating capacity of all alteration assemblages in the study area. Hydrothermal alteration has left these rocks base-cation leached and thus acid-neutralizing potential is negligible. In contrast, propylitic-altered felsic rocks commonly contain trace to minor calcite and abundant chlorite, which provide some amount of acid-neutralization despite the presence of a few percent pyrite.

Introduction

Studies of the geology, hydrothermal alteration, and mineralogy of the Handcart Gulch research watershed were conducted as part of a multidisciplinary approach to understand the hydrology and effects of geology in a typically mineralized alpine watershed (figs. 1 and 2). The study arose out of the donation of four abandoned, deep mineral exploration boreholes for research purposes by Mineral Systems Inc. to the U.S. Geological Survey (Caine and others, 2006; Verplanck and others, 2008). Within the upper portion of Handcart Gulch, no mining has occurred with the exception of one small adit with a waste-rock pile of approximately 300 (ft^3). The watershed therefore provides a unique opportunity to monitor a natural acid-rock-drainage system in an unmined setting. The Handcart Gulch area has rocks that have been pervasively altered, commonly have low acid neutralizing potential, and contain an abundance of finely disseminated pyrite. The high pyrite content and presence of weak base-metal sulfide mineralization explain the natural acidity and elevated concentrations of select metals in surface and groundwater in the watershed.

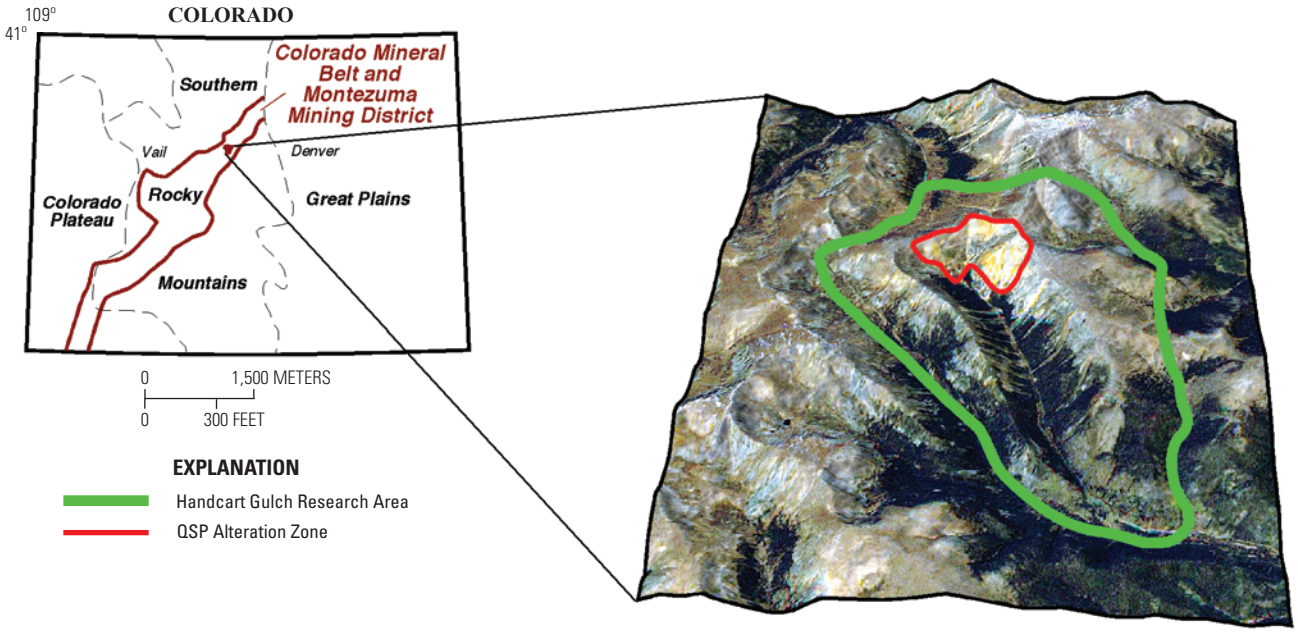

Figure 1. Location of Handcart Gulch, Colo., with physiographic provinces and the Colorado Mineral Belt and Montezuma Mining District. Also shown is a satellite image draped on a tilted digital elevation model. The image shows the extreme topographic relief (2,700 feet with a gradient of approximately 0.1) and the red-orange weathering of the pyrite-rich rocks.

Figure 2. Red Cone Mountain in the upper portion of Handcart Gulch, Colo. The red staining is from the oxidation of pyrite at concentrations of nearly 10 percent of the rock mass. The upper road in the photo cuts across a major rock glacier and was excavated by Mineral Systems, Inc., to drill exploration holes WP3 and WP4 (see fig. 3*A*).

Characterization of the geology of this mineralized area was conducted by mineralogical studies of outcrops and detailed logging of drill core from the four deep exploration boreholes and two shallow boreholes drilled by the U.S. Geological Survey (figs. 3*A–B*). Drill core studies were conducted in conjunction with surficial alteration mapping and related mineralogical studies, and generalized alteration mapping by remote sensing.

Purpose and Scope

This report contains (1) an overview of the geology and mineralization of Handcart Gulch and the surrounding area; (2) detailed drill core logs showing lithology, alteration units, and quantitative mineralogy (figs. 4*A–F*; Appendix A); (3) quantitative mineralogical tables from surface and subsurface samples (Appendixes B and C); (4) electron microprobe analyses of primary and alteration minerals (Appendix D); (5) and laser ablation ICPMS results showing metal abundances from representative pyrite samples. The primary purpose of this report is to present an overview of the geology of this area, which will provide a foundation for interpretation of the hydrology and associated occurrence, transport, and fate of groundwater solutes in this alpine watershed as it is affected by the underlying geology and mineralogy.

Previous Studies

USGS studies (Verplanck and others 2008; Caine and others, 2004) have focused on the surface- and groundwater chemistry of the Handcart Gulch area as a part of a multidisciplinary project to determine the processes that control groundwater chemistry and flow in mineralized alpine environments. Data from these studies are summarized in parts of this report to better understand the affect of geology on water chemistry. In addition, we utilize the geochemistry of Handcart Gulch waters to provide insight into the geochemical and mineralogical nature of specific parts of the watershed that these waters drain.

Geologic Setting

The Handcart Gulch study area is located in the southeastern portion of the Montezuma mining district of the central Colorado Rocky Mountain Front Range (fig. 1). The Montezuma district has a long mining history starting with an initial discovery of silver in 1864 (Lovering, 1935). Metals mined in Montezuma are silver, lead, zinc, and copper and base-metal ore minerals including galena, sphalerite, and tennantite-tetrahedrite (Botinelly, 1979). Molybdenite is also associated with Tertiary-age porphyry stocks. Because of the proximity of the Climax molybdenite deposit, this district has been explored for molybdenum mineralization.

The lithologies in the study area are dominated by Precambrian, amphibolite grade metamorphic rocks composed of biotite-feldspar and biotite sillimanite gneisses, amphibolites, and pegmatites, all cut by small Tertiary-age stocks, plugs, and dikes. Field mapping and outcrop observations indicate that the Precambrian bedrock is complexly deformed. Ductile deformation includes tight, upright folds in the metasediments whose axes are parallel to the major axis of the Handcart valley (for example, Wahlstrom and Kim, 1959). The Montezuma ductile shear zone was mapped by Bryant and others (1981) in the upper reaches of the watershed; however, unpublished maps and mapping by Widmann (2003) show this structure in localities outside of the watershed. Minor stringers of mylonites do exist yet they are not significant in number and they are cut by a few brittle, small-displacement faults (on the order of meters to a few tens of meters), high-intensity joint networks, and several map-scale quartz veins.

The most-well studied Tertiary intrusion in the Montezuma district is the approximately 40 Ma Montezuma stock, a dominantly porphyritic quartz monzonite but which ranges to granite and aplite (Neuerburg and others, 1974; Bookstrom and others, 1987). Although just outside of Handcart watershed proper, the Montezuma stock is the largest outcropping pluton in a swarm of smaller stocks, plugs, cupolas and dikes (Bookstrom and others, 1987). The mean emplacement age for three small granitic to rhyolitic intrusions in the study area, as determined by $^{40}Ar/^{39}Ar$ analyses is 36.90 ± 0.05 Ma (Crook, 2004; Crook, J.C., written commun., 2005). The average ages fall within the 39-35 Ma time span ascertained by fission track analyses on a few of the same and other compositionally similar intrusions in the Handcart Gulch and adjacent areas (Bookstrom and others, 1987).

Methodology

Quantitative mineralogy was determined by X-ray diffraction (XRD) for all samples and is presented in Appendix B (tables B1–B7). The samples were prepared according to the methods described by Środon and others (2001). In summary, 3 grams (g) of sample was mixed with 0.333 g of an internal standard (zincite). The mixture was subsequently ground with 3 milliliters (mL) of methanol in a McCrone mill for 5 minutes, oven dried at 85 °C, passed through a 4 millimeter (mm) sieve, and then side loaded into an aluminum holder to optimize random orientation of mineral samples. Samples were X-rayed from 5 to 65° 2θ with Cu*K*α radiation (40Kv, 30 mA) using a Siemens D500 X-ray diffraction system with a graphite monochromator, 1° slits, a step size of 0.02° 2 θ, and a counting time of 2 seconds (s) per step.

The XRD data were converted into weight percent minerals using the RockJock computer software (Eberl, 2003). The program compares integrated X-ray intensities for minerals present in a sample with that of an internal zincite

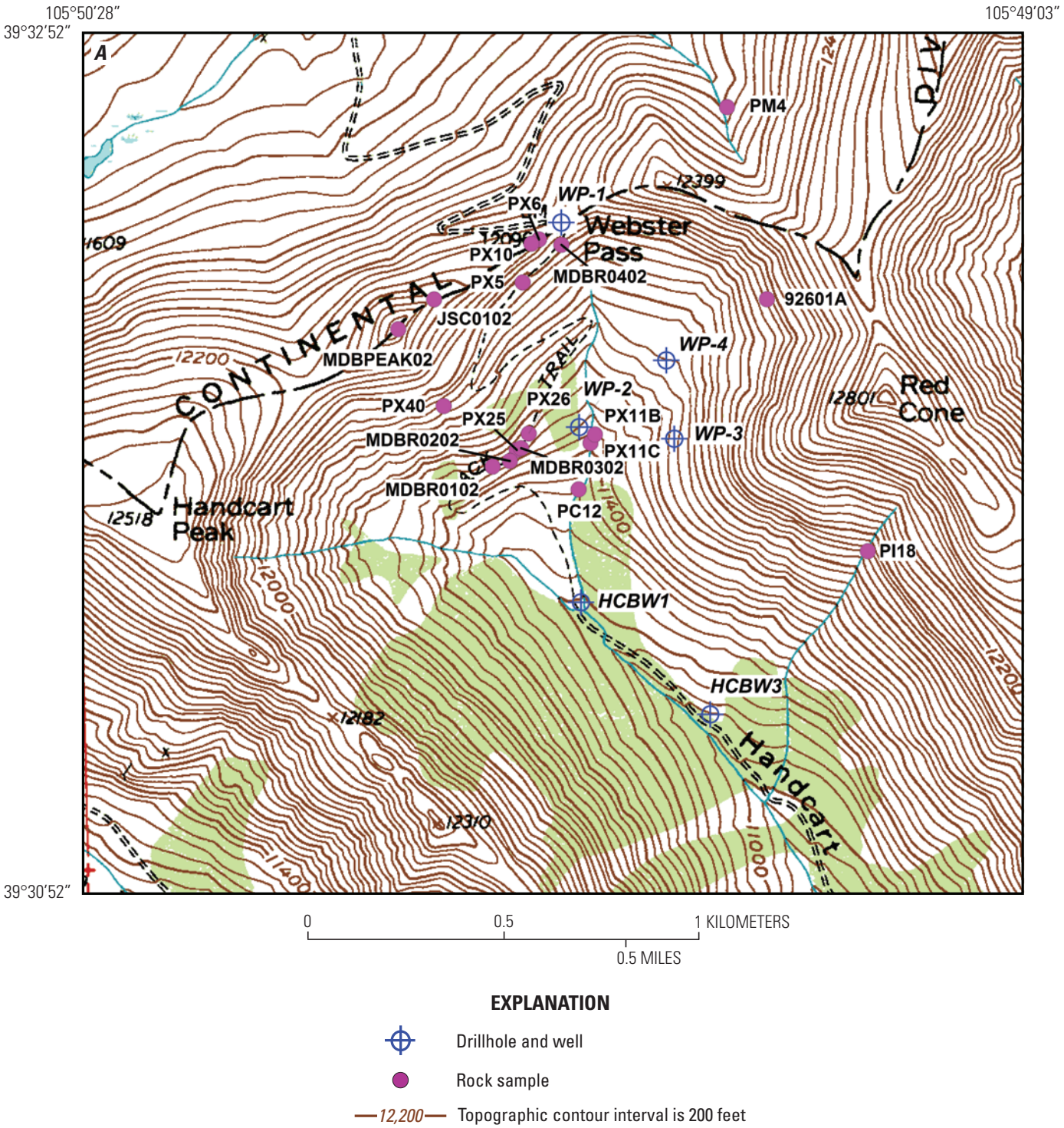

Figure 3. *A,* Handcart Gulch, Colo. *B,* The area immediately north of Handcart Gulch showing drill holes and surface sampling sites. (Mineralogic data from drill holes and samples presented in appendix tables B1–B7).

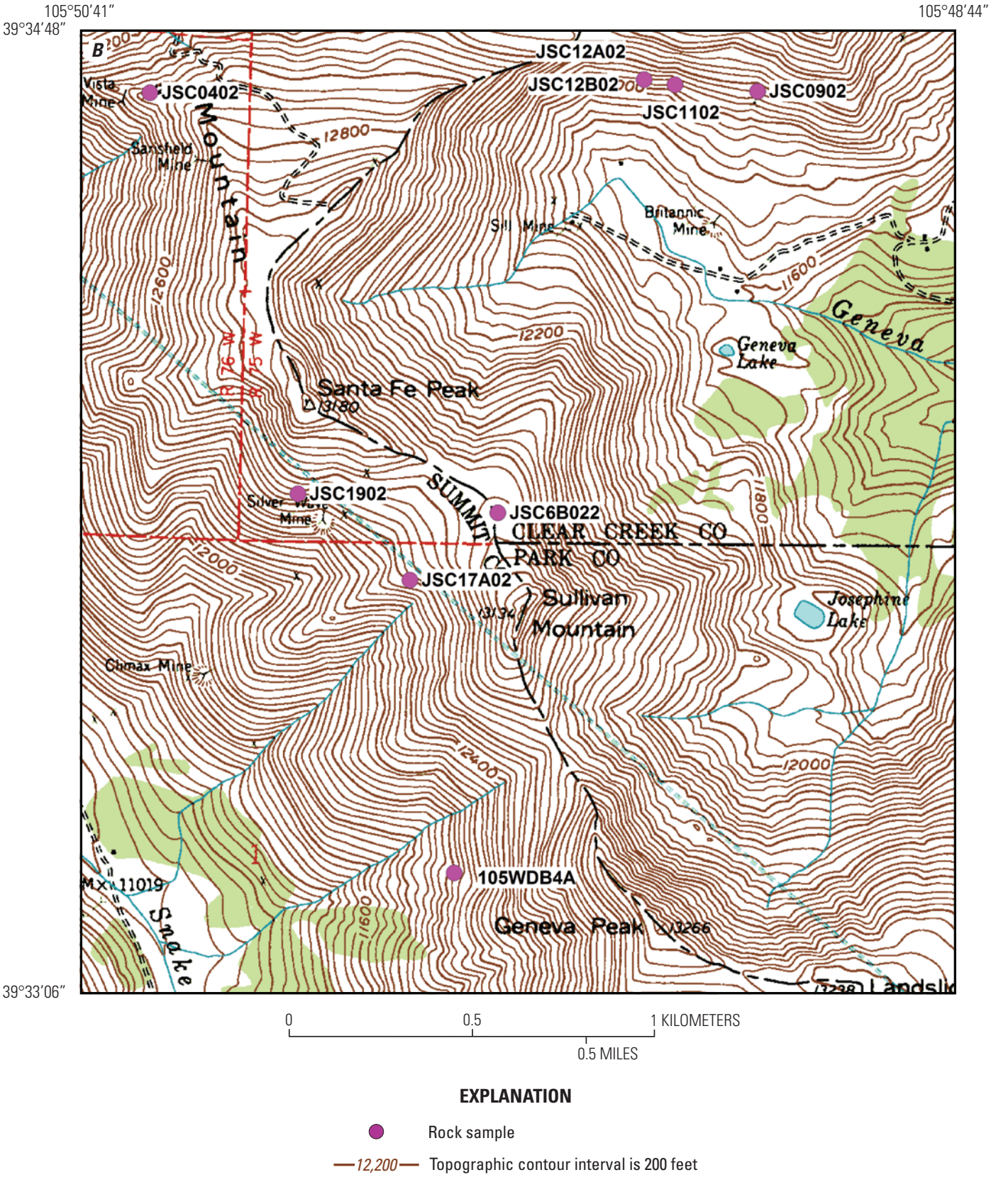

Figure 3. Topographic maps of *A,* Handcart Gulch, Colo. *B,* The area immediately north of Handcart Gulch showing drill holes and surface sampling sites. (Mineralogic data from drill holes and samples presented in appendix tables B1–B7).—Continued

standard in the sample, and weight percents are calculated from previously measured mineral intensity factors (MIFs; also referred to as reference intensity ratios, RIRs). Integrated X-ray intensities for individual minerals were determined by fitting stored XRD patterns for pure mineral phases to the measured XRD pattern using the Solver option in Microsoft Excel. The Solver option minimized the degree of fit parameter between measured and calculated patterns by varying the intensities of the stored standard patterns by multiplying each of these patterns by a separate factor.

The RockJock technique has been checked for accuracy using artificial mixtures, and generally results are within 1 to 2 weight (wt) percent of actual values (Eberl, 2003). Mineral weight percentages were normalized to 100 percent except in a few samples that were run without the zincite standard. X-ray amorphous material was determined to be negligible due to low backgrounds in the XRD patterns and the nature of the rock samples.

Electron microprobe (EMP) analyses of primary, altered, and secondary biotites from dacite intrusions in the core samples (Appendix D, table D5) were used to compare the Webster Pass hydrothermal system to the mineralized molybdenum and copper porphyry deposits characterized by Munoz (1984). Halogen intercept values (Munoz, 1984) of the micas were calculated from the EMP analyses to determine the relative enrichment of F and Cl in the micas and to correct for the opposing effects of Mg/Fe ratio on F=OH and Cl=OH exchange.

All trace element analyses of pyrite were collected by laser ablation inductively coupled plasma mass spectrometry (LA-ICP-MS) at the U.S. Geological Survey (USGS) LA-ICP-MS facility in Denver, Colorado. Pyrite grains were ablated using 25 micron spots generated from a 266 nanometer (nm) laser ablation system (CETAC Technologies LSX-500). The ablated material was introduced directly into the torch of the ICP-MS (Perkins Elmer ELAN6000). The analyses were calibrated using USGS sulfide standard MASS-1 (Wilson and others, 1999). The detection limits for most elements were in the 1-10 parts per million (ppm) range throughout the study. Individual analyses were screened for the presence of micro-inclusions. Data were filtered and processed offline using standard LA-ICP-MS protocol.

Oxygen isotope compositions were determined using the techniques of Taylor and Epstein (1962) and Clayton and Mayeda (1963). Hydrogen isotope compositions of clay and sericite were measured using the techniques of Savin and Epstein (1970). Oxygen and hydrogen isotope measurements were made in the stable isotope laboratories of the USGS in Denver, Colorado.

Study Results

Intrusions, Dikes, and Breccias

The Tertiary intrusions and dikes in the Handcart Gulch area (fig. 5*A*) are dominantly quartz phenocryst-poor (less than 2–3 percent), fluorine deficient (fig. 5*B*), and have compositions ranging from dacite to low-silica rhyolite or granite. At least twelve small stocks or plugs have been identified in the study area. Most are less than 500 m in diameter and are mostly quartz-sericite-pyrite (qsp) altered. Drill hole data indicates that one or more of qsp-altered intrusions were truncated at depth by later intrusions that were likely derived from a similar source (Bookstrom and others, 1987). Drill core intercepts of later, cross-cutting intrusive bodies are largely propylitic-altered and were overprinted by late-stage clays. The cross-section reconstruction in figure 6 depicts the propylitic-altered intrusion intercepted at approximately 970 feet (ft) in drill hole WP1 (fig. 4*A*), which cuts an earlier Tertiary intrusion at Porphyry Peak (see peak location, fig. 3*A*) and intrudes the metamorphic rocks.

A thick sill of high silica rhyolite porphyry (33 Ma), which crops out approximately 4 km north of the study area, resembles the Climax and Henderson intrusions (33-20 Ma) (Bookstrom, 1987). However, no such intrusions have been identified in close proximity to the study area. Electron microprobe analyses of primary and secondary biotites from Handcart Gulch intrusions—focusing on F and Cl content of the micas (Appendix D, table D5)—were used to place the Handcart Gulch/Webster Pass hydrothermal system in the context of the porphyry systems characterized by Munoz (1984). As shown on figure 5B, F and Cl data for the quartz phenocryst-poor intrusions in the Webster Pass area group well outside the field of Climax-type intrusions, overlapping the field of micas from porphyry Cu deposits.

Figure 4. (click to open PDF files) Core logs showing lithology, alteration assemblages, and quantitative mineralogy in drill holes *A*, WP1. *B*, WP2. *C*, WP3. *D*, WP4. *E*, HCBW1. *F*, HCBW3. See Appendix A for key to all lithology and alteration types.

Breccias are common in zones of hydrothermally altered rock and vary widely in character, geometry, and likely in genesis. Most breccias are concentrated in zones (less than 1 m to as much as 100 m across) comprised of narrow clastic veins or irregular dikes with sharp contacts that anastamose throughout undisturbed country

Figure 5. *A,* Core sample from drill hole in Handcart Gulch, Colo., showing relatively fresh intrusion of porphyritic dacite with larger phenocrysts of potassium feldspar that range up to 2 centimeters across. *B,* Intercept value of fluorine-chloride in relation to intercept value of fluorine. In figure 5*B*, fluorine values of biotites from Webster Pass are relatively low in comparison to biotites from Climax-type molybdenum-porphyry systems (Henderson intrusion), copper-porphyry systems, and a subeconomic copper-molybdenum porphyry system near Lake City, Colo. Biotite data from Henderson. Data on copper-porphyry deposits from Munoz (1984), and Lake City data from Bove (1988).

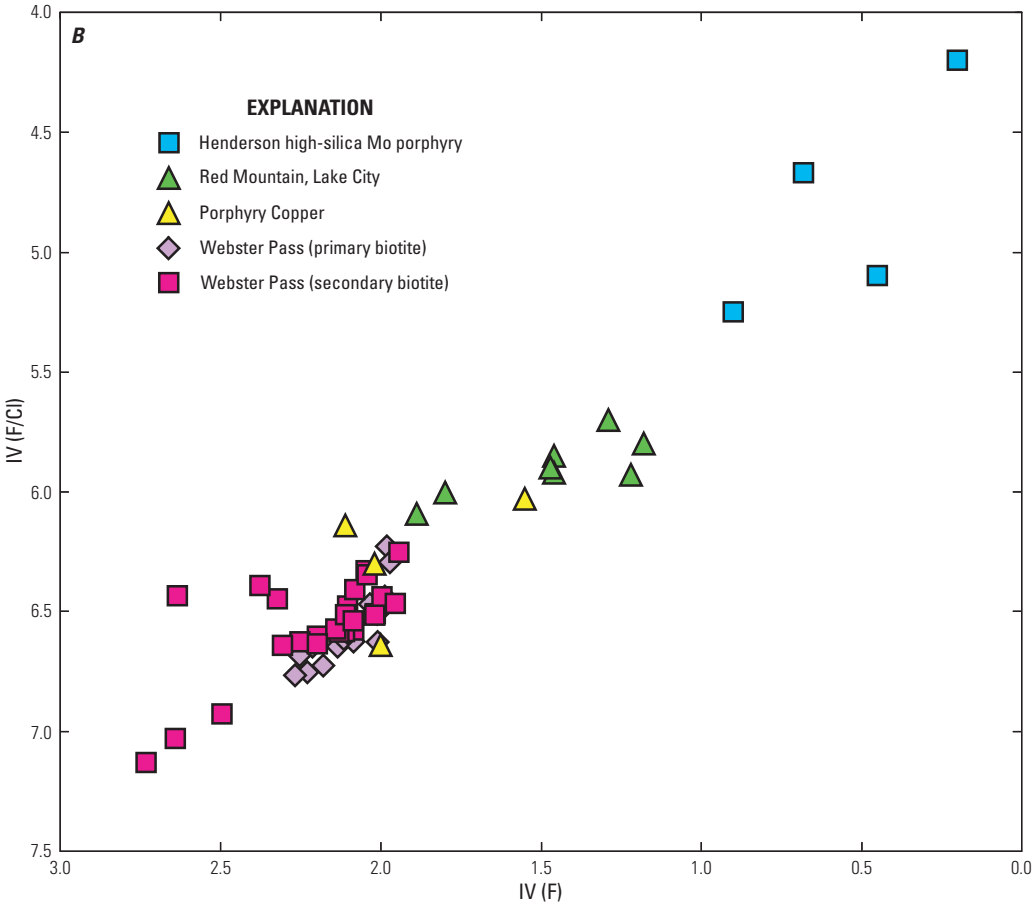

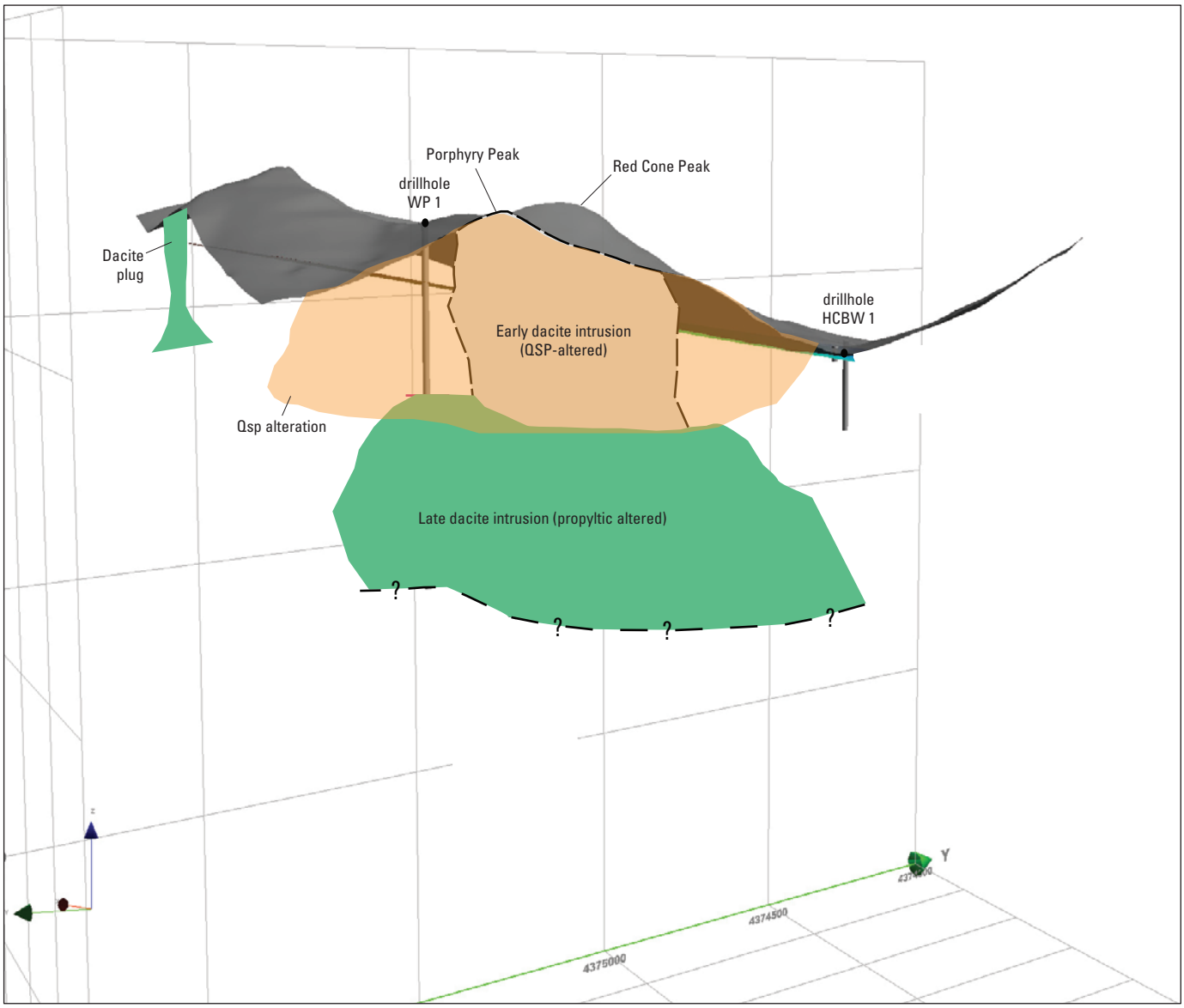

Figure 6. Cross-section reconstruction from surface mapping and drill-core logs showing Tertiary dacite intrusions and related alteration in Handcart Gulch, Colo. Profile is looking northeast from Porphyry Peak, Handcart Gulch, Colo. (See figure 3*A*; QSP=quartz-sericit-pyrite).

rock. Breccias within these composite zones vary from a monolithologic variety (fig. 7*A*) to more matrix-supported types, the latter containing rounded and internally rotated clasts of multiple lithology and alteration type. Both matrix and clasts in the above described breccias are commonly cut by pyrite ± quartz veinlets of varying density and are superimposed by later qsp alteration.

Another major type of breccia is largely clast-supported and contains subangular clasts derived from adjacent wall rock mixed with smaller clastic pyrite grains (fig. 7*B*). The breccia matrix is well sorted and may be preferentially altered to argillic clays comprised of kaolinite and smectite (fig. 7*B*). Pyrite is neither cogenetic with the argillic clays nor does it appear to post-date brecciation. These breccia zones generally have sharp contacts with their wall rocks—some with slickensides—that are commonly lined with a dark-gray, finely pyritic clay (fig. 7*D*).

Hydrothermal Alteration and Mineralization

Handcart Gulch was the locus of intense hydrothermal alteration that overprinted an area of roughly 2.8 km^2 (fig. 1). The pervasive hydrothermal alteration and weak mineralization is spatially and genetically associated with the many small 39-35 Ma stocks and plugs as noted above (Crook, J.C., written commun., 2005; Crook, 2004; Bookstrom, 1987). Although fine-grained pyrite averages 8 weight percent in the seven drill holes (fig. 8), other metal sulfides including molybdenite, chalcopyrite, galena, and sphalerite—with exception of a discrete interval in the upper part of drill hole WP1—are present in only minor to trace abundances (see copper, lead, and zinc abundances, fig. 9). Thus, the Handcart Gulch study area was not mined. Studies conducted on nearly 123 pyrite samples by Laser Ablation Induced Coupled Plasma Mass Spectrometry (LA-ICP-MS) from the six drill holes show that on average the pyrite has limited metal substitution in its crystal structure (median value of Cu, Pb, Zn less than 22 ppm (fig. 10).

The only significant metallic mineralization observed during this study was in a breccia zone in drill hole WP1 (interval about 300–400 ft beneath the surface) that was cemented with abundant pyrite, chalcopyrite, and luzonite (Cu_3AsS_4). Luzonite and chalcopyrite are intergrown with the pyrite, whereas both sulfides are post-dated by clays, fine-grained barite, secondary copper oxides, and secondary copper sulfates. The secondary copper oxides and sulfates appear to be related to the oxidation and alteration of the primary sulfides, luzonite and chalcopyrite. Chalcocite is notably abundant in this core interval and is present mostly as thin coatings or as sooty fine-grained aggregates on or around pyrite. The dark fine-grained chalcocite masses are commonly lined by a drusy, light gray mineral coating. Scanning electron micrograph (SEM) studies reveal that these light gray coatings are composed of a mixture of barite, crandallite, chalcocite, and kaolinite (fig. 20). Although secondary copper is mostly in the form of chalcocite, a few mineral specimens contain a copper sulfate mineral phase that appears to be related to the alteration of primary copper-bearing sulfides. Geochemical data from 10 ft core splits (Robinson and others, unpub. data, 2002) from this breccia zone show Cu enrichment over a 50 ft core interval reaching a maximum of about 1,100 ppm; zinc, lead, and other trace metal abundances are relatively low in this interval. A fist-sized ore sample contains about 20–30 percent copper, greater than Fe (largely from pyrite), and minor As (determined by energy dispersive X-ray flouresence, Richard Grauch, USGS, oral commun., 2009)

A weighted average of five sericite $^{40}Ar/^{39}Ar$ ages from several altered intrusions yielded an age of 37.81 ± 0.04 Ma, which is slightly older than the intrusions themselves (Crook, J.C., written commun., 2005). However, the sericite ages may be slightly younger than the data indicate due to argon recoil during irradiation (Crook, J.C., written commun., 2005), and thus would explain why the sericite ages are as much as 0.9 Ma older than the average age of the intrusions that they alter. Although the precise timing of mineralization and intrusive activity cannot be resolved by these isotopic ages, it is likely that mineralization is closely tied to magmatic activity as indicated by (1) the close proximity in the ages of the sericites and the Webster Pass intrusions, and (2) the alternating episodes of intrusion and qsp-dominated hydrothermal alteration.

Alteration of Felsic Lithologies

Felsic lithologies at the ground surface are dominantly altered to a qsp mineral assemblage. Quartz-sericite-pyrite alteration post-dates low grade but pervasive albitic alteration, which appears to be the earliest episode of alteration in the study area. The intensity of hydrothermal alteration decreases to the west of Handcart Gulch and north and south of Red Cone Peak and Webster Pass (locations shown on fig. 3*A*), transitioning outward from qsp to propylitic alteration, then into relatively fresh rocks. Alteration assemblages are more variable in the subsurface, ranging from a qsp assemblage—typically in the upper portions of the drill holes—to a propylitic type assemblage with a late clay overprint. The qsp assemblage is characterized by the complete replacement of plagioclase and nearly wholesale replacement of potassium feldspar by sericite (15–40 percent of rock total) and fine-grained quartz (35–65 percent). Primary ferromagnesian minerals are completely altered to Fe-Ti oxides and clays, whereas pyrite, which is largely present as finely disseminated grains and in veinlets, averages 10 percent (approximately 8 percent median). In contrast, propylitic-altered rocks contain varying amounts of chlorite, epidote, calcite, and sericite, with primary feldspar crystals that are nearly fresh to partially altered. Mineralogical changes illustrating the progressive effects of increasing alteration in the Tertiary dacite intrusions—a relatively homogeneous protolith—are illustrated in figure 11. Variations in mineralogy in the other main felsic lithologies are shown in Appendix C (tables C1–C3).

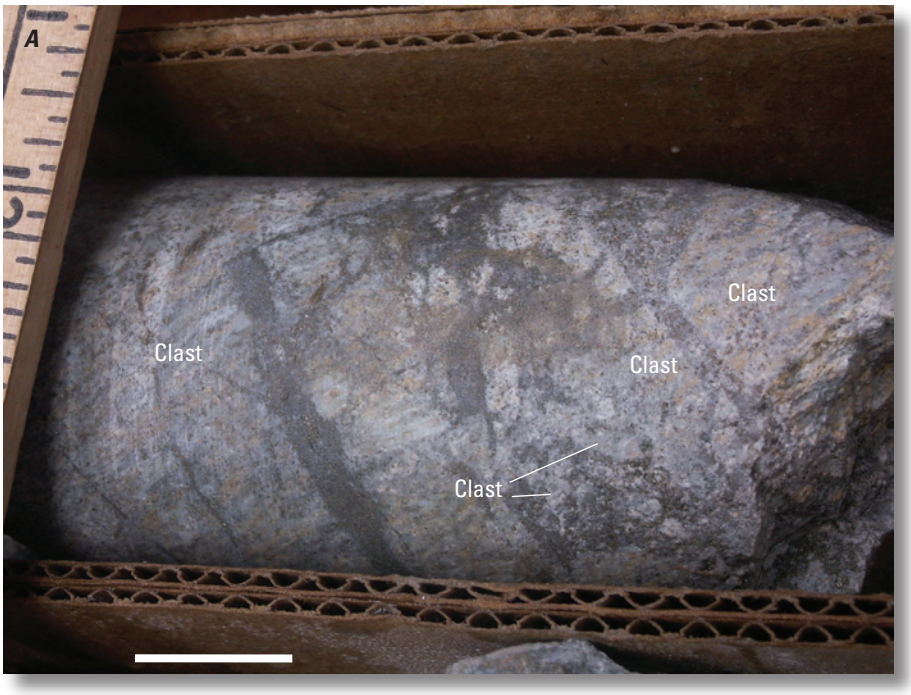

Figure 7. Cores from *A,* Drill hole showing coarse clast-supported breccia with monolithologic clasts of foliated felsite with cross-cutting pyrite veinlets. *B,* Drill hole showing clast-supported breccia with clasts derived from adjacent wall rock. *C,* Drill hole showing clast-supported breccia with light-gray kaolinite and smectite-altered matrix. *D,* Drill hole showing dark gray pyritic clay, likely of clastic origin that lines the sharp contact between breccia and wall rock, Handcart Gulch, Colo. The scale is in inches. In figure 7*A*, note the abundance of fine-grained pyrite (dark material) in breccia matrix that distinguishes clast boundaries. Fine pyrite in matrix post-dates brecciation. In figure 7*B*, note the clastic pyrite grains and sharp contact between the breccia and wall rock.

Figure 7. Cores from *A,* Drill hole showing coarse clast-supported breccia with monolithologic clasts of foliated felsite with cross-cutting pyrite veinlets. *B,* Drill hole showing clast-supported breccia with clasts derived from adjacent wall rock. *C,* Drill hole showing clast-supported breccia with light-gray kaolinite and smectite-altered matrix. *D,* Drill hole showing dark gray pyritic clay, likely of clastic origin that lines the sharp contact between breccia and wall rock, Handcart Gulch, Colo. The scale is in inches. In figure 7*A*, note the abundance of fine-grained pyrite (dark material) in breccia matrix that distinguishes clast boundaries. Fine pyrite in matrix post-dates brecciation. In figure 7*B*, note the clastic pyrite grains and sharp contact between the breccia and wall rock.—Continued

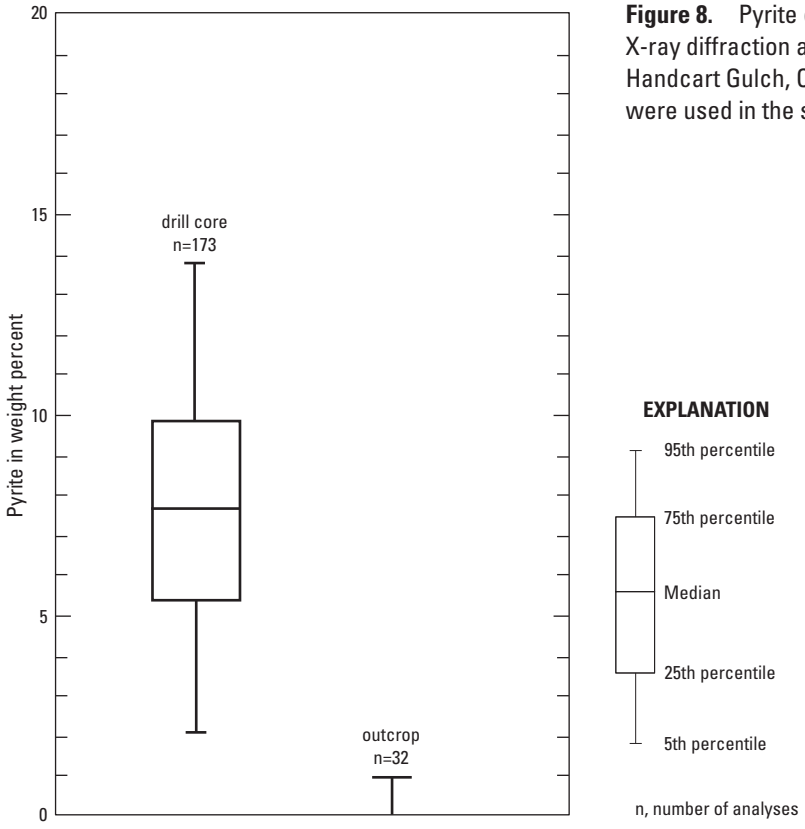

Figure 8. Pyrite content in weight percent as ascertained by quantitative X-ray diffraction analyses from drill core and surface samples from Handcart Gulch, Colo. Thin sections devoid of pyrite from outcrop samples were used in the statistical count.

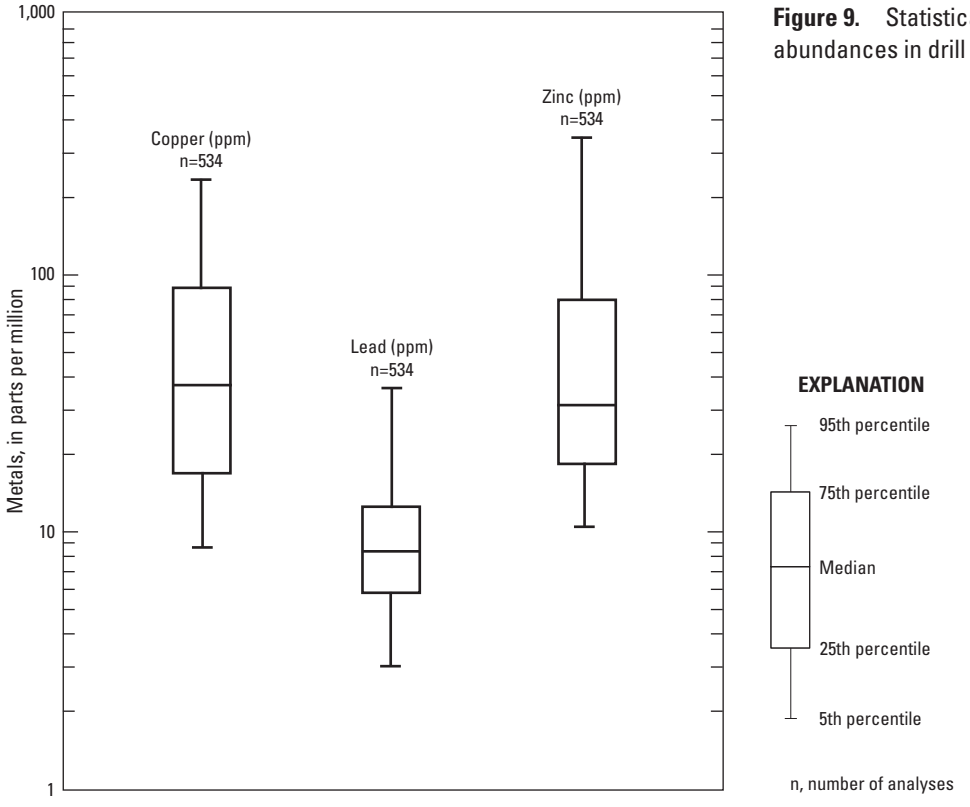

Figure 9. Statistical data for copper, lead, and zinc abundances in drill holes WP1-WP4, Handcart Gulch, Colo.

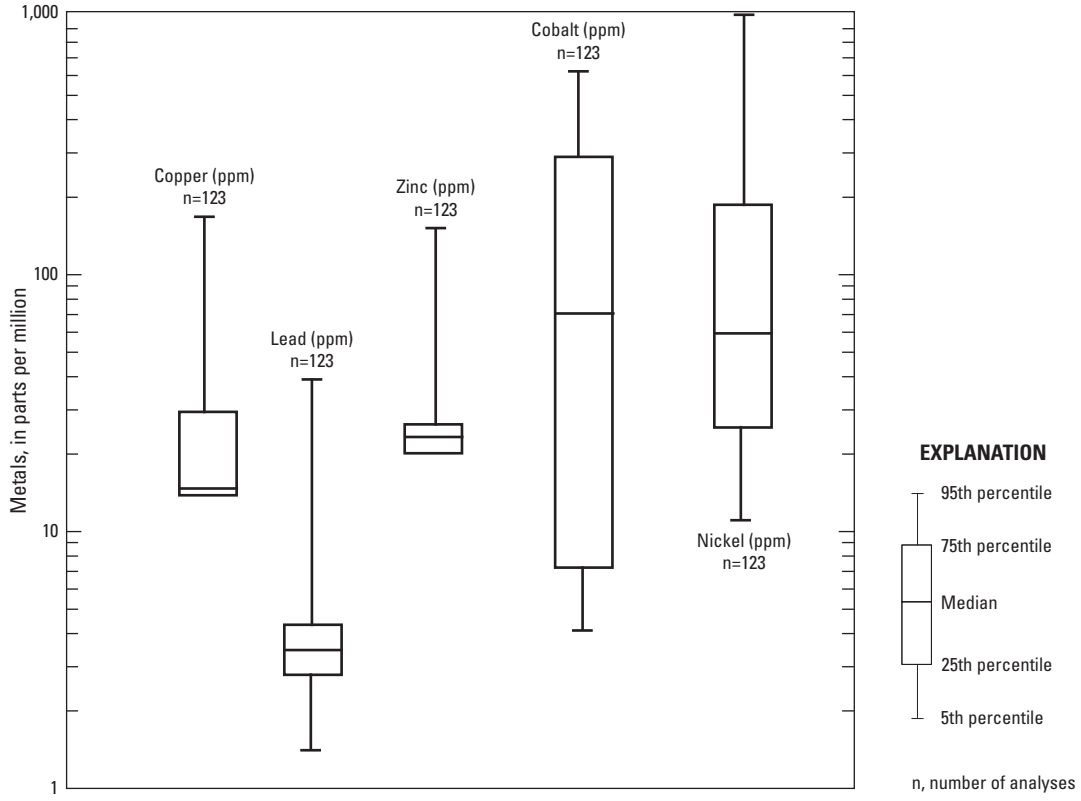

Figure 10. Statistical data from LA-ICPMS analyses of pyrite from drill holes WP1-4, HCBW-1, and HCBW-3, Handcart Gulch, Colo.

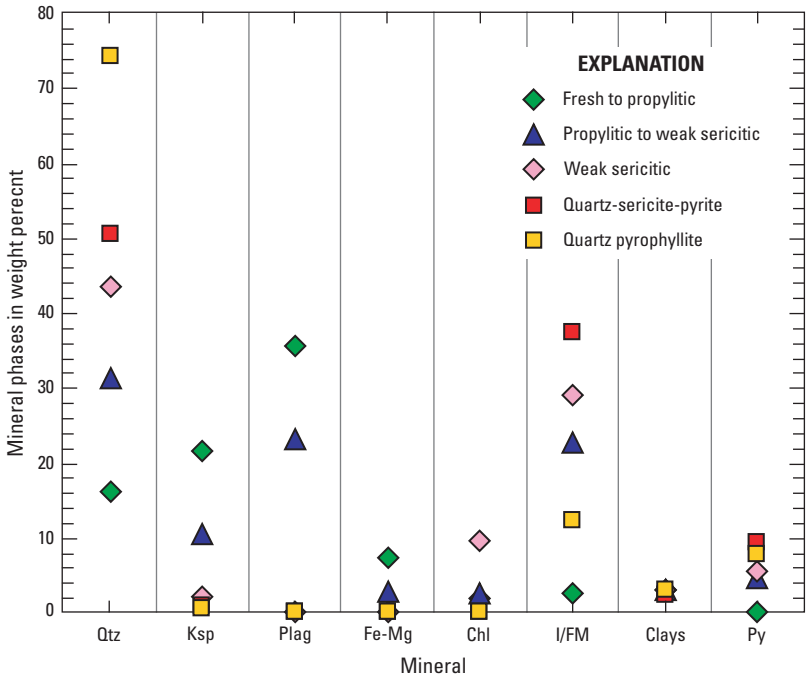

Figure 11. Variation of mineralogy in dacite and rhyolite intrusions in drill holes/cores in Handcart Gulch, Colo., reflecting the characteristics of the major alteration assemblages. Data are shown in weight percent as determined by quantitative X-ray diffraction. Samples represented on graph are considered to be generally representative of alteration assemblages. (Qtz=quartz; Ksp=potassium feldspar; Fe-Mg = sum of biotite, pyroxene, and amphibole; chl=chlorite; I/FM=illite or fine muscovite; and py=pyrite).

The depth of pervasive qsp-altered rock extends to 300 m in drill hole WP1 (fig. 4*A*) in an interval where felsic metamorphic rocks predominate. Tertiary age dacite intrusive rocks, which were intercepted below 300 m in drill hole WP1, are largely propylitic-altered and weakly argillized (late smectite and kaolinite). In contrast, qsp-altered Tertiary intrusive rocks were encountered throughout most of the entire 530 m of drill hole WP4 (fig. 4*D*) and in the top 200 m of drill hole WP2 (fig. 4*B*). Propylitic-altered intrusive rocks in the deeper levels of drill holes WP1 and WP2 (figs. 4*A* and 4*B*) are cut by intermittent intervals of qsp-altered rock. These sporadic qsp zones are characterized by haloes a few millimeters up to several meters wide centered around pyrite ± quartz-veins (figs. 12*A* and 12*B*). In some instances, these qsp zones grade outward into weak sericite-pyrite altered rocks; however, some thin qsp selvages have strongly chloritized margins. Regardless of thickness, the qsp alteration haloes are accompanied by a dense network of tiny pyrite ± quartz filled fractures. Although a similar dense network of fine fractures may persist in relatively unaltered rocks outside of the qsp envelopes, these fractures are devoid of pyrite and quartz. The pervasive or composite qsp zones in the upper levels of drill core and at the surface likely represent a progressive overlap of these individual qsp zones through time.

Alteration of Mafic Lithologies

Hydrothermal alteration of amphibolites—the dominant lithologies in drill holes WP3 and HCBW1 (figs. 4*C* and 4*E*)—produced alteration mineral assemblages distinct from those of the more felsic lithologies (tables C1–C4). For example, in core intervals where felsic rocks are interleaved with amphibolites, the felsic rocks may be strongly qsp-altered, whereas, adjacent amphibolites may only show a local lightening in coloration due to alteration to smectite, kaolinite, epidote, and minor sericite. More commonly however, hydrothermally altered amphibolites are characterized by biotitic alteration of amphibole, and subsequent alteration of both primary and secondary biotite to chlorite. Although fine-grained pyrite is abundant, most is restricted to small veinlets, whereas, disseminated

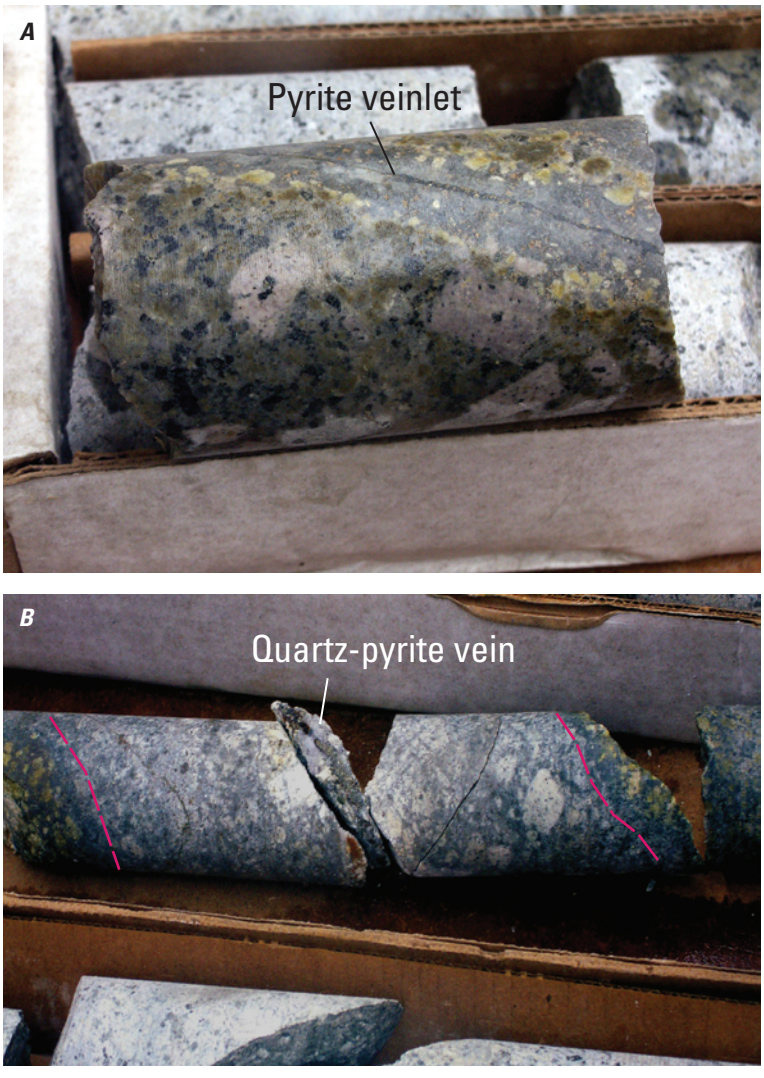

Figure 12. Cores from *A,* Drill hole showing quartz-sericite-pyrite alteration haloes centered around fractures filled by pyrite. *B,* Drill hole showing quartz and pyrite, Handcart Gulch, Colo. Rock on the margins of quartz-sericite-pyrite zones are superimposed by weak, late-stage argillic alteration (light green).

pyrite and sericite are locally abundant adjacent to pyrite veins but decrease markedly a few millimeters from these discrete zones.

Late-Stage Argillic Alteration of Felsic Lithologies

Late-stage argillic alteration is characterized by the presence of more than 2–5 percent clays consisting of kaolinite and(or) smectite (fig. 13). SEM studies indicate that kaolinite and smectite are superimposed on earlier-formed clays (mostly illite/sericite) of the propylitic, weak sericitic, and qsp assemblages.

Kaolinite-rich rocks are most prevalent in the upper 180 to 300 m of drill holes WP1,WP2, WP3, and WP4 (figs. 4*A*–4*D*; appendix tables B2–B5). In these zones, kaolinite typically formed in and around discrete, narrow 1-5 mm fractures. The kaolinite-filled fractures are markedly abundant in brecciated and less silicified core intervals. These intervals are commonly soft, friable, and highly broken owing to the general abundance of kaolinite. In comparison, more silicified qsp-altered rocks, which are generally characterized by a high density of quartz veins and a more silicified rock matrix, are significantly less affected by late-stage clays.

Kaolinite is also found in the matrix of clast-supported breccias (fig. 7*C*). In some instances, fractures or small faults are lined with soft, waxy, nearly monomineralic kaolinite (figs. 14*A* and 14*B*). Some fault movement was cogenetic with or post-dated late-stage kaolinite alteration as evidenced by slickensides etched in the clay (fig. 14*A*).

In contrast, quantitative XRD data indicate that late-stage clays comprised of both kaolinite and smectite are more prevalent in propylitic to weak sericite-pyrite alteration assemblages, which retained much of their primary mineralogy during the earlier hydrothermal alteration. In drill core, smectite-rich rocks—particularly the dacite intrusions—have a characteristic light-greenish hue. As shown in figure 15, authigenic smectite formed from the dissolution of chlorite, plagioclase and sericite (minerals rich in Ca, K, Na, Mg, and Fe. Although all smectites are dioctahedral montmorillonites, their composition changes locally (appendix table D7). The largest variations are in Fe, K, Na, and Mg. SEM studies reveal that these compositional changes reflect the composition of the reactant or dissolved mineral phases.

Similar to the kaolinite-dominated zones in the upper 180–300 m of the WP drill holes, kaolinite and smectite-rich clays also are localized along fractures and small faults. These clays are most abundant proximal to fractures where both the plagioclase phenocrysts and the rock matrix (as observed in the Tertiary intrusive rocks) are pervasively argillized (fig. 16). As the degree of alteration diminishes distal to the fractures, biotite, K-feldspar, and the rock matrix (in the case of intrusive rocks) remain relatively unaltered, whereas, plagioclase is

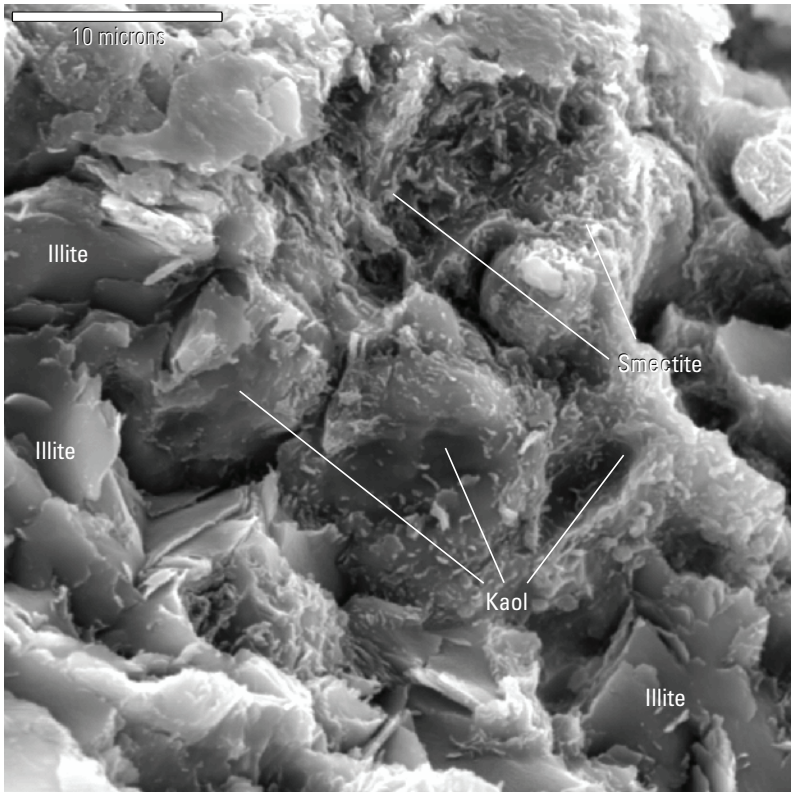

Figure 13. Scanning electron micrograph image showing late-stage kaolinite and smectite that formed after illite.

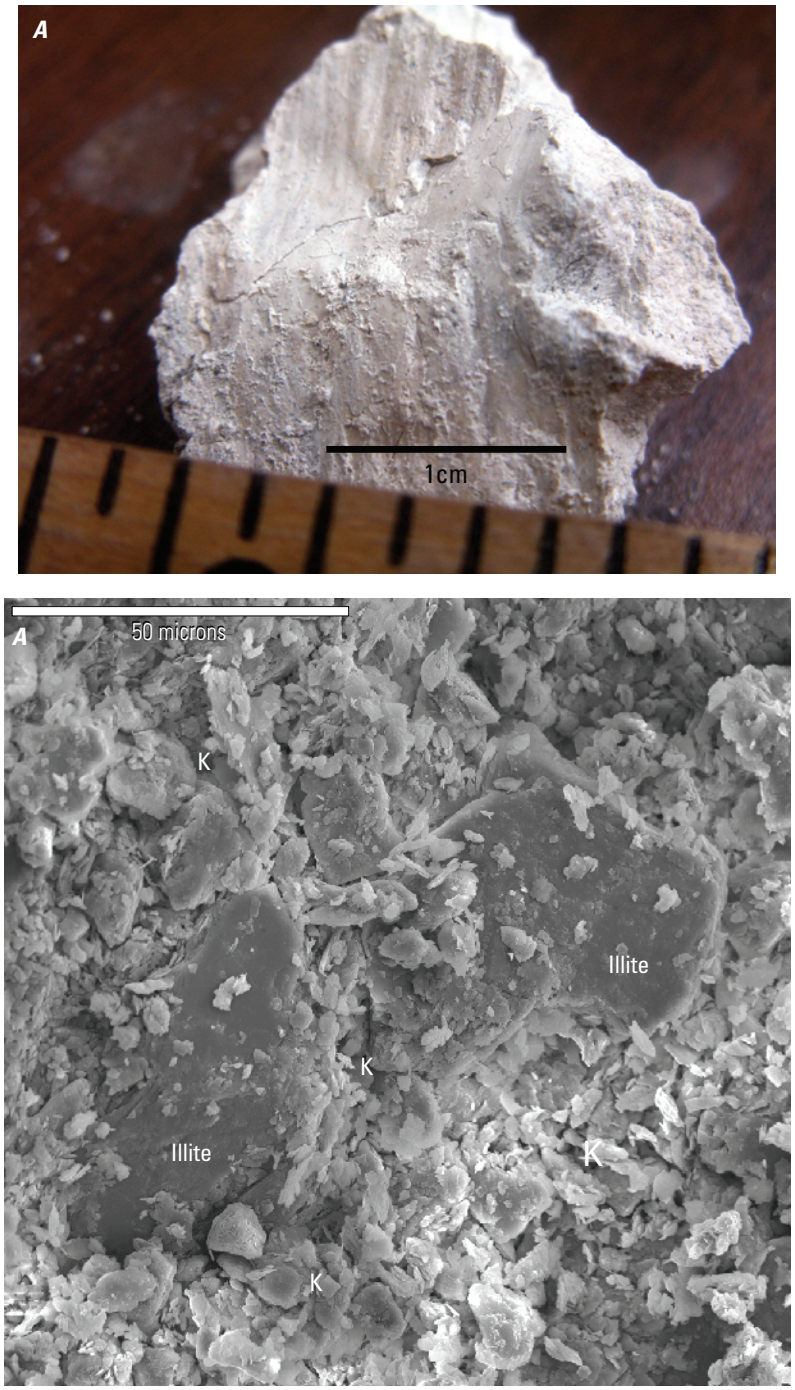

Figure 14. *A,* Waxy kaolinite from fracture in a breccia zone with vertical slickensides. *B,* Scanning electron micrograph image showing kaolinite morphology of waxy kaolinite. (image of sample shown in fig. 13*A*). Note the grains of illite (sericite) are partially replaced by the later kaolinite. Although the illite grains are volumetrically abundant in this scanning electron micrograph view, they are rare in the entire sample.

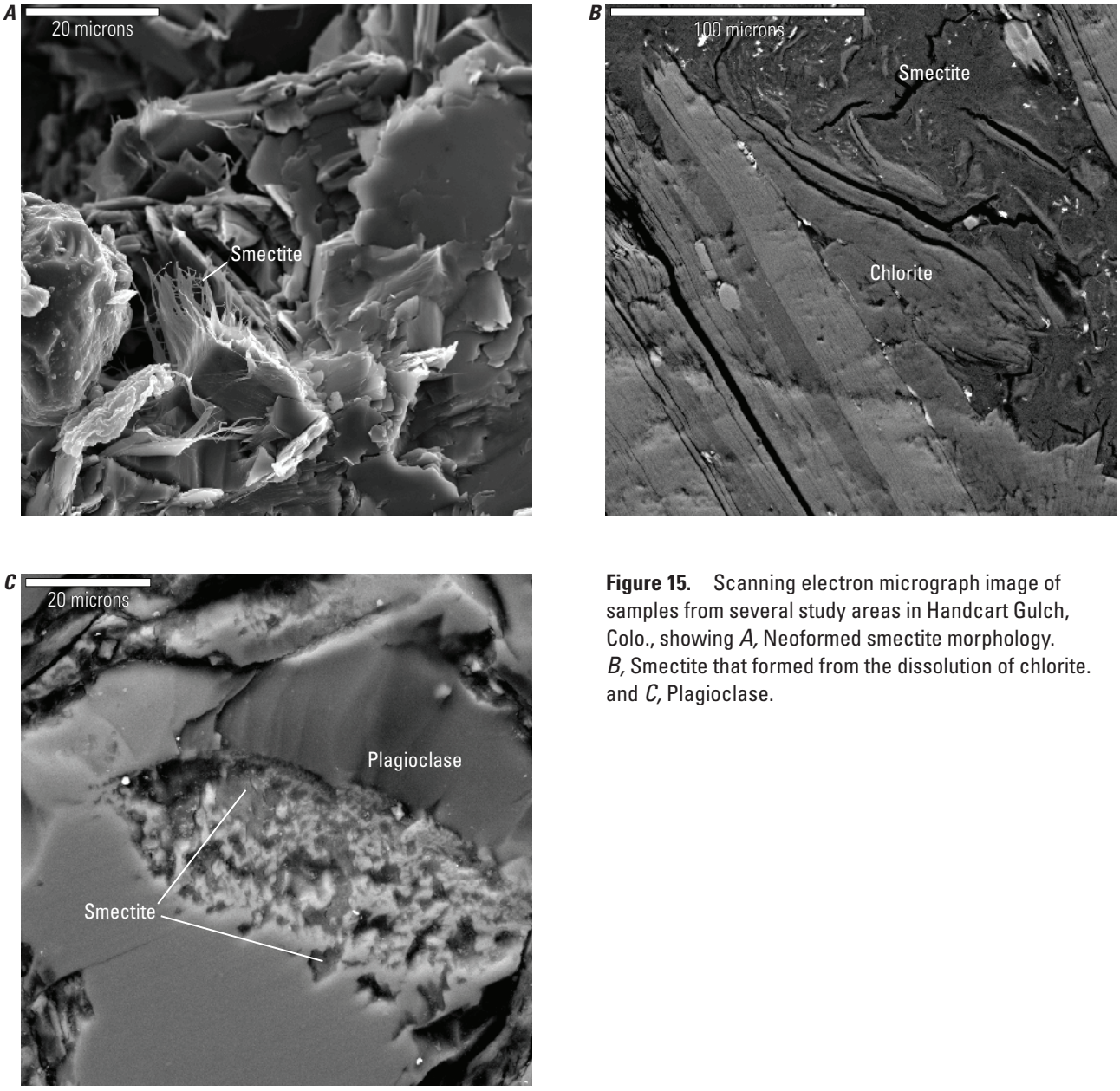

Figure 15. Scanning electron micrograph image of samples from several study areas in Handcart Gulch, Colo., showing *A,* Neoformed smectite morphology. *B,* Smectite that formed from the dissolution of chlorite. and *C,* Plagioclase.

still strongly altered to kaolinite and smectite. As shown in figure 16, jarosite and iron oxy-hydroxides also tend to be localized along these clay-altered fractures.

Stable isotope data from clay mineral separates from the WP1 drillcore (fig. 17) show that late-stage kaolinite and smectite are isotopically distinct in comparison to earlier formed sericite. The late-stage clays plot near the kaolinite line, whereas the sericite data are postitioned to the far left of the line. The sericites plot in a field typically occupied by hypogene and higher temperature clays, whereas clays plotting near the kaolinite line are generally formed in equilibrium with lower temperature, near-surface waters (Taylor, 1974).

Late-Stage Chlorite Alteration

Chlorite is present in the upper 900 ft of drill hole WP1, where it fills fractures that post-date qsp-alteration and was localized along foliation planes in metamorphic rocks (fig. 18*A*). Late fracture-filling chlorite, as shown in figure 18*B*, is commonly intergrown with euhedral, coarse-grained pyrite. Late-stage chlorite contains more magnesium and less iron than replacement chlorite (see tables D3 and D4). Late-stage chlorite post-dates qsp alteration where it was observed in drill hole WP1.

Figure 16. Core from drill hole WP1, Handcart Gulch, Colo., showing strong late-stage clay alteration and jarosite localized at the site of a prominent fracture zone.

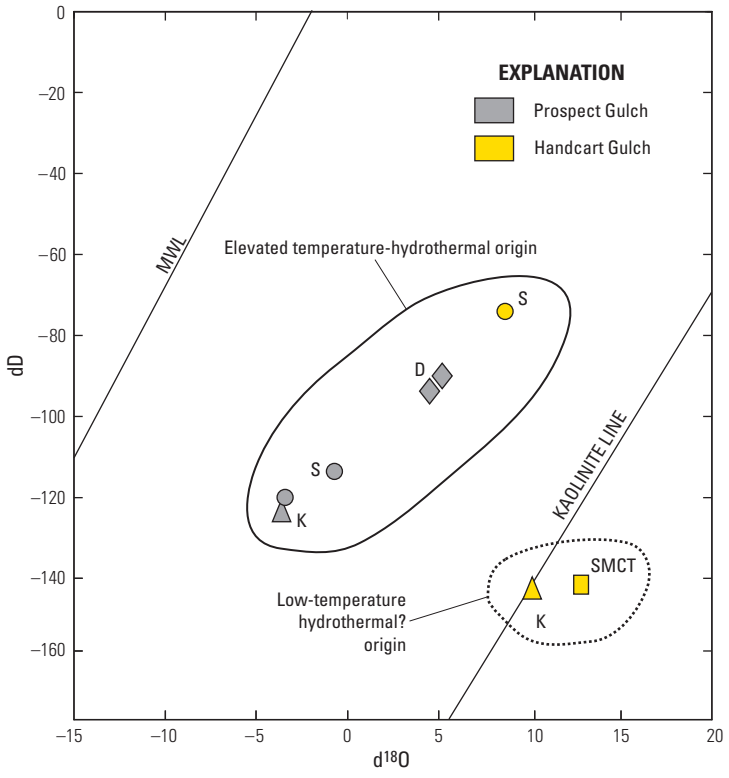

Figure 17. Plot of stable isotopes $d^{18}O$ in relations to dD for clays from the Handcart Gulch area, Colo., and hydrothermal clays from a magmatic hydrothermal acid-sulfate system in the Red Mountain Pass area, near Silverton, Colorado. (From Bove and others, 2007; S=sericite, K=kaolinite, SMCT=smectite, D=Dickite).

Figure 18. *A,* Core from drill hole in Handcart Gulch, Colo., showing late-stage chlorite that formed along foliation planes in quartz-sericite-pyrite-altered gneiss and with fracture-filling pyrite. *B,* Scanning electron micrograph image showing late stage chlorite and intergrown pyrite. In figure 17*A*, the late-stage chlorite is in green.

Sulfide Oxidation

Drillcore data show that zones of pyrite oxidation—as noted by the alteration of pyrite to hematite and other fe-oxyhydroxides—range in depth from approximately 30 to 70 m below the surface at the highest elevations to just a few meters at the lowest elevation along the trunk stream. In addition, pyrite is oxidized in nearly all outcrops examined (fig. 8), marked by characteristic brown (goethite) and red (jarosite and minor hematite) staining on rock surfaces. Discrete pyrite oxidation zones are also present in drillcore to depths of several hundred meters below the pervasive near-surface oxidation zones (fig. 19). These deeper oxidation zones, which are present where fresh pyrite predominates, are spatially associated with fractures, quartz veins, faults, and breccias.

Geochemical and mineralogical data indicate that chalcopyrite, which is present in trace to minor quantities in unoxidized and pyritic rocks, has been mobilized in the near-surface oxidation zone due to pyrite weathering (fig. 20). Detailed studies of drillcore from WP1 show a discrete zone of weak secondary copper enrichment in an approximately 150-ft interval just below the base of the upper pyrite oxidation elevation. Chalcocite is notably abundant in this core interval and is present mostly as thin coatings or as sooty fine-grained aggregates on or around pyrite.

Mineralized Zones and Water Geochemical Data

Data from previous water geochemical studies have been utilized in conjunction with geologic data gathered for this study. The authors present the data that are most pertinent to mineralization and related metal concentrations in the ground and surface waters.

After the cores were collected from the drill holes, the holes were used as monitoring wells to sample groundwater. Dissolved copper concentrations in the monitoring well converted from the WP1 borehole ranged from 10 to 20 mg/L (Verplanck and others, 2008). With the exception of Fe and Cu, concentrations of other base-metal concentrations were low in the WP1 well water. Copper concentrations were relatively low (less than 0.01 to 460 µg/L) in monitoring wells WP2, WP3, WP4, HCBW1, and HCBW3 (fig. 3*A*) and were less than 50 µg/L in the trunk stream, upstream from drill hole HCBW3 (Verplanck and others, 2009).

Stream tracer studies (Verplanck and others, 2008) show an abrupt increase in dissolved copper in the trunk stream and in small inflows in the lower reaches of Handcart Gulch (downstream of drill hole HCBW3; fig. 3*A*). Samples from groundwater monitoring wells in the lower part of the watershed (downstream of drill hole HCBW3) were also enriched in dissolved copper, with concentrations that

Figure 19. Core from drill hole WP1 in Handcart Gulch, Colo., showing zone of localized oxidation surrounded by rock containing mostly unoxidized pyrite. Core depth is 685 feet and below the level of pervasive pyrite oxidation (see figure 4*B*). Oxidation is in orange yellow.

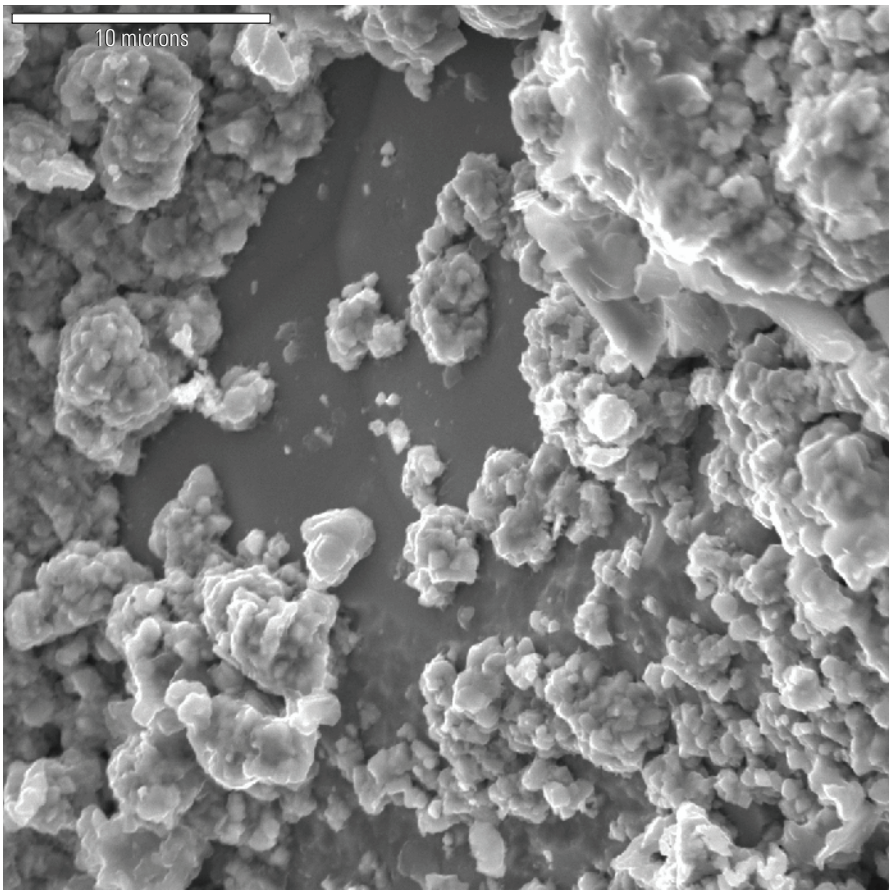

Figure 20. Scanning electron micrograph image showing oxidized pyrite coated by chalcocite, copper sulfates, and clay. Oxidized pyrite is the dark smooth surface, and chalcocite, copper sulfates, and clay are the light colored aggregates.

ranged from 1 to 2 mg/L (Verplanck and others, 2008). In the Summary and Discussion section of this report, these data will be evaluated to assess the controls of mineralization on water geochemistry and to determine whether localized sources of metal loading to surface groundwater could be identified.

Summary and Discussion

Handcart Gulch was the center of intense hydrothermal alteration exposed in an area roughly 2.8 km^2 (fig. 1). Hydrothermal alteration and weak mineralization are spatially and genetically associated with small dacite to low-silica rhyolite stocks and plugs (approximately 37–36 Ma). As indicated by Bookstrom (1987), the dacite to rhyolite intrusions may be low silica and molybdenum-poor precursors of younger and more differentiated intrusions of the Climax and Henderson molybdenite deposits, nearby. Instead, halogen data by EMP indicate that these intrusions are more akin to those that produced porphyry copper deposits.

The only substantial mineralization observed in the Handcart Gulch area was in a localized pyrite-chalcopyrite-luzonite cemented breccia, which was intercepted at shallow depths in drill hole WP1 beneath Porphyry Peak (fig. 6). The high dissolved copper concentrations in the WP1 monitoring well (10-20 mg/L) in the absence of other base metals besides Fe, may indicate the interaction of local groundwater with these copper-rich breccias. There are two plausible explanations for the copper-bearing salts noted in the breccia zone: (1) they precipitated during dry seasons, then dissolved as the water table rose in wet periods, subsequently enriching copper concentrations in the local groundwater; or (2) they formed after the core was removed from the hole due to subsequent drying in the core box.

In comparison, copper concentrations were relatively low (less than 0.01 to 460 µg/L) in monitoring wells WP2, WP3, WP4, HCBW1, and HCBW3 (fig. 3*A*) and were less than 50 µg/L in the trunk stream, upstream of drill hole HCBW3 (Verplanck and others, 2009). These data indicate that sources of mineralization in the upper reaches of Handcart Gulch may be localized, perhaps mostly in the vicinity of Porphyry Peak.

Interpretations of geophysical data by induced polarization (Mineral Systems Inc., unpublished data, 2006) are consistent with the presence of a strongly pyritic zone in the vicinity and immediately southeast of Red Cone Peak (fig. 3*A*). There was a sharp increase in the concentration of dissolved copper noted in samples from the trunk stream and in small inflows in the lower reaches of Handcart Gulch (downstream of drill hole HCBW3; fig. 3*A*) during stream tracer studies. Groundwater monitoring wells in the lower part of the watershed—downstream of drill hole HCBW3—were also enriched in dissolved copper (1–2 mg/L). These combined geologic, geophysical, and water geochemical data indicate there may be a concentrated source of pyrite and copper sulfides near Red Cone Peak, perhaps similar to the mineralized interval identified in drill hole WP1.

Felsic lithologies are commonly altered to a qsp mineral assemblage at the ground surface. Pyrite, which is typically unoxidized in the subsurface beneath 100 m, is very fine-grained and present mostly as disseminations and in veinlets. Alteration assemblages in felsic lithologies are more varied in the subsurface than those observed in outcrop, (figures 4*A*–4*D*), ranging from qsp-dominant in upper drillcore to a propylitic variant that is more typical in deeper drillcore intervals. In contrast, hydrothermally altered amphibolites reflect a propylitic style of alteration (figs. 4*C* and 4*E*), characterized by biotite alteration of amphibole, and chlorite replacement of primary and secondary biotite. Although fine-grained pyrite is present in the amphibolites, most is restricted to small veinlets, whereas, disseminated grains are rare. The characteristics of this hydrothermal mineral assemblage may reflect the mafic and potassium deficient composition of the amphibolite and (or) may have buffered hydrothermal solutions, limiting sericitic alteration of plagioclase and biotite in the amphibolites.

Late-stage argillic alteration (greater than 2–5 percent kaolinite and (or) smectite) was superimposed over earlier-formed alteration assemblages. Late-stage clays are almost entirely composed of kaolinite (a clay mineral containing only Si and Al cations) in rocks where the later alteration overprinted qsp alteration assemblages. The removal of Ca, Fe, Na, and Mg from primary rock minerals during earlier qsp alteration likely explains the scarcity of smectite in the late argillic assemblage (where overprinting qsp rocks), as these cations are key constituents of the local smectitic clays.

Smectite is mostly neoformed resulting from dissolution of chlorite, plagioclase, and minor illite in more weakly altered rocks. Although all smecites are diocathedral montmorillonites, their composition changes locally. The largest variations are in Fe, Na, Mg, and K, which reflect the composition of the reactant phases. Stable isotope data from clay mineral separates from the WP1 drill hole indicate that both kaolinite and smectite formed at relatively low temperatures compared to paragenetically earlier sericite (Bove and others, 2006). Where spatially associated with smectite, late-stage kaolinite is always observed to be a paragenetic precursor. Late-stage kaolinite may have formed in more permeable pathways that conducted acidic waters. In contrast, smectite formation must have occurred when the pH and cation concentrations of fluids increased. It is plausible that some of the low temperature clays, especially those associated with zones of pyrite oxidation, could have formed due to acid weathering processes. However, the great volumetric extent and depth of the late stage clays (see figures 4*A–D*) and common association with unoxidized pyrite, indicates that they were dominantly formed during the collapse or cooling of the hydrothermal system.

Zones of pyrite oxidation range in depth from 30 to 70 m below the ground-surface at higher elevations to just a few meters near the base of the study area. Although almost entirely oxidized in these shallow zones, pyrite is present in trace to minor abundances, especially in more silicified rocks. Because near-surface rocks appear to have a high fracture density and thus a high surface area to volume ratio (Caine and others, 2006; Verplanck and others, 2008), it is probable that much of the rock in the shallow oxidized zone would no longer contribute much acidity, sulfate, or base metal content to surface and groundwaters. However, studies of similarly altered rock in southwest Colorado and northern New Mexico (Bove and others, 2007; Verplanck and others, 2008), indicate that even minor isolated zones of unoxidized pyrite in otherwise oxidized rock can produce low pH, high sulfate, and metal-rich waters, depending on precipitation, topography, degree of silicification, and weathering rates.

Discrete zones of pyrite oxidation are common in drillcore to depths as much as several hundred meters below the pervasive near-surface oxidation zones. These deep oxidation zones contain jarosite and other iron oxides and are spatially associated with fractures, faults, and breccias that also host late-stage kaolinite and smectite clays. This indicates that recent oxidizing and Fe-rich waters have followed along pathways that were open during the evolution of the hydrothermal system. Thus, fractures along which the oxidized pyrite is found at depth may have been discrete zones of high permeability that conducted rapid groundwater flow to depth. If this flow were sufficiently rapid (relative to pyrite oxidation kinetics), the water may have transported dissolved oxygen to depths well below the shallow zone of pervasive oxidation where oxygen was widely available from diffusion from the surface. Alternatively, the deep oxidation zones could also reflect dry climatic periods accompanied by large drops in the groundwater table.

A discrete zone of weak secondary copper enrichment, just below the base of the upper pyrite oxidation level–within the interval of the range of variation of the present-day water table–was intersected between approximately 250–450 ft in drill hole WP1. Chalcocite is common in this drillcore interval and is present mostly as thin coatings or as fine-grained aggregates on or around pyrite. Secondary copper enrichment processes were likely initiated by the dissolution of chalcopyrite and other copper-bearing sulfides in low pH and oxygenated water generated by pyrite oxidation above the water table. The copper in solution probably became saturated at or below the water table where iron in pyrite was partially replaced by copper to form chalcocite.

Quartz-sericite-pyrite altered rocks containing unoxidized pyrite, primarily below the unsaturated zone, have the highest acid-generating capacity of all alteration assemblages in the study area. Hydrothermal alteration has left these rocks base-cation leached and thus acid-neutralizing potential is negligible. Although fine-grained pyrite in qsp-altered rocks undoubtedly generate some low pH and sulfate rich waters, they have very low trace-metal concentrations and thus contribute very little with respect to trace metal concentrations in these waters. Propylitic-altered felsic rocks commonly contain trace to minor calcite and abundant chlorite, which likely provide some amount of acid-neutralization despite the presence of a few percent pyrite.

Acknowledgments

The authors thank Dr. Charles S. Robinson of Mineral Systems Inc. who donated the drill core from the deep boreholes in the study area. The authors also thank Andy Manning and Douglas Yager of the USGS for their helpful reviews.

References Cited

Bookstrom, A.R., Naeser, C.W., and Shannon, J.R., 1987, Isotopic age determinations, unaltered and hydrothermally altered igneous rocks, north-central Colorado Mineral Belt: Isochron/West, no. 49, p. 13–20.

Bove, D.J., 1988, Evolution of the Red Mountain alunite deposit, Lake City caldera, San Juan Mountains, Colorado: Boulder, Colo., University of Colorado, unpublished, M.S. thesis, 179 p.

Bove, D.J., Mast, M.A., Dalton, J.B., Wright, W.G., and Yager, D.B., 2007, Major styles of mineralization and hydrothermal alteration and related solid- and aqueous-phase geochemical signatures, Chapter E3 *in* Church, S.E., von Guerard, Paul, and Finger, S.E., eds., Integrated investigations of environmental effects of historical mining in the Animas River watershed, San Juan County, Colorado: U.S. Geological Survey Professional Paper 1651, p. 160–230.

Botinelly, T., 1979, Mineralogy as a guide for exploration in the Montezuma District, central Colorado: U.S. Geological Survey Open-File Report 79–1177, 18 p.

Bryant, B., McGrew, L.W., and Wobus, R.A., 1981, Geologic map of the Denver 1 degree by 2 degrees Quadrangle, north-central Colorado: U.S. Geological Survey Miscellaneous Investigations Series Map I-1163, 2 sheets, scale 1:250,000.

Caine, J.S., Bove, D.J., Manning, A.H., and Verplanck, P.L., 2004, Preliminary characterization of geological controls on groundwater flow and solute transport in an alpine hydrothermal metal deposit: Handcart Gulch, Montezuma Mining District, Colorado Rocky Mountain Front Range: Annual Meeting, Denver, Colorado, Geological Society of America Abstracts with Programs, v. 36, p. 539.

Caine, J.S., Manning, A.H., Verplanck, P.L., Bove, D.J., Kahn, K.G., and Ge, Shemin, 2006, Well construction information, lithologic logs, water level data, and overview of research in Handcart Gulch, Colorado: An alpine watershed affected by metalliferous hydrothermal alteration: U.S. Geological Survey Open-File Report 2006–1189, 14 p.

Clayton, R.N., and Mayeda, T.K., 1963, The use of bromine pentafluoride in extraction of oxygen from oxides and silicates for isotopic analysis: Geochimica et Cosmochima Acta, v. 27, p. 43–52.

Crook, J.C, 2004, Hydrothermal alteration associated with a copper-molybdenum porphyry system, Webster Pass area, Park and Summit Counties, Colorado: New Mexico Geology, v. 26, p. 72.

Eberl, D.D., 2003, User guide to RockJock—A program for determining quantitative mineralogy from X-ray diffraction data: U.S. Geological Survey Open-File Report 2003–78, 40 p.

Koenig, A.E., and Bove, D.J., Trace elements in pyrite from six areas affected by large scale-pervasive hydrothermal alteration: acid rock drainage (ARD) and signatures of mineralization style: Geological Society of America Abstracts with Programs, vol. 37, no. 7, p. 510.

Lamothe, P.J., Meier, A.L., and Wilson, S.A., 2002, The determination of forty-four elements in aqueous samples by inductively coupled plasma-mass spectrometry, *in* Taggart, J.E., ed., Analytical methods for chemical analysis of geologic and other materials, U.S. Geological Survey: U.S. Geological Survey Open-File Report 02–223, chap. H, 13 p.

Leake, B.E., Woolley, A.R., Arps, C.E.S., Birch, W.D., Gilbert, M.C., Grice, J.D., Hawthorne, F.C., Kato, A., Kisch, H.J., Krivovichev, V.G., Linthout, K., Laird, J., Mandarino, J.A., Maresch, W.V., Nickel, E.H., Rock, N.M.S., Schumacher, J.C., Smith, D.C., Stephenson, N.C.N., Ungaretti, L., Whittaker, E.J.W., and Youzhi, G., 1997, Nomenclature of the amphiboles: Report of the subcommittee on amphiboles of the International Mineralogical Association, Commission on New Minerals and Mineral Names: American Mineralogist, v. 82, p. 1019–1037.

Lovering, T.S., 1935, Geology and ore deposits of the Montezuma Quadrangle Colorado: U.S. Geological Survey Professional Paper 178, 119 p.

Mast, M.A., Evans, J.B., Leib, K.J., and Wright, W.G., 2000, Hydrologic and water-quality data at selected sites in the upper Animas River watershed, southwestern, Colorado, 1997–1999: U.S. Geological Survey Open-File Report 00–53, 20 p.

Millan, C., Pride, D., and Robinson, C., 2002, Interesting ocurrences of breccia near Webster Pass, Colorado: Geological Society of America, Abstracts with Programs, 336 p.

Munoz, J.L., 1984, F-OH and Cl-OH exchange in Micas with applications to hydrothermal ore deposits, *in* Bailey, S.W., ed., Reviews in mineralogy: Micas, v. 13, Mineralogical Society of America, p. 469–491.

Neubert, J.T., Kurtz, J.P., Bove, D.J., and Sares, M.A., 2011, Natural acid rock drainage associated with hydrothermally altered terrane in Colorado: Colorado Geological Survey Bulletin 54, 114 p.

Neuerburg, G.J., Botinelly, T., and Watterson, J., 1974, Molybdenite in the Montezuma District of central Colorado: U.S. Geological Survey Circular 0704, 21 p.

Nordstrom, D.K., McCleskey, R.B., Hunt, A.G., and Naus, C.A., 2005, Questa baseline and pre-mining ground-water quality investigation. 14. Interpretation of ground-water geochemistry in catchments other than the Straight Creek catchment, Red River Valley, Taos County, New Mexico, 2002–2003: U.S. Geological Survey Scientific Investigations Report 2005–5050, 84 p.

Savin, S.M., and Epstein, S, 1970, The oxygen and hydrogen isotope geochemistry of clay minerals, Geochimica et Cosmochima Acta, v. 34, p. 25–42.

Środon, J., Drits, V.A., McCarty, D.K., Hsieh, J.C., and Eberl, D.D., 2001, Quantitative mineral analysis by powder X-ray diffraction from random preparations: Clays and Clay Minerals, v. 49, p. 514–528.

Taylor, H.P., and Epstein, S., 1962, Relationship between 18O/16O ratios in coexisting minerals in igneous and metamorphic rocks, Part I: Geological Society of America Bulletin 73, p. 461–480.

Taylor, H.P., 1974, The application of of oxygen and hydrogen isotope studies to problems of hydrothermal alteration and ore deposition, Economic Geology, v. 69, p. 843–883.

Verplanck, P.L., ed., 2008, Understanding contaminants associated with mineral deposits: U.S. Geological Survey Circular 1328, 96 p.

Verplanck, P.L., Nordstrom, D.K., Bove, D.J., Plumlee, G.S., and Runkel, R.L., 2009, Naturally acidic surface and groundwaters draining porphyry-related mineralized areas of the southern Rocky Mountains, Colorado and new Mexico: Applied Geochemistry, v. 22, p. 1899–1918.

Verplanck, P.L., Manning, A.H., Kimball, B.A., McCleskey, R.B., Runkel, R.L., Caine, J.S., Adams, Monique, Gemery-Hill, P.A., and Fey, D.L., 2008, Ground- and surface-water chemistry of Handcart Gulch, Park County, Colorado, 2003–2006: U.S. Geological Survey Open-File Report 2007–1020, 31 p.

Wahlstrom, E.E., and Kim, O.J., 1959, Precambrian rocks of the Hall Valley area, Front Range, Colorado: Geological Society of America Bulletin, v. 70, p. 1217–1244.

Watanabe, Y., and Hedenquist, J.W., 2001, Mineralogic and stable isotope zonation at the surface over the El Salvador Porphyry Copper Deposit, Chile: Economic Geology, v. 96, p. 1775–1797.

Widmann, B. L., 2003, Geologic map of Keystone Quadrangle, Summit County, Colorado: Colorado Geological Survey, OF 02-03, 1:24,000 scale.

Wilson, S.A., Ridley, W.I., and Koenig, A.E., 2002, Development of sulfide calibration standards for the laser ablation inductively-coupled plasma mass spectrometry technique: Journal of Analytical Atomic Spectrometry, v. 17, p. 405–409.

Publishing support provided by:
Denver Publishing Service Center

For more information concerning this publication, contact:
Center Director, USGS Central Mineral and Environmental Resources Science Center

Box 25046, Mail Stop 973
Denver, CO 80225
(303) 236-1562

Or visit the Central Mineral and Environmental Resources Science Center Web site at:
http://minerals.cr.usgs.gov/

Appendixes

Appendix A

Note: Numbers in parenthesis correspond with numerical designations for lithology and alteration units in tables B1–B7; mineral abundances in descriptions below are in weight percent and reflect data and statistics from tables B1–B7.

Description of Lithologic Units

Quaternary Surficial Deposits

Soil or saprolite (#13)
Ferricrete deposits (#12)

Tertiary Age Intrusions, Dikes, and Breccias

Breccia lithologies undifferentiated (#2)—Includes hydrothermal breccia bodies and dikes, fault breccias, and intrusion-related breccias

Dacite to low-silica rhyolite/granite intrusions and dikes (#1)—Characterized by 30–50 percent phenocrysts of plagioclase, orthoclase, biotite, quartz, plus or minus (±) minor quartz, hornblende, or pyroxene in a microcrystalline groundmass. Plagioclase phenocrysts (dominantly oligoclase) are subhedral to euhedral, tabular to lath-shaped, and 1 to 5 millimeters (mm) long. Orthoclase phenocrysts are mostly euhedral, tabular, and as much as 1 to 5 centimeters (cm) in length. Quartz is rounded, embayed, and ranges from 1 to 5 mm.

Plagioclase-biotite dacite to andesite porphyritic dikes (#14)—Relatively narrow (less than 0.3 m) dikes containing phenocrysts of plagioclase (andesine and albite) and biotite in a black aphanitic groundmass.

Precambrian Rocks

Includes biotite-feldspar-quartz gneiss, biotite-sillimanite-quartz gneiss, porphyroblastic gneiss, feldspar-biotite-quartz gneiss, foliated felsite, felsite, and amphibolite. All of the Precambrian units are intimately intruded by granite and granite pegmatite.

Pegmatite (#3)
Biotite-sillimanite-quartz gneiss and porphyroblastic gneiss (#4)
Biotite-sillimanite-quartz gneiss and porphyroblastic gneiss intimately intermingled or cut by pegmatite (#5)
Biotite-sillimanite-quartz gneiss and porphyroblastic gneiss, and (or) feldspar-biotite-quartz gneiss (#8)
Amphibolite intermingled or cut by pegmatite (#6)
Amphibolite (#7)
Foliated felsite may include feldspar-biotite-quartz gneiss (#9)
Felsite with intervals of feldspar-biotite-quartz gneiss (#11)

Silver Plume granite (#15) Samples of Silver Plume granite in table B1 are highly altered and from outcrops north of Webster Pass (see fig. 3*B*). Silver Plume granite was not identified in drill core.

Description of Alteration Units

Note: The following alteration assemblages are specific to all lithologies except the amphibolite units (#6 and #7).

Propylitic (#1)—Contains varying amounts of chlorite, epidote, calcite, and illite (sericite) in the presence of metastable to stable primary feldspar crystals. Plagioclase grains show significant replacement by mixtures of chlorite, calcite, and illite. Ferromagnesian minerals (biotite, pyroxene, and hornblende) are partially altered to fine-grained chlorite, smectite, illite, quartz, iron-oxides, and epidote. Hematite, chlorite, and other iron oxides are typically abundant along fractures, especially in metamorphic lithologies distal to the Handcart Gulch/Webster Pass areas. Quantitative analysis (tables B1–B7) show that propylitic-altered Tertiary intrusive rocks generally contain less than 30 percent quartz, greater than 10 to 15 percent plagioclase, greater than 10 to 20 percent potassium feldspar, and less than 20 percent illite. Pyrite, when present is less than about 2 percent. Secondary albite is widespread, abundant (as much as 10–15 percent), and present in most lithologies in the study area. Paragenetic studies indicate that albitization was one of the earliest alteration events in the study area, perhaps accompanying propylitic alteration. Similar to potassium feldspar, albite is less susceptible to hydrothermal breakdown as noted in all but quartz-sericite-pyrite altered rocks.

Propylitic to weak sericitic (#2)—Assemblage designation pertains only to potassium feldspar-bearing lithologies including Tertiary intrusions, pegmatites, and felsites. Potassium feldspar is mostly unaltered and abundances range from about 10–15 percent. In contrast to the propylitic assemblage, plagioclase content is commonly less than

10 to 15 percent owing to partial alteration to sericite. Sericite content typically ranges from about 15 to 20 percent, whereas quartz typically exceeds 30 percent owing to weak silicification. Fine-grained pyrite averages 4 percent and is most abundant in narrow veinlets but is also present as disseminated grains.

Weak sericite-pyrite (#4)—Characterized by the near complete alteration of plagioclase to sericite; biotite is completely altered. Chlorite, an alteration product of biotite, pyroxene, and amphibole is commonly metastable. Potassium feldspar, where present in original lithologies, is partially altered to sericite (less than 5–8 percent). Quartz content generally exceeds 30–35 percent owing to silicification, whereas pyrite, which is present as finely disseminated grains and in narrow veinlets, averages 6 percent.

Quartz-sericite-pyrite (qsp) (#5)—Characterized by the complete alteration of plagioclase and near complete alteration of potassium feldspar (less than 2 percent) to sericite and fine-grained quartz. Ferromagnesian minerals and chlorite are absent. Sericite is commonly pseudomorphous after biotite, whereas Fe-Ti oxides are altered to fine hematite, maghemite, and minor anatase or rutile. Rocks containing unoxidized pyrite are typically gray to light gray, although some rocks have a highly bleached appearance. Pyrite is almost always absent in outcrop, where these rocks are bleached or stained brown (goethite or limonite) or red (jarosite and hematite) as a result of oxidation. Pyrite is present as finely disseminated grains (0.1 to 0.5 mm) and in veinlets (1–3 mm) with or without quartz; pyrite content in quartz-sericite-pyrite-altered rock averages 9 percent.

Quartz-sericite-pyrite zones are pervasive and widespread to about 1,000 ft below land surface in drill holes WP1-WP4 (tables B2–B5), perhaps due to coalescence of individual hydrothermal cells. Below this depth, quartz-sericite-pyrite (qsp) zones are more sporadic and irregularly distributed as haloes a few millimeters to several meters wide about prominent fractures containing pyrite. Pyrite grains are euhedral and as much as 5mm in these fractures, which may also contain minor quartz.

Pyrite ± quartz veinlet densities vary widely in qsp-altered rock. Veinlets can be sparsely dispersed or present in a relatively dense stockwork arrangement. Although the density of the fine fracture network is generally similar in both the qsp and adjacent zones of weaker alteration, pyrite content decreases sharply in the fracture network just outside the qsp zones

Silicified with pyrophyllite (#9)—Rocks are highly silicified (mostly greater than 55 percent quartz) and also contain pyrophyllite, the latter being ascertained by XRD and (or) mineral maps by remote spectroscopy (Airborne Visible/Infrared Imaging Spectrometer or AVIRIS). This assemblage is commonly associated with brecciated rocks of varying lithologies. Remote mineral mapping by AVIRIS (E. Livo, USGS, oral commun., 2004) shows a strong spatial correlation between silicified and pyrophyllite-bearing rocks and areas rich in jarosite. Silicified and pyrophyllite-altered rocks are only noted in a few outcrop areas and near the top of drill holes WP1, WP3, and HCBW3. Pyrite is oxidized in all observed silicified and pyrophyllite-altered rocks owing to near surface exposure. The presence of pyrophyllite in these silicified and commonly brecciated rocks indicates that these areas may have been local centers of hydrothermal alteration. Hydrothermal fluids in these centers were likely higher temperature than those that produced sericite in the absence of pyrophyllite in surrounding rocks (Watanabe and Hedenquist, 2001)

Note: The following assemblages are specific to amphibolite and other mixed amphibolite lithologies (see drill holes WP3 and HCBW-1, tables B4 and B6, figures 4*C* and 4*E*).

Propylitic-altered amphibolite (#31)—Dark gray to black, amphibole and plagioclase-rich rock. Amphibole is partially altered to biotite, which in turn is partially replaced by chlorite. Magnetite alters to maghemite as propylitic alteration intensity increases. Minor epidote is present and is typically associated with vein quartz bands that tend to parallel foliation. As much as 7 to 8 percent pyrite is present but mostly in small fractures or veinlets; disseminated grains are rare.

High propylitic-altered amphibolite (#32)—Altered amphibolites are characterized by a brown to greenish-brown hue. Amphibole is minor due to near complete alteration to biotite;

biotite that formed after amphibole is in turn altered to chlorite. Epidote is minor to moderately abundant and is associated with irregular quartz veins. Minor smectite is also present and commonly forms replacements after original biotite and amphibole. Sericite is minor. Pyrite is abundant in small fractures and veinlets but rare as disseminations.

Argillic-altered amphibolite (#33)—Rocks are characteristically brown with primary amphibolite features well preserved and easily recognized. Original minerals are mostly altered to smectite, kaolinite, epidote, and minor sericite. Argillic alteration zones are commonly coincident with faults; slickenside surfaces are abundant and well preserved in these deformation zones.

Mixed Alteration Assemblages

Mix of weak sericitic altered felsic rocks and propylitic altered amphibolite (#34)

Mix of quartz-sericite-pyrite altered felsic rocks and propylitic, high propylitic, and argillic-altered amphibolite (#35)

Late-Stage Clay and Vein-Related Alteration

Late-Stage Argillic Alteration

Late-stage argillic alteration is characterized by more than 2 to 5 percent clays consisting of kaolinite and (or) smectite superimposed over earlier-formed alteration assemblages. Late-stage clays are almost exclusively composed of kaolinite in quartz-sericite-pyrite altered rocks. These kaolinite-rich rocks are most prevalent in the upper 600 to 1,000 ft of drill holes WP1,WP2, WP3, and WP4 (fig. 4*A*). Kaolinitic clay-altered rocks are typically white, soft, and have a waxy or porcelain-like appearance. In some instances, prominent fractures or small faults are lined with a soft, waxy, nearly pure kaolinite.

In contrast, clays composed of both kaolinite and smectite are present in more weakly altered rocks (propylitic to weak sericite-pyrite) that retained much of their primary mineralogy during the alteration process. Late kaolinite and smectite are prevalent in intrusive rocks beneath about 1,000 ft in drill holes WP1, WP2, and WP4, where they overprint earlier formed clays in propylitic to weak sericitic assemblages. Late-stage clays containing both kaolinite and smectite impart a characteristic greenish-brown hue, especially on more weakly altered intrusive rocks. Although this greenish coloration tends to be evenly distributed in the matrix of intrusive rocks, it is most striking in altered plagioclase phenocrysts. Similar to the higher level kaolinite dominated zones, kaolinite/smectite was localized along fractures and faults.

Note: Letters below in parentheses are used in conjunction with numerical codes as listed above (see tables B1–B7) to denote that the primary mineral assemblage is overprinted by late stage clay or vein-related alteration. For example, alteration unit 5a represents a qsp-altered rock that was overprinted by weak argillic alteration.

Weak argillic [suffix (a)] Contains 2 to 5 percent kaolinite and smectite

Argillic [suffix (b)] Contains greater than 5 percent kaolinite and smectite

Late chlorite [suffix (c)] Observed only in the upper 900 ft of drill hole WP1, where it imparts a distinctly greenish hue on quartz-sericite-pyrite-altered metamorphic rocks. Chlorite precipitated mostly along fractures and infiltrated into the interior of the rock, commonly parallel to foliation. Fracture-filling chlorite is commonly intergrown with euhedral pyrite; both chlorite and pyrite post-date earlier episodes of qsp-alteration. Chlorite compositions from the study area fall in the range of clinochlore; however, late-stage chlorite precipitates contain more magnesium and less iron than replacement chlorite (see tables D3 and D4).

Late chlorite and kaolinite [suffix (d)] Identical in character to late-stage chlorite as described above; however, kaolinite is also abundant. Although chlorite is spatially associated with kaolinite, the paragenetic relation between these minerals has not been determined.

Diffuse quartz veins with epidote [suffix (e)] Rocks cut by diffuse milky quartz veins with associated epidote and calcite. May be associated garnet (grossular). Mineral assemblage observed only in drill hole HCBW-1.

Table B1. Quantitative X-ray diffraction results from surface samples.

[All samples normalized to 100 percent. Pre-normalization totals are recorded in samples run with zincite standard, otherwise samples were run without an internal standard. See Appendix A for key to lithology and alteration codes. Lower values for degree of fit suggest more accurate analyses with values less than 0.1 considered ideal. Mineral percentages are blank where absent in the sample and therefore not analyzed]

Sample number	LINC-PORPH	PM4	PX40	PX26	MDBR01
Lithology	1	1	1	1	1
Alteration	0	0	0	1	1
			Non-clays		
Quartz	23.2	16.1	17.2	24.4	26.3
Potassium Feldspar	15.7	21.4	18.2	24.5	27.0
Plagioclase	48.7	30.6	27.5	17.3	20.1
Albite	5.3	5.0	8.9	12.5	11.2
Amphibole	0.4	2.0	1.4	0.0	
Biotite	3.5	4.3	4.9	0.4	0.0
Pyroxene	0.5	1.0	0.0		
Titanite		0.4	0.0	1.7	
Magnetite	1.4	2.5	1.4	0.5	1.2
Anatase		0.0	0.0	0.2	
Apatite		1.6	1.7	1.0	0.8
Rutile	0.5	0.0	0.1	0.7	0.6
Garnet					
Sillimanite				0.4	
Calcite		0.5	0.2	0.0	
Siderite		0.1	0.2		
Epidote		0.4	0.6	0.7	
Laumontite					
Svanbergite					
Hematite		0.0	0.0	0.3	
Maghemite		6.0	3.0	0.5	
Goethite		0.0	0.1	0.3	
Jarosite	0.0	0.3	0.3	0.6	0.0
Anhydrite		0.2	0.0	0.0	
Gypsum		0.5	0.0	0.3	
Pyrite		0.0	0.6	0.0	0.8
			Clays		
Illite/Fine Muscovite	0.0	2.4	5.4	8.7	5.8
Smectite		2.5	2.6	0.3	
Kaolinite		0.5	0.9	3.8	0.8
Pyrophyllite					
Chlorite	0.8	1.8	4.8	1.0	5.4
			Total clays		
Full pattern region degree of fit	0.0820	0.1144	0.1036	0.1715	0.0883
Clay region degree of fit	0.0497				0.0562
Pre-normalization total	99.9	114.2	117.7		105.8

Table B1. Quantitative X-ray diffraction results from surface samples.—Continued

[All samples normalized to 100 percent. Pre-normalization totals are recorded in samples run with zincite standard, otherwise samples were run without an internal standard. See Appendix A for key to lithology and alteration codes. Lower values for degree of fit suggest more accurate analyses with values less than 0.1 considered ideal. Mineral percentages are blank where absent in the sample and therefore not analyzed]

Sample number	MDBR0202	MDBPEAK02	MDBR0302	MDBR0402
Lithology	1	1	9	7
Alteration	4	5	4	5
		Non-clays		
Quartz	50.1	61.4	31.8	81.3
Potassium Feldspar	2.4	0.7	0.5	0.0
Plagioclase	0.2		6.9	0.0
Albite	1.0		16.1	0.0
Amphibole	0.8		0.0	0.0
Biotite	0.6		0.3	0.0
Pyroxene				
Titanite	0.2		0.2	0.0
Magnetite	0.1		0.0	0.0
Anatase	0.0		0.0	0.0
Apatite	0.0		0.1	0.0
Rutile	0.7	0.4	0.1	0.3
Garnet				
Sillimanite	0.4		0.7	0.0
Calcite	0.1		0.0	0.0
Siderite				
Epidote	0.0		0.0	0.0
Laumontite				
Svanbergite				
Hematite	0.0		0.0	0.0
Maghemite	0.0	2.0	0.2	0.0
Goethite	0.1		0.8	0.0
Jarosite	2.1	1.3	0.4	0.0
Anhydrite	0.0		0.0	0.3
Gypsum	1.0		0.3	0.0
Pyrite	0.0		0.0	0.0
		Clays		
Illite/Fine Muscovite	35.0	34.2	40.2	18.1
Smectite	1.9		1.0	0.0
Kaolinite	2.4		0.0	0.0
Pyrophyllite				
Chlorite	1.0		0.5	0.0
		Total clays		
Full pattern region degree of fit	0.1402	0.0965	0.1779	0.1503
Clay region degree of fit		0.0654		
Pre-normalization total	98.3	93.6	103.2	101.9

Table B1. Quantitative X-ray diffraction results from surface samples.—Continued

[All samples normalized to 100 percent. Pre-normalization totals are recorded in samples run with zincite standard, otherwise samples were run without an internal standard. See Appendix A for key to lithology and alteration codes. Lower values for degree of fit suggest more accurate analyses with values less than 0.1 considered ideal. Mineral percentages are blank where absent in the sample and therefore not analyzed]

Sample number	105WDB4A	JSC19	9 26 1A	JSC0102	JSC0402
Lithology	9	4	9	1	9
Alteration	5a	1	2	5	5
			Non-clays		
Quartz	50.7	23.2	23.2	66.1	36.4
Potassium Feldspar		1.6	29.5	0.0	1.5
Plagioclase				0.0	0.0
Albite		0.6		0.0	0.0
Amphibole				0.0	0.3
Biotite		13.1	3.5	0.0	0.4
Pyroxene				0.0	0.0
Titanite		0.0		0.0	0.0
Magnetite		0.0	6.2	0.0	0.0
Anatase					
Apatite				0.0	0.0
Rutile	2.2				
Garnet					
Sillimanite		20.1		0.0	1.4
Calcite				0.0	0.0
Siderite					
Epidote				0.0	0.0
Laumontite					
Svanbergite					
Hematite				0.0	0.0
Maghemite	2.9	2.0	3.1	0.0	0.2
Goethite				0.3	0.0
Jarosite	7.2			0.0	1.6
Anhydrite					
Gypsum				0.0	0.2
Pyrite	0.3			0.0	0.0
			Clays		
Illite/Fine Muscovite	31.6	25.9	13.0	33.6	57.6
Smectite				0.0	0.0
Kaolinite	5.2			0.0	0.4
Pyrophyllite				0.0	0.0
Chlorite		13.5	21.6	0.0	0.0
			Total clays		
Full pattern region degree of fit	0.0864	0.1168	0.1049	0.1283	0.1218
Clay region degree of fit	0.0624	0.0798	0.0788		
Pre-normalization total	106.9	103.2	110.0	105.1	101.1

Table B1. Quantitative X-ray diffraction results from surface samples.—Continued

[All samples normalized to 100 percent. Pre-normalization totals are recorded in samples run with zincite standard, otherwise samples were run without an internal standard. See Appendix A for key to lithology and alteration codes. Lower values for degree of fit suggest more accurate analyses with values less than 0.1 considered ideal. Mineral percentages are blank where absent in the sample and therefore not analyzed]

Sample number	JSC0602	JSC6A02	JSC6B02	JSC6C02	JSC902
Lithology	9	9	15	9	4
Alteration	1	1	5	5	5
			Non-clays		
Quartz	42.8	36.2	57.2	46.5	57.7
Potassium Feldspar	3.7	4.8	0.4	1.6	0.0
Plagioclase	14.9	27.5	0.0	0.0	0.0
Albite	8.2	11.9	0.0	0.0	0.0
Amphibole	0.0	0.0	0.1	1.0	
Biotite	2.3	5.3	0.9	0.7	0.0
Pyroxene	0.0	0.0	0.0	0.7	
Titanite	0.0	0.7	0.0	0.3	0.0
Magnetite	0.0	0.1	0.4	0.0	0.0
Anatase					0.0
Apatite	0.1	0.1	0.0	0.0	0.0
Rutile					0.1
Garnet					
Sillimanite	0.3	0.7	0.8	0.0	0.0
Calcite	0.0	0.0	0.0	0.0	0.0
Siderite					
Epidote	0.0	0.0	0.0	0.0	0.0
Laumontite					
Svanbergite					
Hematite	0.0	0.0	0.0	0.2	0.0
Maghemite	0.0	0.0	0.0	0.6	0.0
Goethite	0.1	0.0	0.0	0.5	0.1
Jarosite	0.2	0.9	1.5	2.1	0.0
Anhydrite					1.0
Gypsum	0.8	1.0	0.7	0.2	0.0
Pyrite	0.0	0.0	0.0	0.0	0.0
			Clays		
Illite/Fine Muscovite	18.7	7.5	37.8	44.9	41.2
Smectite	0.0	0.0	0.0	0.0	
Kaolinite	1.0	0.4	0.1	0.0	0.0
Pyrophyllite	0.0	0.0	0.0	0.0	0.0
Chlorite	6.7	3.1	0.0	0.8	0.0
			Total clays		
Full pattern region degree of fit	0.1244	0.1555	0.1392	0.1331	0.1366
Clay region degree of fit					
Pre-normalization total	97.6	103.9	104.4	104.8	102.2

Table B1. Quantitative X-ray diffraction results from surface samples.—Continued

[All samples normalized to 100 percent. Pre-normalization totals are recorded in samples run with zincite standard, otherwise samples were run without an internal standard. See Appendix A for key to lithology and alteration codes. Lower values for degree of fit suggest more accurate analyses with values less than 0.1 considered ideal. Mineral percentages are blank where absent in the sample and therefore not analyzed]

Sample number	JSC1102	JSC12B02	JSC12A02	JSC1902	JSC17A02
Lithology	4	15	4	4	4
Alteration	2	5	5	1	2
			Non-clays		
Quartz	44.4	60.4	63.1	58.0	34.1
Potassium Feldspar	10.8	0.0	0.0	1.1	17.3
Plagioclase	12.6	0.0	0.0	1.1	12.6
Albite	18.0	0.0	0.0	1.4	6.4
Amphibole	0.0	0.0		0.0	
Biotite	4.0	0.0	0.0	4.9	0.0
Pyroxene	0.0	0.6		0.0	
Titanite	0.7	0.2	0.0	0.2	0.0
Magnetite	0.5	0.0	0.0	0.3	0.0
Anatase			0.0		1.0
Apatite	0.0	0.0	0.0	0.0	0.0
Rutile			0.2		0.9
Garnet					
Sillimanite	0.0	0.0	0.0	13.2	5.0
Calcite	0.0	0.0	0.0	0.0	0.0
Siderite					
Epidote	0.0	0.0	0.0	1.0	0.0
Laumontite					
Svanbergite					
Hematite	0.0	0.0	0.0	0.0	0.0
Maghemite	0.0	0.0	0.0	0.5	0.0
Goethite	0.0	0.0	0.0	0.1	0.0
Jarosite	0.0	0.4	0.6	0.0	0.5
Anhydrite			0.4		0.6
Gypsum	0.0	0.9	0.1	0.5	0.5
Pyrite	0.0	0.0	0.0	0.0	0.0
			Clays		
Illite/Fine Muscovite	5.0	37.4	35.6	12.7	18.2
Smectite	0.0	0.0		0.0	
Kaolinite	0.0	0.0	0.0	0.0	1.4
Pyrophyllite	0.0	0.0	0.0	0.0	0.0
Chlorite	4.0	0.0	0.0	4.9	1.5
			Total clays		
Full pattern region degree of fit	0.1543	0.1314	0.1834	0.1789	0.1393
Clay region degree of fit					
Pre-normalization total	95.9	105.8	108.1	105.0	104.1

Table B1. Quantitative X-ray diffraction results from surface samples.—Continued

[All samples normalized to 100 percent. Pre-normalization totals are recorded in samples run with zincite standard, otherwise samples were run without an internal standard. See Appendix A for key to lithology and alteration codes. Lower values for degree of fit suggest more accurate analyses with values less than 0.1 considered ideal. Mineral percentages are blank where absent in the sample and therefore not analyzed]

Sample number	PC12	PX5	PI18	PX6	PX10
Lithology	1	1	1	1	2b
Alteration	4	5	5	5	9
			Non-clays		
Quartz	48.2	52.5	51.3	62.0	48.1
Potassium Feldspar	1.3	0.7	0.0	0.0	0.0
Plagioclase	2.2	0.2	0.0	0.0	0.0
Albite	2.6	0.0	0.0	0.0	0.0
Amphibole					
Biotite	0.0				
Pyroxene					
Titanite	0.4	0.0	0.0	0.0	0.0
Magnetite	0.0	0.0	0.0	0.0	0.0
Anatase	0.0	0.0	0.0	0.0	0.0
Apatite	0.0	0.0	0.0	0.0	0.0
Rutile	0.8	0.9	0.1	0.3	0.5
Garnet					
Sillimanite	0.1	0.0	0.0	0.0	
Calcite	0.0				
Siderite					
Epidote	0.0	0.1	0.0	0.0	
Laumontite					
Svanbergite					
Hematite	0.0	0.0	0.0	0.0	0.0
Maghemite	0.0	0.0	0.0	0.0	0.0
Goethite	0.2	0.0	0.0	0.0	2.9
Jarosite	1.0	1.7	1.8	0.0	0.0
Anhydrite	0.5	0.0	0.6	0.6	0.0
Gypsum	0.1	0.0	0.0	0.0	0.0
Pyrite	0.0	0.0	0.0	0.0	0.0
			Clays		
Illite/Fine Muscovite	40.3	43.2	46.2	37.1	43.1
Smectite					
Kaolinite	1.8	0.6	0.0	0.0	0.0
Pyrophyllite	0.0				5.3
Chlorite	0.5				0.0
			Total clays		
Full pattern region degree of fit	0.1441	0.1439	0.1426	0.1207	0.1486
Clay region degree of fit					
Pre-normalization total	101.8	102.9	101.6	98.3	102.5

Table B1. Quantitative X-ray diffraction results from surface samples.—Continued

[All samples normalized to 100 percent. Pre-normalization totals are recorded in samples run with zincite standard, otherwise samples were run without an internal standard. See Appendix A for key to lithology and alteration codes. Lower values for degree of fit suggest more accurate analyses with values less than 0.1 considered ideal. Mineral percentages are blank where absent in the sample and therefore not analyzed]

Sample number	PX11b	PX11C	PX25
Lithology	1	1	1
Alteration	5b	5	4
		Non-clays	
Quartz	35.5	58.2	56.8
Potassium Feldspar	0.0	0.0	0.0
Plagioclase	0.0	0.0	2.5
Albite	0.0	0.0	0.0
Amphibole			0.0
Biotite			0.0
Pyroxene			
Titanite	0.8	0.0	0.0
Magnetite	0.0	0.0	0.1
Anatase	0.0	0.0	0.0
Apatite	0.1	0.0	0.2
Rutile	0.8	0.5	0.5
Garnet			
Sillimanite			0.0
Calcite			0.0
Siderite			
Epidote			0.0
Laumontite			
Svanbergite			
Hematite	0.0	0.0	0.0
Maghemite	1.9	0.0	0.1
Goethite	9.1	0.3	0.3
Jarosite	0.4	0.2	0.0
Anhydrite	0.0	0.1	1.0
Gypsum	0.9	0.0	0.0
Pyrite	0.1	0.1	0.0
		Clays	
Illite/Fine Muscovite	41.3	40.6	38.4
Smectite			0.0
Kaolinite	7.1	0.0	0.0
Pyrophyllite	1.0	0.0	
Chlorite	1.0	0.0	0.2
		Total clays	
Full pattern region degree of fit	0.1391	0.1612	0.1350
Clay region degree of fit			
Pre-normalization total	104.5	105.2	96.9

Table B2. Quantitative X-ray diffraction results from drill hole WP-1 in weight percent.

[All samples normalized to 100 percent. Pre-normalization totals are recorded in samples run with zincite standard, otherwise samples were run without an internal standard. See Appendix A for key to lithology and alteration codes. Lower values for degree of fit suggest more accurate analyses with values less than 0.1 considered ideal. Mineral percentages are blank where absent in the sample and therefore not analyzed]

Sample number	WP1-49	WP1-85	WP1-102	WP1-144	WP1-185
Lithology	9	11	9	11	11
Alteration	5	5	5b	5b	9
			Non-Clays		
Quartz	62.6	65.8	67.7	85.6	56.3
Potassium Feldspar				0.0	
Albite					
Plagioclase					
Amphibole					
Biotite					
Pyroxene					
Titanite	0.1	1.0	0.2	0.6	0.6
Magnetite	0.0	0.6	1.0	0.2	
Anatase				0.0	
Rutile	0.8	1.0	1.8	0.1	0.0
Calcite					
Epidote					
Laumontite					
Svanbergite					
Hematite	0.2	0.3	0.2	0.1	0.0
Maghemite					
Goethite	3.0	4.1	0.4	5.0	2.9
Anhydrite					
Gypsum					
Jarosite		0.0	0.0	0.0	
Pyrite	0.3	0.5	0.5	0.4	0.0
			Clays		
Illite/Fine Muscovite	33.0	26.7	23.9	2.7	28.7
Smectite					
Kaolinite			4.3	5.4	
Pyrophyllite					11.5
Chlorite					
Total clays	**33.0**	**26.7**	**28.2**	**8.0**	**40.2**
Full pattern region degree of fit	0.1046	0.1377	0.1341	0.1246	0.1153
Clay region degree of fit	0.0709	0.0884	0.0784	0.1136	0.0831
Pre-normalization total	100.4	97.1	102.2	107.0	100.8

Table B2. Quantitative X-ray diffraction results from drill hole WP-1 in weight percent.—Continued

[All samples normalized to 100 percent. Pre-normalization totals are recorded in samples run with zincite standard, otherwise samples were run without an internal standard. See Appendix A for key to lithology and alteration codes. Lower values for degree of fit suggest more accurate analyses with values less than 0.1 considered ideal. Mineral percentages are blank where absent in the sample and therefore not analyzed]

Sample number	WP1-226	WP1-255	WP1-265	WP1-276	WP1-281
Lithology	9	8	8	9	2
Alteration	5	5	5	5d	5b
			Non-clays		
Quartz	88.2	29.6	29.5	40.5	41.7
Potassium Feldspar					
Albite					
Plagioclase					
Amphibole					
Biotite					
Pyroxene					
Titanite	0.0				
Magnetite	0.2	0.0	0.3	0.7	0.1
Anatase		0.0	0.1	0.0	0.0
Rutile	0.7	0.8	1.0	1.6	1.1
Calcite					
Epidote					
Laumontite		1.4			
Svanbergite					
Hematite	0.0				
Maghemite					
Goethite	0.9				
Anhydrite					
Gypsum					
Jarosite				0.0	
Pyrite	0.8	12.0	12.8	3.7	9.7
			Clays		
Illite/Fine Muscovite	8.1	56.1	54.3	23.9	42.6
Smectite					
Kaolinite			2.0	20.8	4.8
Pyrophyllite	1.0				
Chlorite				8.9	
Total clays	**9.1**	**56.1**	**56.3**	**53.6**	**47.4**
Full pattern region degree of fit	0.1047	0.1045	0.1058	0.0975	0.0992
Clay region degree of fit	0.0853	0.0745	0.0835	0.0792	0.0625
Pre-normalization total	105.1	96.9	102.6	99.1	96.3

Table B2. Quantitative X-ray diffraction results from drill hole WP-1 in weight percent.—Continued

[All samples normalized to 100 percent. Pre-normalization totals are recorded in samples run with zincite standard, otherwise samples were run without an internal standard. See Appendix A for key to lithology and alteration codes. Lower values for degree of fit suggest more accurate analyses with values less than 0.1 considered ideal. Mineral percentages are blank where absent in the sample and therefore not analyzed]

Sample number	WP1-287	WP1-360-clast	WP1-360-matrix	WP1-378
Lithology	2	2	2	2
Alteration	5d	5b	5b	5b
		Non-clays		
Quartz	31.5	30.7	46.8	49.8
Potassium Feldspar				
Albite				
Plagioclase				
Amphibole				
Biotite				
Pyroxene				
Titanite		0.0	0.0	
Magnetite	0.5	0.4	0.0	0.6
Anatase	0.0			0.1
Rutile	1.6	1.3	1.2	1.3
Calcite				
Epidote				
Laumontite				
Svanbergite		0.8	1.0	
Hematite				
Maghemite				
Goethite				
Anhydrite				
Gypsum				
Jarosite				
Pyrite	7.3	9.2	17.1	12.6
		Clays		
Illite/Fine Muscovite	43.6	26.8	22.7	31.2
Smectite				
Kaolinite	8.9	20.3	11.3	4.5
Pyrophyllite				
Chlorite	6.6			
Total clays	**59.1**	**47.0**	**34.0**	**35.6**
Full pattern region degree of fit	0.1897	0.1181	0.1118	0.1046
Clay region degree of fit	0.0591	0.0896	0.0747	0.0859
Pre-normalization total	102.3	114.1	110.8	99.5

Table B2. Quantitative X-ray diffraction results from drill hole WP-1 in weight percent.—Continued

[All samples normalized to 100 percent. Pre-normalization totals are recorded in samples run with zincite standard, otherwise samples were run without an internal standard. See Appendix A for key to lithology and alteration codes. Lower values for degree of fit suggest more accurate analyses with values less than 0.1 considered ideal. Mineral percentages are blank where absent in the sample and therefore not analyzed]

Sample number	WP1-385	WP1-411	WP1-483	WP1-549
Lithology	2	8	8	3
Alteration	5b	5b	5d	5d
		Non-clays		
Quartz	36.0	71.2	41.5	35.6
Potassium Feldspar				
Albite				
Plagioclase				
Amphibole				
Biotite				
Pyroxene				
Titanite	0.4		0.4	0.0
Magnetite	0.9	0.5		0.1
Anatase	0.0	0.1	0.0	
Rutile	1.9	0.8	1.1	0.9
Calcite				
Epidote				
Laumontite				
Svanbergite				
Hematite			0.6	0.6
Maghemite			0.2	
Goethite				0.6
Anhydrite				
Gypsum				
Jarosite				0.4
Pyrite	19.5	6.0	12.9	7.3
		Clays		
Illite/Fine Muscovite	25.1	16.3	36.2	36.1
Smectite				
Kaolinite	16.3	5.0	6.5	3.2
Pyrophyllite				
Chlorite			0.6	15.2
Total clays	**41.4**	**21.3**	**43.3**	**54.5**
Full pattern region degree of fit	0.1077	0.1313	0.1079	0.0924
Clay region degree of fit	0.0713	0.0652	0.0664	0.0556
Pre-normalization total	101.6	112.3	107.0	104.4

Table B2. Quantitative X-ray diffraction results from drill hole WP-1 in weight percent.—Continued

[All samples normalized to 100 percent. Pre-normalization totals are recorded in samples run with zincite standard, otherwise samples were run without an internal standard. See Appendix A for key to lithology and alteration codes. Lower values for degree of fit suggest more accurate analyses with values less than 0.1 considered ideal. Mineral percentages are blank where absent in the sample and therefore not analyzed]

Sample number	WP1-629	WP1-647	WP1-700	WP1-708	WP1-856
Lithology	8	8	2	8	3
Alteration	5d	5d	5d	5d	4d
			Non-clays		
Quartz	46.3	39.1	49.4	45.9	35.9
Potassium Feldspar			0.1		1.0
Albite			0.7		18.9
Plagioclase					4.4
Amphibole					
Biotite					
Pyroxene					
Titanite	0.0	0.3			0.0
Magnetite	0.3	0.0	0.1	0.2	0.0
Anatase	0.0		0.1	0.0	
Rutile	1.1	1.0	1.1	1.2	0.2
Calcite					
Epidote					
Laumontite					
Svanbergite					
Hematite		0.4			
Maghemite					
Goethite		0.7	0.9	0.0	0.7
Anhydrite					
Gypsum					
Jarosite		0.8	0.9		0.7
Pyrite	2.7	8.1	4.3	2.5	2.4
			Clays		
Illite/Fine Muscovite	28.2	37.7	19.8	30.6	23.1
Smectite			2.0		1.9
Kaolinite	3.2	0.0	7.6	0.0	3.9
Pyrophyllite					
Chlorite	18.1	12.0	13.3	19.7	7.0
Total clays	**49.6**	**49.7**	**42.6**	**50.2**	**35.8**
Full pattern region degree of fit	0.1035	0.1874	0.0994	0.1642	0.0925
Clay region degree of fit	0.0796	0.0626	0.0538	0.0624	0.0602
Pre-normalization total	103.4	102.9	102.1	98.1	106.4

Table B2. Quantitative X-ray diffraction results from drill hole WP-1 in weight percent.—Continued

[All samples normalized to 100 percent. Pre-normalization totals are recorded in samples run with zincite standard, otherwise samples were run without an internal standard. See Appendix A for key to lithology and alteration codes. Lower values for degree of fit suggest more accurate analyses with values less than 0.1 considered ideal. Mineral percentages are blank where absent in the sample and therefore not analyzed]

Sample number	WP1-869	WP1-1100	WP1-1108	WP1-1173	WP1-1175
Lithology	2	1	1	1	1
Alteration	5d	1b	2	5	4a
		Non-clays			
Quartz	30.6	23.9	26.6	42.1	43.4
Potassium Feldspar	0.1	14.6	13.7	1.0	2.1
Albite	11.8	2.2	11.7		0.0
Plagioclase	6.7	20.8	4.9		0.0
Amphibole		0.2			
Biotite		5.1	3.4		
Pyroxene			0.7		
Titanite		0.7	0.0	0.0	
Magnetite	0.8	0.5	0.0	0.0	0.0
Anatase	0.1	0.0	0.0	0.0	0.0
Rutile	1.2	0.3	0.3	0.8	0.6
Calcite		0.6			0.3
Epidote					
Laumontite					
Svanbergite					
Hematite		0.3		0.4	0.3
Maghemite		3.7	1.0	3.4	2.9
Goethite	1.7	0.2	0.6	0.5	1.6
Anhydrite					
Gypsum					
Jarosite	0.7	0.5	0.2	1.0	2.1
Pyrite	2.3	1.7	1.9	13.5	5.4
		Clays			
Illite/Fine Muscovite	25.5	10.7	14.8	35.8	28.9
Smectite	7.1	1.7	5.3		
Kaolinite	2.0	4.2	8.9	1.4	3.0
Pyrophyllite					
Chlorite	9.3	8.2	6.1		9.5
Total clays	**44.0**	**24.8**	**35.0**	**37.2**	**41.4**
Full pattern region degree of fit	0.1012	0.1054	0.0862	0.1350	0.1233
Clay region degree of fit	0.6065	0.0634	0.0609	0.0641	0.0946
Pre-normalization total	98.7	112.4	93.5	97.4	90.6

Table B2. Quantitative X-ray diffraction results from drill hole WP-1 in weight percent.—Continued

[All samples normalized to 100 percent. Pre-normalization totals are recorded in samples run with zincite standard, otherwise samples were run without an internal standard. See Appendix A for key to lithology and alteration codes. Lower values for degree of fit suggest more accurate analyses with values less than 0.1 considered ideal. Mineral percentages are blank where absent in the sample and therefore not analyzed]

Sample number	WP1-1225	WP1-1372	WP1-1496	WP1-1616	WP1-1627
Lithology	1	1	14	1	1
Alteration	1b	2	1b	2	4b
			Non-clays		
Quartz	23.3	31.8	16.3	34.0	35.4
Potassium Feldspar	8.7	16.8	0.0	3.3	3.0
Albite	12.4	7.5	24.1	0.3	
Plagioclase	17.4	5.7	7.2	0.7	
Amphibole	0.0	0.0		0.0	
Biotite	8.2	3.8	19.1	3.5	
Pyroxene					
Titanite	0.0	0.4	0.6	1.0	
Magnetite	0.1	0.0	0.5	0.0	0.3
Anatase		0.0			0.1
Rutile					1.8
Calcite	0.9	0.8	1.3	1.1	0.1
Epidote					
Laumontite	0.0	0.0		0.0	
Svanbergite					
Hematite					
Maghemite	0.5	0.0	0.5	0.5	
Goethite					
Anhydrite					
Gypsum					
Jarosite		0.0		0.0	
Pyrite	2.1	2.1	1.5	3.2	3.9
			Clays		
Illite/Fine Muscovite	9.5	17.8	13.4	29.2	15.4
Smectite	7.9	4.7	4.5	11.5	7.0
Kaolinite	3.3	4.8	5.8	8.4	19.1
Pyrophyllite					
Chlorite	5.7	3.8	5.1	3.4	13.8
Total clays	**26.4**	**31.1**	**28.8**	**52.5**	**55.3**
Full pattern region degree of fit	0.0884	0.0897	0.0988	0.1153	0.0941
Clay region degree of fit	0.0827	0.0870	0.0911	0.0942	0.0742
Pre-normalization total	102.5	91.6	99.1	97.0	92.9

Table B2. Quantitative X-ray diffraction results from drill hole WP-1 in weight percent.—Continued

[All samples normalized to 100 percent. Pre-normalization totals are recorded in samples run with zincite standard, otherwise samples were run without an internal standard. See Appendix A for key to lithology and alteration codes. Lower values for degree of fit suggest more accurate analyses with values less than 0.1 considered ideal. Mineral percentages are blank where absent in the sample and therefore not analyzed]

Sample number	WP1-1681	WP1-1725	WP1-1785
Lithology	1	1	1
Alteration	52b	52b	1b
		Non-clays	
Quartz	31.5	20.3	22.7
Potassium Feldspar	9.4	20.5	13.0
Albite	6.7	17.8	16.9
Plagioclase	6.1	3.6	16.1
Amphibole	0.0		0.0
Biotite	3.3	7.0	8.4
Pyroxene			
Titanite	0.3	0.0	0.5
Magnetite	0.9	0.0	1.1
Anatase			
Rutile			
Calcite	0.4	0.7	1.3
Epidote			
Laumontite	0.0	0.0	0.0
Svanbergite			
Hematite			
Maghemite	0.0	0.9	0.3
Goethite		0.1	
Anhydrite			
Gypsum			
Jarosite	0.0	0.0	0.0
Pyrite	1.5	3.7	2.1
Clays			
Illite/Fine Muscovite	20.7	16.2	6.8
Smectite	7.1	2.5	3.6
Kaolinite	7.0	5.7	2.6
Pyrophyllite			
Chlorite	5.1	1.0	4.5
Total clays	**39.9**	**25.4**	**17.5**
Full pattern region degree of fit	0.0883	0.0834	0.0965
Clay region degree of fit	0.0750	0.0870	0.0689
Pre-normalization total	98.6	101.2	98.9

Table B3. Quantitative X-ray diffraction results from drill hole WP-2 in weight percent.

[All samples normalized to 100 percent. Pre-normalization totals are recorded in samples run with zincite standard, otherwise samples were run without an internal standard. See Appendix A for key to lithology and alteration codes. Lower values for degree of fit suggest more accurate analyses with values less than 0.1 considered ideal. Mineral percentages are blank where absent in the sample and therefore not analyzed]

Sample number	WP2 31-41	WP2-51-61	WP2 151-61	WP2 251-261
Lithology	1	1	2	1
Alteration	5a	5	5	5
		Non-Clays		
Quartz	62.0	80.2	51.5	45.5
Potassium Feldspar		0.3		
Albite				
Plagioclase				
Amphibole				
Biotite				
Pyroxene				
Titanite		0.2		
Magnetite		0.0		
Anatase		0.0	0.1	
Rutile		0.4	0.5	0.6
Calcite				
Epidote				
Laumontite				
Svanbergite				
Hematite	0.2	0.0		
Maghemite		1.3		
Goethite		0.6		
Anhydrite				1.9
Gypsum				
Jarosite	0.3	0.2		0.0
Pyrite	3.7	4.7	9.9	7.7
		Clays		
Illite/Fine Muscovite	30.1	12.1	36.6	41.6
Smectite				
Kaolinite	3.7		1.4	1.7
Pyrophyllite				0.9
Chlorite				
Total clays	**33.8**	**12.1**	**37.9**	**44.3**
Full pattern region degree of fit	0.1094	0.0822	0.1328	0.1281
Clay region degree of fit	0.0880	0.0636	0.0752	0.0630
Pre-normalization total	103.9	106.8	105.5	105.4

Table B3. Quantitative X-ray diffraction results from drill hole WP-2 in weight percent.—Continued

[All samples normalized to 100 percent. Pre-normalization totals are recorded in samples run with zincite standard, otherwise samples were run without an internal standard. See Appendix A for key to lithology and alteration codes. Lower values for degree of fit suggest more accurate analyses with values less than 0.1 considered ideal. Mineral percentages are blank where absent in the sample and therefore not analyzed]

Sample number	WP2 351-61	WP2 381-91	WP2 451-61	WP2 481-91
Lithology	5	5	5	5
Alteration	5	5	5	5a
		Non-clays		
Quartz	49.9	50.2	57.3	47.7
Potassium Feldspar				1.3
Albite				
Plagioclase				
Amphibole				
Biotite				
Pyroxene				
Titanite				
Magnetite				
Anatase		0.0		0.0
Rutile	0.5	0.5	0.8	0.7
Calcite				
Epidote				
Laumontite				
Svanbergite				
Hematite				
Maghemite				
Goethite	0.5			
Anhydrite			2.0	1.1
Gypsum	0.5			
Jarosite	0.0		1.4	1.3
Pyrite	8.8	7.3	8.3	10.1
		Clays		
Illite/Fine Muscovite	38.9	40.4	29.1	33.8
Smectite				
Kaolinite	0.8	1.5	1.0	4.0
Pyrophyllite				
Chlorite				
Total clays	**39.7**	**41.9**	**30.0**	**37.8**
Full pattern region degree of fit	0.0871	0.1187	0.0933	0.1055
Clay region degree of fit	0.0687	0.0734	0.0628	0.0614
Pre-normalization total	100.3	103.4	101.2	98.4

Table B3. Quantitative X-ray diffraction results from drill hole WP-2 in weight percent.—Continued

[All samples normalized to 100 percent. Pre-normalization totals are recorded in samples run with zincite standard, otherwise samples were run without an internal standard. See Appendix A for key to lithology and alteration codes. Lower values for degree of fit suggest more accurate analyses with values less than 0.1 considered ideal. Mineral percentages are blank where absent in the sample and therefore not analyzed]

Sample number	WP2 551-561	WP2 611	WP2 651-661	WP2 746-56
Lithology	1	1	1	1
Alteration	5a	2b	2b	2a
		Non-clays		
Quartz	42.0	30.7	40.9	32.7
Potassium Feldspar		17.6	2.9	16.8
Albite			4.0	5.9
Plagioclase				10.7
Amphibole				
Biotite		1.5	2.1	2.1
Pyroxene				
Titanite				
Magnetite		0.7		0.6
Anatase				
Rutile	1.3	1.2	1.3	0.5
Calcite				
Epidote			0.9	1.1
Laumontite				
Svanbergite				
Hematite				
Maghemite				
Goethite				
Anhydrite	1.0			
Gypsum				
Jarosite	0.2			0.4
Pyrite	8.4	2.5	8.2	4.7
		Clays		
Illite/Fine Muscovite	42.7	5.0	27.6	15.3
Smectite		6.2		1.9
Kaolinite	4.4	22.9	5.2	1.3
Pyrophyllite				
Chlorite		11.8	6.8	5.8
Total clays	**47.0**	**45.8**	**39.6**	**24.4**
Full pattern region degree of fit	0.1177	0.0901	0.1016	0.0858
Clay region degree of fit	0.0623	0.0603	0.0748	0.0503
Pre-normalization total	103.0	101.0	105.2	92.4

Table B3. Quantitative X-ray diffraction results from drill hole WP-2 in weight percent.—Continued

[All samples normalized to 100 percent. Pre-normalization totals are recorded in samples run with zincite standard, otherwise samples were run without an internal standard. See Appendix A for key to lithology and alteration codes. Lower values for degree of fit suggest more accurate analyses with values less than 0.1 considered ideal. Mineral percentages are blank where absent in the sample and therefore not analyzed]

Sample number	WP2 842-56	WP2 946-56	WP2 1046-56
Lithology	1	1	1
Alteration	4a	4b	4a
		Non-clays	
Quartz	44.8	43.9	43.5
Potassium Feldspar	2.6	2.1	1.6
Albite	0.0		
Plagioclase			
Amphibole			
Biotite	0.0		
Pyroxene			
Titanite			
Magnetite			
Anatase			
Rutile	0.5	0.5	0.7
Calcite			
Epidote	0.8		
Laumontite			
Svanbergite			
Hematite			
Maghemite			
Goethite			
Anhydrite	0.3		
Gypsum			
Jarosite		0.5	0.3
Pyrite	6.2	16.3	9.9
		Clays	
Illite/Fine Muscovite	29.2	28.5	39.1
Smectite	2.0	3.3	2.6
Kaolinite	2.4	4.9	2.2
Pyrophyllite			
Chlorite	11.1		
Total clays	44.7	36.7	44.0
Full pattern region degree of fit	0.1495	0.1151	0.1525
Clay region degree of fit	0.0712	0.0561	0.0583
Pre-normalization total	99.1	98.7	101.3

Table B3. Quantitative X-ray diffraction results from drill hole WP-2 in weight percent.—Continued

[All samples normalized to 100 percent. Pre-normalization totals are recorded in samples run with zincite standard, otherwise samples were run without an internal standard. See Appendix A for key to lithology and alteration codes. Lower values for degree of fit suggest more accurate analyses with values less than 0.1 considered ideal. Mineral percentages are blank where absent in the sample and therefore not analyzed]

Sample number	WP2 1146-56	WP2 1246-56	WP2 1346-56	WP2 1446-56
Lithology	1	1	1	1
Alteration	2	2b	2b	2b
		Non-clays		
Quartz	31.1	37.0	36.8	34.0
Potassium Feldspar	10.3	3.2	7.7	7.4
Albite	10.6	5.8	5.8	6.5
Plagioclase	11.4	1.1	3.7	2.9
Amphibole				
Biotite	2.6	1.6	2.4	4.4
Pyroxene				
Titanite	0.0	0.0	0.0	0.0
Magnetite	0.0	0.0	0.0	0.0
Anatase	0.0	0.0	0.0	0.0
Rutile	0.3	0.5	0.5	0.6
Calcite	1.0	0.0	0.0	0.1
Epidote	0.7	0.0	0.0	0.3
Laumontite				
Svanbergite				
Hematite				
Maghemite	0.0	0.0	0.0	0.0
Goethite	0.0	0.1	0.2	0.4
Anhydrite				
Gypsum	0.0	0.2	0.0	0.2
Jarosite	0.3	0.3	0.3	0.3
Pyrite	4.5	9.3	3.3	5.0
		Clays		
Illite/Fine Muscovite	22.5	34.0	26.4	26.9
Smectite	2.0	2.5	3.2	3.0
Kaolinite		2.6	8.6	6.6
Pyrophyllite				
Chlorite	2.6	1.6	1.2	1.4
Total clays	**27.0**	**40.8**	**39.4**	**37.8**
Full pattern region degree of fit	0.1008	0.0899	0.1054	0.0819
Clay region degree of fit				
Pre-normalization total	102.3	105.1	103.0	103.7

Table B4. Quantitative X-ray diffraction results from drill hole WP-3 in weight percent.

[All samples normalized to 100 percent. Pre-normalization totals are recorded in samples run with zincite standard, otherwise samples were run without an internal standard. See Appendix A for key to lithology and alteration codes. Lower values for degree of fit suggest more accurate analyses with values less than 0.1 considered ideal. Mineral percentages are blank where absent in the sample and therefore not analyzed]

Sample number	WP3 0-10	WP3 30-40	WP3 54-64	WP3 74-84	WP3 94 -104
Lithology	8	8	8	8	4
Alteration	9	5	5	9	9
		Non-clays			
Quartz	65.3	50.2	50.3	61.8	60.3
Potassium Feldspar	2.8	2.3	1.0	1.6	1.9
Albite	0.0	0.0	0.0	0.0	
Plagioclase	0.0		0.0	0.0	
Amphibole	0.0		0.0	0.0	
Biotite					
Pyroxene					
Titanite					
Magnetite					
Anatase					
Rutile	0.5	1.2	1.3	0.8	0.8
Ankerite					
Calcite					
Siderite					
Epidote					
Laumontite					
Hematite					
Maghemite					
Goethite					
Alunite					
Anhydrite					
Gypsum					
Jarosite	5.1	8.8	5.6	6.8	9.3
Pyrite			0.0	0.0	0.5
Sphalerite					
		Clays			
Illite/Fine Muscovite	17.2	37.5	41.8	19.8	20.5
Smectite					
Kaolinite	0.0	0.0	0.0	0.0	
Pyrophyllite	9.1	0.0	0.0	9.2	6.6
Chlorite					
Total clays	**26.3**	**37.5**	**41.8**	**29.0**	**27.2**
Full pattern region degree of fit	0.1214	0.1977	0.1250	0.1394	0.1027
Clay region degree of fit	0.0932	0.1527	0.1172	0.1004	0.0712
Pre-normalization total	103.3	92.6	91.6	102.5	101.1

Table B4. Quantitative X-ray diffraction results from drill hole WP-3 in weight percent.—Continued

[All samples normalized to 100 percent. Pre-normalization totals are recorded in samples run with zincite standard, otherwise samples were run without an internal standard. See Appendix A for key to lithology and alteration codes. Lower values for degree of fit suggest more accurate analyses with values less than 0.1 considered ideal. Mineral percentages are blank where absent in the sample and therefore not analyzed]

Sample number	WP3 134-144	WP3 184-194	WP3 194-204	WP3 214-224
Lithology	4	4	4	4
Alteration	9	5	5	5a
		Non-clays		
Quartz	64.3	67.3	55.3	54.2
Potassium Feldspar	1.5	2.9	2.2	0.0
Albite	0.0	0.0	0.0	0.0
Plagioclase	0.0	0.0	0.0	0.0
Amphibole	0.0	0.0	0.0	0.0
Biotite				
Pyroxene				
Titanite				
Magnetite				
Anatase				0.0
Rutile	1.1	1.0	1.4	1.0
Ankerite				
Calcite				
Siderite				
Epidote				
Laumontite				
Hematite				
Maghemite				
Goethite				
Alunite				
Anhydrite				
Gypsum				
Jarosite	9.8	6.5	3.9	
Pyrite	0.0	1.5	4.9	7.9
Sphalerite				
		Clays		
Illite/Fine Muscovite	19.4	20.8	32.2	32.9
Smectite				
Kaolinite		0.0	0.0	3.9
Pyrophyllite	3.9		0.0	0.0
Chlorite				
Total clays	**23.3**	**20.8**	**32.2**	**36.8**
Full pattern region degree of fit	0.1065	0.1087	0.1216	0.1164
Clay region degree of fit	0.0830	0.0815	0.0774	0.1077
Pre-normalization total	94.3	96.1	95.1	99.9

Table B4. Quantitative X-ray diffraction results from drill hole WP-3 in weight percent.—Continued

[All samples normalized to 100 percent. Pre-normalization totals are recorded in samples run with zincite standard, otherwise samples were run without an internal standard. See Appendix A for key to lithology and alteration codes. Lower values for degree of fit suggest more accurate analyses with values less than 0.1 considered ideal. Mineral percentages are blank where absent in the sample and therefore not analyzed]

Sample number	WP3 314-324	WP3 334-344	WP3 384-95	WP3 464-74
Lithology	4	4	1	4
Alteration	5	5	5	5a
		Non-clays		
Quartz	51.0	59.7	47.7	54.4
Potassium Feldspar	0.0	0.0	0.0	
Albite	0.0	0.0	0.0	
Plagioclase		0.0	0.0	
Amphibole	0.0	0.0	0.0	
Biotite				
Pyroxene				
Titanite				
Magnetite				
Anatase	0.0	0.1	0.1	0.0
Rutile	1.0	0.9	0.9	0.9
Ankerite				
Calcite				
Siderite				
Epidote				
Laumontite	0.0			
Hematite				
Maghemite				
Goethite				
Alunite	0.7	0.8	1.0	0.7
Anhydrite				
Gypsum				
Jarosite		1.8	0.5	
Pyrite	9.9	7.9	12.9	10.6
Sphalerite				
		Clays		
Illite/Fine Muscovite	37.4	28.9	36.8	30.1
Smectite				
Kaolinite				3.3
Pyrophyllite				
Chlorite				
Total clays	**37.4**	**28.9**	**36.8**	**33.4**
Full pattern region degree of fit	0.1137	0.1004	0.0877	0.1026
Clay region degree of fit	0.1024	0.0783	0.0749	0.0750
Pre-normalization total	105.8	106.8	105.2	102.4

Table B4. Quantitative X-ray diffraction results from drill hole WP-3 in weight percent.—Continued

[All samples normalized to 100 percent. Pre-normalization totals are recorded in samples run with zincite standard, otherwise samples were run without an internal standard. See Appendix A for key to lithology and alteration codes. Lower values for degree of fit suggest more accurate analyses with values less than 0.1 considered ideal. Mineral percentages are blank where absent in the sample and therefore not analyzed]

Sample number	WP3 504-514	WP3 671-681	WP3 771-82	WP3 871-881
Lithology	4	4	4	4
Alteration	5a	5b	5b	5b
		Non-clays		
Quartz	55.0	47.7	42.2	44.5
Potassium Feldspar		0.0		
Albite		0.0		
Plagioclase		0.0		
Amphibole		0.0		
Biotite				
Pyroxene				
Titanite				
Magnetite				
Anatase	0.0	0.0	0.0	
Rutile	1.0	1.0	1.4	1.0
Ankerite				
Calcite				
Siderite				
Epidote				
Laumontite				
Hematite				
Maghemite				
Goethite				
Alunite	0.5	0.6		
Anhydrite				
Gypsum				
Jarosite		0.0		
Pyrite	11.6	11.4	14.4	8.0
Sphalerite				
		Clays		
Illite/Fine Muscovite	29.0	29.8	36.7	39.5
Smectite				
Kaolinite	2.8	9.5	5.4	7.0
Pyrophyllite	0.0	0.0	0.0	0.0
Chlorite				
Total clays	**31.8**	**39.3**	**42.0**	**46.5**
Full pattern region degree of fit	0.0960	0.0988	0.1948	0.1415
Clay region degree of fit	0.0721	0.0656	0.0715	0.0816
Pre-normalization total	101.4	102.5	97.7	102.7

Table B4. Quantitative X-ray diffraction results from drill hole WP-3 in weight percent.—Continued

[All samples normalized to 100 percent. Pre-normalization totals are recorded in samples run with zincite standard, otherwise samples were run without an internal standard. See Appendix A for key to lithology and alteration codes. Lower values for degree of fit suggest more accurate analyses with values less than 0.1 considered ideal. Mineral percentages are blank where absent in the sample and therefore not analyzed]

Sample number	WP3 911-22	WP3 931-42	WP3 971-982	WP3 999-1011
Lithology	2	2	2	7
Alteration	5b	5b	7	32
		Non-clays		
Quartz	44.8	47.3	12.1	8.0
Potassium Feldspar	0.0	0.0	0.0	0.0
Albite	0.0	0.0	0.0	0.0
Plagioclase	0.0	0.0	29.1	38.6
Amphibole	0.0	0.0	14.1	11.1
Biotite		0.0	3.2	4.8
Pyroxene				
Titanite		0.0	1.0	0.0
Magnetite		0.0	4.1	3.4
Anatase	0.0	0.2	0.0	0.0
Rutile	1.0	1.1	1.0	1.6
Ankerite				
Calcite				
Siderite				
Epidote		0.0	6.5	2.1
Laumontite				
Hematite				
Maghemite				
Goethite				
Alunite	0.0	0.0	0.0	0.0
Anhydrite				
Gypsum				
Jarosite	1.0	0.0	0.0	0.0
Pyrite	9.1	10.6	8.5	8.9
Sphalerite				
		Clays		
Illite/Fine Muscovite	34.4	25.2	0.0	4.6
Smectite		0.0	0.0	2.0
Kaolinite	9.6	15.6	0.0	0.0
Pyrophyllite	0.0	0.0	0.0	0.0
Chlorite		0.0	20.4	15.0
Total clays	**44.1**	**40.8**	**20.4**	**21.6**
Full pattern region degree of fit	0.1122	0.0952	0.1271	0.0949
Clay region degree of fit	0.0820	0.0670	0.0706	0.0657
Pre-normalization total	98.2	99.2	97.3	95.0

Table B4. Quantitative X-ray diffraction results from drill hole WP-3 in weight percent.—Continued

[All samples normalized to 100 percent. Pre-normalization totals are recorded in samples run with zincite standard, otherwise samples were run without an internal standard. See Appendix A for key to lithology and alteration codes. Lower values for degree of fit suggest more accurate analyses with values less than 0.1 considered ideal. Mineral percentages are blank where absent in the sample and therefore not analyzed]

Sample number	WP3 1031-1041	WP3 1091-1101	WP3 1111-1121	WP3 1181-1191
Lithology	6	8	7	7
Alteration	35	4a	33	31
		Non-clays		
Quartz	46.5	0.3	20.7	9.7
Potassium Feldspar	1.2		3.6	
Albite	0.0		0.0	
Plagioclase	0.0	0.9	0.6	33.6
Amphibole	0.0		8.3	28.5
Biotite	0.9	2.5	4.0	4.4
Pyroxene				
Titanite	0.0	0.8	0.1	
Magnetite	0.4	0.0	1.3	5.6
Anatase	0.0	0.0		
Rutile	0.7		0.2	0.9
Ankerite				
Calcite				
Siderite			7.3	
Epidote	0.0			
Laumontite				
Hematite		0.4	1.5	
Maghemite				
Goethite				
Alunite	0.0			
Anhydrite				
Gypsum				
Jarosite	0.0			
Pyrite	7.6	6.9	8.9	7.1
Sphalerite				
		Clays		
Illite/Fine Muscovite	20.5	26.5	8.2	
Smectite	0.0			
Kaolinite	3.1	4.1	17.9	
Pyrophyllite	0.0	54.7		
Chlorite	19.0	2.9	17.5	10.3
Total clays	**42.6**	**88.2**	**43.6**	**10.3**
Full pattern region degree of fit	0.0995	0.1161	0.0958	0.1313
Clay region degree of fit	0.0651	0.0623	0.0789	0.0974
Pre-normalization otal	101.3	107.0	96.6	100.4

Table B4. Quantitative X-ray diffraction results from drill hole WP-3 in weight percent.—Continued

[All samples normalized to 100 percent. Pre-normalization totals are recorded in samples run with zincite standard, otherwise samples were run without an internal standard. See Appendix A for key to lithology and alteration codes. Lower values for degree of fit suggest more accurate analyses with values less than 0.1 considered ideal. Mineral percentages are blank where absent in the sample and therefore not analyzed]

Sample number	WP3 1266-1275	WP3 1321-1330	WP3 1330-1340	WP3 1386-1396
Lithology	7	6	3	7
Alteration	8	35	5	8
		Non-clays		
Quartz	12.8	38.7	59.8	31.5
Potassium Feldspar				
Albite				
Plagioclase	26.1			5.6
Amphibole	27.5			1.1
Biotite	5.6	1.8		12.7
Pyroxene				
Titanite	0.0	0.5		0.0
Magnetite	4.6			2.4
Anatase	0.0	0.0	0.0	0.0
Rutile	0.2	0.3	0.1	0.0
Ankerite				
Calcite				
Siderite				
Epidote	0.0			
Laumontite				
Hematite	0.6	0.3	0.4	1.1
Maghemite				
Goethite		0.4		
Alunite				
Anhydrite				
Gypsum				
Jarosite				
Pyrite	6.8	11.6	6.0	11.2
Sphalerite				
		Clays		
Illite/Fine Muscovite	0.0	17.2	33.7	5.6
Smectite				
Kaolinite		7.0		
Pyrophyllite				
Chlorite	15.7	22.2		28.8
Total clays	**15.7**	**46.4**	**33.7**	**34.3**
Full pattern region degree of fit	0.1266	0.1038	0.0923	0.0861
Clay region degree of fit	0.0973	0.0585	0.0666	0.0576
Pre-normalization total	99.6	95.9	107.9	104.0

Table B4. Quantitative X-ray diffraction results from drill hole WP-3 in weight percent.—Continued

[All samples normalized to 100 percent. Pre-normalization totals are recorded in samples run with zincite standard, otherwise samples were run without an internal standard. See Appendix A for key to lithology and alteration codes. Lower values for degree of fit suggest more accurate analyses with values less than 0.1 considered ideal. Mineral percentages are blank where absent in the sample and therefore not analyzed]

Sample number	WP3 1494-1504	WP3 1544-1554	WP3 1594-1604	WP3 1614-1624
Lithology	6	7	3	6
Alteration	35	31	5	35
		Non-clays		
Quartz	39.4	16.0	57.5	38.3
Potassium Feldspar	0.0	0.5	0.8	
Albite	0.0	0.6		
Plagioclase	0.6	27.8	0.0	1.3
Amphibole		7.6		
Biotite	3.1	19.5		16.7
Pyroxene				
Titanite	0.6	0.4		0.2
Magnetite	0.0	2.0	0.2	0.5
Anatase	0.0		0.0	0.0
Rutile	0.0		0.5	1.0
Ankerite				
Calcite				
Siderite				
Epidote				
Laumontite				
Hematite	0.5			
Maghemite				
Goethite				
Alunite				
Anhydrite				
Gypsum				
Jarosite				0.8
Pyrite	14.6	11.3	7.4	13.9
Sphalerite				
		Clays		
Illite/Fine Muscovite	29.5	4.9	23.3	18.6
Smectite				
Kaolinite	0.0	0.8	4.4	5.8
Pyrophyllite				
Chlorite	18.0	8.5	5.9	2.9
Total clays	**47.5**	**14.2**	**33.6**	**27.3**
Full pattern region degree of fit	0.1832	0.1089	0.1006	0.1089
Clay region degree of fit	0.0601	0.0748	0.0744	0.0651
Pre-normalization total	102.7	97.4	94.7	96.9

Table B4. Quantitative X-ray diffraction results from drill hole WP-3 in weight percent.—Continued

[All samples normalized to 100 percent. Pre-normalization totals are recorded in samples run with zincite standard, otherwise samples were run without an internal standard. See Appendix A for key to lithology and alteration codes. Lower values for degree of fit suggest more accurate analyses with values less than 0.1 considered ideal. Mineral percentages are blank where absent in the sample and therefore not analyzed]

Sample number	WP3 1684-1694	WP3 1774-84	WP3 1834-1844	WP3 1864-1874
Lithology	6	7	6	3
Alteration	34	31	35	5
		Non-clays		
Quartz	40.6	13.4	43.0	51.9
Potassium Feldspar	21.0	0.4	0.8	0.0
Albite	0.0	0.9	0.0	
Plagioclase	0.0	23.9	1.9	0.0
Amphibole		26.3	0.5	
Biotite	5.1	6.2	7.7	
Pyroxene				
Titanite	0.2	0.0	0.0	
Magnetite	0.0	2.6	1.6	0.4
Anatase	0.0			0.1
Rutile	0.5		0.6	0.2
Ankerite				
Calcite				
Siderite				
Epidote				
Laumontite				
Hematite				
Maghemite				
Goethite				
Alunite				
Anhydrite				
Gypsum				
Jarosite				
Pyrite	8.2	6.4	9.7	9.9
Sphalerite				
		Clays		
Illite/Fine Muscovite	17.5	5.7	17.5	35.6
Smectite				
Kaolinite	0.0		8.4	1.9
Pyrophyllite				
Chlorite	7.0	14.3	8.3	
Total clays	**24.5**	**20.0**	**34.2**	**37.6**
Full pattern region degree of fit	0.0941	0.1309	0.0833	0.1668
Clay region degree of fit	0.0549	0.0969	0.0655	0.0959
Pre-normalization total	98.6	99.6	97.3	109.3

Table B4. Quantitative X-ray diffraction results from drill hole WP-3 in weight percent.—Continued

[All samples normalized to 100 percent. Pre-normalization totals are recorded in samples run with zincite standard, otherwise samples were run without an internal standard. See Appendix A for key to lithology and alteration codes. Lower values for degree of fit suggest more accurate analyses with values less than 0.1 considered ideal. Mineral percentages are blank where absent in the sample and therefore not analyzed]

Sample number	WP3 1904-1914	WP3 1941-1951	WP3 1954-64	WP3 1984-1994
Lithology	7	7	6	6
Alteration	31	31	35	35
		Non-clays		
Quartz	13.3	26.6	48.1	45.3
Potassium Feldspar		6.7		
Albite	0.7			
Plagioclase	29.2		1.9	6.6
Amphibole	19.4	4.7		
Biotite	9.8	3.3	7.4	
Pyroxene				
Titanite	0.0	2.0	0.5	
Magnetite	2.7	0.6	0.1	0.2
Anatase			0.0	
Rutile			0.1	0.3
Ankerite	0.0			
Calcite				
Siderite	0.1	2.2		
Epidote				
Laumontite				
Hematite				
Maghemite				
Goethite				
Alunite				
Anhydrite				
Gypsum	3.9	1.9		
Jarosite			0.3	0.6
Pyrite	12.5	13.7	11.0	10.1
Sphalerite				
		Clays		
Illite/Fine Muscovite	0.0	6.2	25.0	36.7
Smectite		4.9		
Kaolinite		11.3	5.7	0.2
Pyrophyllite				
Chlorite	8.5	15.9		
Total clays	**8.5**	**38.2**	**30.7**	**36.8**
Full pattern region degree of fit	0.1308	0.1039	0.0873	0.1607
Clay region degree of fit	0.0657	0.0593	0.0708	0.0625
Pre-normalization total	103.9	102.4	102.3	90.6

Table B4. Quantitative X-ray diffraction results from drill hole WP-3 in weight percent.—Continued

[All samples normalized to 100 percent. Pre-normalization totals are recorded in samples run with zincite standard, otherwise samples were run without an internal standard. See Appendix A for key to lithology and alteration codes. Lower values for degree of fit suggest more accurate analyses with values less than 0.1 considered ideal. Mineral percentages are blank where absent in the sample and therefore not analyzed]

Sample number	WP3 2084-2094	WP3 2164-74	WP3 2184-2194	WP3 2254-2264
Lithology	6	6	6	3
Alteration	35	35	34	5
		Non-clays		
Quartz	51.1	41.2	29.4	52.6
Potassium Feldspar			2.8	0.4
Albite	0.0		1.8	
Plagioclase	1.9	2.8	30.4	0.3
Amphibole	1.5		6.5	
Biotite	12.3	11.0	14.9	
Pyroxene				
Titanite	0.4		0.0	
Magnetite	0.0	0.0	0.1	
Anatase		0.0		0.1
Rutile		0.5		0.5
Ankerite				
Calcite				
Siderite				
Epidote				
Laumontite				2.3
Hematite				
Maghemite				
Goethite				
Alunite				
Anhydrite				
Gypsum				
Jarosite				0.9
Pyrite	9.4	8.6	4.3	19.5
Sphalerite				
		Clays		
Illite/Fine Muscovite	23.4	22.4	5.8	21.4
Smectite				2.0
Kaolinite		7.1		
Pyrophyllite				
Chlorite		6.4	4.0	
Total clays	**23.4**	**36.0**	**9.9**	**23.4**
Full pattern region degree of fit	0.1001	0.1011	0.0929	0.1212
Clay region degree of fit	0.0775	0.0528	0.0584	0.0922
Pre-normalization total	96.5	106.4	96.5	102.1

Table B4. Quantitative X-ray diffraction results from drill hole WP-3 in weight percent.—Continued

[All samples normalized to 100 percent. Pre-normalization totals are recorded in samples run with zincite standard, otherwise samples were run without an internal standard. See Appendix A for key to lithology and alteration codes. Lower values for degree of fit suggest more accurate analyses with values less than 0.1 considered ideal. Mineral percentages are blank where absent in the sample and therefore not analyzed]

Sample number	WP3 2284-2294	WP3 2414-2424	WP3 2434-2444	WP3 2474-2484
Lithology	3	6	6	3
Alteration	4a	35	35	4
		Non-clays		
Quartz	58.0	35.5	26.3	60.2
Potassium Feldspar	1.2		0.0	0.0
Albite		3.1	3.4	
Plagioclase	1.3	13.8	24.9	5.0
Amphibole		1.1		
Biotite		4.3	20.6	
Pyroxene				
Titanite		0.0	0.0	
Magnetite	0.0	0.5	0.7	0.2
Anatase	0.0			0.0
Rutile	0.2			0.2
Ankerite		0.1	0.0	
Calcite			0.0	
Siderite		0.8	0.6	
Epidote			1.8	
Laumontite				
Hematite				
Maghemite				
Goethite				
Alunite				
Anhydrite				
Gypsum		0.4	1.1	
Jarosite	0.0			0.0
Pyrite	6.5	8.8	8.9	5.0
Sphalerite				
		Clays		
Illite/Fine Muscovite	28.8	14.0	1.7	25.1
Smectite			5.6	2.1
Kaolinite	4.0	1.5	1.0	1.2
Pyrophyllite				
Chlorite		16.0	3.5	0.9
Total clays	**32.8**	**31.5**	**11.8**	**29.3**
Full pattern region degree of fit	0.0906	0.1047	0.1117	0.1265
Clay region degree of fit	0.0667	0.0572	0.0633	0.0592
Pre-normalization total	95.6	97.3	101.0	103.7

Table B4. Quantitative X-ray diffraction results from drill hole WP-3 in weight percent.—Continued

[All samples normalized to 100 percent. Pre-normalization totals are recorded in samples run with zincite standard, otherwise samples were run without an internal standard. See Appendix A for key to lithology and alteration codes. Lower values for degree of fit suggest more accurate analyses with values less than 0.1 considered ideal. Mineral percentages are blank where absent in the sample and therefore not analyzed]

Sample number	WP3 2514-2524	WP3 2554-2564	WP3 2584-2594	WP3 2624-2634
Lithology	6	6	3	6
Alteration	35	35	5	35
		Non-clays		
Quartz	37.3	21.5	63.2	48.0
Potassium Feldspar	0.2	0.0	0.3	2.9
Albite	8.8	3.2	0.0	
Plagioclase	7.1	18.5	1.8	8.0
Amphibole	1.8	4.0		0.3
Biotite	7.0	22.2	1.4	7.3
Pyroxene				
Titanite	0.2	0.0		0.0
Magnetite	0.2	0.8	0.1	0.1
Anatase				
Rutile				
Ankerite	0.0	0.5		
Calcite	0.6	1.0		0.0
Siderite	0.0	0.0		
Epidote				
Laumontite				
Hematite				
Maghemite				
Goethite				
Alunite				
Anhydrite				
Gypsum	2.9	1.2	1.0	0.5
Jarosite				
Pyrite	6.5	7.6	8.8	7.0
Sphalerite				
		Clays		
Illite/Fine Muscovite	13.3	5.0	17.6	24.9
Smectite			2.5	
Kaolinite	0.0	0.0	2.3	1.0
Pyrophyllite				
Chlorite	14.0	14.4	1.1	
Total clays	**27.3**	**19.4**	**23.4**	**25.9**
Full pattern region degree of fit	0.1156	0.0870	0.0975	0.1058
Clay region degree of fit	0.0537	0.0598	0.0580	0.0766
Pre-normalization total	102.7	93.1	92.9	100.6

Table B4. Quantitative X-ray diffraction results from drill hole WP-3 in weight percent.—Continued

[All samples normalized to 100 percent. Pre-normalization totals are recorded in samples run with zincite standard, otherwise samples were run without an internal standard. See Appendix A for key to lithology and alteration codes. Lower values for degree of fit suggest more accurate analyses with values less than 0.1 considered ideal. Mineral percentages are blank where absent in the sample and therefore not analyzed]

Sample number	WP3 2644-2654	WP3 2674-2684	WP3 2754-2764
Lithology	6	3	3
Alteration	35	2	2
		Non-clays	
Quartz	32.1	39.4	38.9
Potassium Feldspar	9.7	10.3	7.8
Albite	3.1	6.4	3.9
Plagioclase	8.4	5.6	8.7
Amphibole			
Biotite	12.3	9.8	9.5
Pyroxene			
Titanite			0.4
Magnetite	0.0	0.0	0.1
Anatase		0.0	
Rutile		0.0	0.2
Ankerite	0.1		
Calcite	0.6		0.4
Siderite	0.0		
Epidote			
Laumontite			
Hematite			
Maghemite			
Goethite			
Alunite			
Anhydrite	0.3		0.5
Gypsum	2.4		0.7
Jarosite		0.0	0.2
Pyrite	8.4	8.0	7.6
Sphalerite			
		Clays	
Illite/Fine Muscovite	17.1	20.5	15.1
Smectite	1.8		
Kaolinite	3.6		1.8
Pyrophyllite			
Chlorite			4.3
Total clays	**22.6**	**20.5**	**21.2**
Full pattern region degree of fit	0.1152	0.1060	0.0869
Clay region degree of fit	0.0550	0.0485	0.0461
Pre-normalization total	98.7	101.8	105.6

Table B4. Quantitative X-ray diffraction results from drill hole WP-3 in weight percent.—Continued

[All samples normalized to 100 percent. Pre-normalization totals are recorded in samples run with zincite standard, otherwise samples were run without an internal standard. See Appendix A for key to lithology and alteration codes. Lower values for degree of fit suggest more accurate analyses with values less than 0.1 considered ideal. Mineral percentages are blank where absent in the sample and therefore not analyzed]

Sample number	WP3 2774-2784	WP3 2814-2824	WP3 2834-2844	WP3 2864-2874
Lithology	6	3	3	3
Alteration	34	4	4	4
		Non-clays		
Quartz	36.5	57.6	49.7	54.4
Potassium Feldspar	0.5	11.8	13.2	7.1
Albite		0.0	6.9	1.6
Plagioclase	14.7	0.0	1.7	3.3
Amphibole				0.4
Biotite	17.8	1.9	2.9	3.4
Pyroxene				
Titanite	0.0	1.6	0.5	0.3
Magnetite	0.1	0.0	0.1	0.0
Anatase				
Rutile				0.3
Ankerite	0.3			
Calcite		0.0		0.2
Siderite	0.0			0.9
Epidote				
Laumontite				
Hematite				
Maghemite				
Goethite				
Alunite				
Anhydrite	0.0	0.8		0.0
Gypsum		1.0	2.0	2.3
Jarosite		0.0		0.0
Pyrite	8.5	7.7	6.9	6.8
Sphalerite				0.9
		Clays		
Illite/Fine Muscovite	16.6	15.6	15.1	17.5
Smectite	2.2	0.2		
Kaolinite	1.1	1.9	0.9	0.6
Pyrophyllite				
Chlorite	1.7			
Total clays	**21.6**	**17.7**	**16.0**	**18.1**
Full pattern region degree of fit	0.1020	0.1414	0.0965	0.1070
Clay region degree of fit	0.0613	0.0708	0.0560	0.0516
Pre-normalization total	94.1	111.0	93.3	107.8

Table B4. Quantitative X-ray diffraction results from drill hole WP-3 in weight percent.—Continued

[All samples normalized to 100 percent. Pre-normalization totals are recorded in samples run with zincite standard, otherwise samples were run without an internal standard. See Appendix A for key to lithology and alteration codes. Lower values for degree of fit suggest more accurate analyses with values less than 0.1 considered ideal. Mineral percentages are blank where absent in the sample and therefore not analyzed]

Sample number	WP3 2894-2904	WP3 2924-2934	WP3 2944-2954	WP3 3024-3034
Lithology	1	6	6	3
Alteration	4	34	34	4
		Non-clays		
Quartz	41.2	39.6	36.9	50.7
Potassium Feldspar	3.0	18.1	2.8	11.9
Albite	1.8		10.5	7.2
Plagioclase	8.2	10.1	7.5	2.2
Amphibole			2.3	
Biotite	6.3	4.9	6.8	3.8
Pyroxene				
Titanite		1.1	0.0	0.4
Magnetite	0.2	0.1	0.9	
Anatase		0.0		
Rutile		0.0		0.0
Ankerite	0.0			
Calcite	1.1	0.0	1.0	
Siderite	0.0		0.0	
Epidote				
Laumontite				
Hematite				
Maghemite				
Goethite				
Alunite				
Anhydrite	1.0	0.4		0.6
Gypsum	3.8	3.3	0.3	
Jarosite		0.0		
Pyrite	10.9	6.4	7.7	3.7
Sphalerite				
		Clays		
Illite/Fine Muscovite	21.1	15.4	8.0	16.3
Smectite				
Kaolinite	1.4	0.6	0.0	0.0
Pyrophyllite				
Chlorite			15.3	3.3
Total clays	**22.5**	**16.0**	**23.2**	**19.6**
Full pattern region degree of fit	0.1078	0.1509	0.0819	0.1079
Clay region degree of fit	0.0614	0.0515	0.0524	0.0542
Pre-normalization total	96.0	99.8	101.8	110.0

Table B4. Quantitative X-ray diffraction results from drill hole WP-3 in weight percent.—Continued

[All samples normalized to 100 percent. Pre-normalization totals are recorded in samples run with zincite standard, otherwise samples were run without an internal standard. See Appendix A for key to lithology and alteration codes. Lower values for degree of fit suggest more accurate analyses with values less than 0.1 considered ideal. Mineral percentages are blank where absent in the sample and therefore not analyzed]

Sample number	WP3 3174-3184	WP3 3224-3234	WP3 3254-3264	WP3 3344-3354
Lithology	6	6	6	6
Alteration	34	34	34	34
		Non-clays		
Quartz	38.2	35.3	42.3	35.4
Potassium Feldspar	9.8	13.0	9.8	1.7
Albite	7.4	4.1	5.9	4.3
Plagioclase	14.6	18.8	12.7	19.2
Amphibole				
Biotite	12.3	8.8	10.7	11.9
Pyroxene				
Titanite			0.0	
Magnetite	0.0	0.0		0.8
Anatase			0.0	
Rutile			0.0	
Ankerite	0.1	0.2		0.0
Calcite				
Siderite	0.0			0.3
Epidote				
Laumontite				
Hematite				
Maghemite				
Goethite				
Alunite				
Anhydrite				
Gypsum				
Jarosite				
Pyrite	5.7	8.3	5.7	6.4
Sphalerite				
		Clays		
Illite/Fine Muscovite	8.9	10.1	8.8	11.9
Smectite		0.0		
Kaolinite	2.5		1.4	5.1
Pyrophyllite				
Chlorite	0.5	1.5	2.8	3.0
Total clays	**11.9**	**11.5**	**13.0**	**19.9**
Full pattern region degree of fit	0.1002	0.1023	0.0822	0.1147
Clay region degree of fit	0.0553	0.0581	0.0572	0.0498
Pre-normalization total	102.2	96.4	102.3	96.9

Table B4. Quantitative X-ray diffraction results from drill hole WP-3 in weight percent.—Continued

[All samples normalized to 100 percent. Pre-normalization totals are recorded in samples run with zincite standard, otherwise samples were run without an internal standard. See Appendix A for key to lithology and alteration codes. Lower values for degree of fit suggest more accurate analyses with values less than 0.1 considered ideal. Mineral percentages are blank where absent in the sample and therefore not analyzed]

Sample number	WP3 3384-3394	WP3 3414-3424	WP3 3424-3434	WP3 3444-3454
Lithology	6	3	3	6
Alteration	34	4	4	34
		Non-clays		
Quartz	27.6	64.7	58.7	29.0
Potassium Feldspar	8.6	14.9	17.5	3.1
Albite	2.8	0.6	1.3	7.6
Plagioclase	31.9	0.0	0.3	17.4
Amphibole				
Biotite	12.1		0.0	10.6
Pyroxene				
Titanite				
Magnetite	0.7	0.0	0.0	0.7
Anatase	0.0	0.0	0.0	0.0
Rutile	0.0	0.2	0.2	0.7
Ankerite	0.1			
Calcite		0.1	0.3	3.9
Siderite	0.4		0.0	0.0
Epidote				
Laumontite				
Hematite		0.0	0.0	0.0
Maghemite		0.0	0.0	0.7
Goethite		0.0	0.0	0.0
Alunite				
Anhydrite				
Gypsum				
Jarosite				
Pyrite	4.0	1.1	1.6	1.9
Sphalerite				
		Clays		
Illite/Fine Muscovite	4.3	18.4	19.2	17.4
Smectite				
Kaolinite	2.8		0.9	2.1
Pyrophyllite				
Chlorite	4.9		0.0	4.8
Total clays	**12.0**	**18.4**	**20.1**	**24.4**
Full pattern region degree of fit	0.0828	0.1259	0.1097	0.1019
Clay region degree of fit	0.0425			
Pre-normalization total	100.1	100.0	100.0	100.0

Table B4. Quantitative X-ray diffraction results from drill hole WP-3 in weight percent.—Continued

[All samples normalized to 100 percent. Pre-normalization totals are recorded in samples run with zincite standard, otherwise samples were run without an internal standard. See Appendix A for key to lithology and alteration codes. Lower values for degree of fit suggest more accurate analyses with values less than 0.1 considered ideal. Mineral percentages are blank where absent in the sample and therefore not analyzed]

Sample number	WP3 3464-3474	WP3 3474-3484	WP3 3494-3501
Lithology	6	3	3
Alteration	34	4	4
		Non-clays	
Quartz	38.1	45.3	42.2
Potassium Feldspar	4.8	16.9	26.8
Albite	5.5	5.9	2.8
Plagioclase	11.9	4.5	0.0
Amphibole			
Biotite	7.3	0.1	0.2
Pyroxene			
Titanite			
Magnetite	0.5	0.3	0.2
Anatase	0.0	0.0	0.0
Rutile	0.6	0.9	0.5
Ankerite			
Calcite	3.3	2.6	1.5
Siderite	0.0	0.0	0.0
Epidote			
Laumontite			
Hematite	0.0	0.0	0.0
Maghemite	0.5	0.4	0.5
Goethite	0.0	0.0	0.0
Alunite			
Anhydrite			
Gypsum			
Jarosite			
Pyrite	2.6	5.1	4.0
Sphalerite			
		Clays	
Illite/Fine Muscovite	20.1	16.8	18.2
Smectite			
Kaolinite	1.4	1.2	3.0
Pyrophyllite			
Chlorite	3.7	0.0	0.0
Total clays	**25.2**	**18.0**	**21.3**
Full pattern region degree of fit	0.1081	0.1279	0.1371
Clay region degree of fit			
Pre-normalization total	100.0	100.0	100.0

Table B5. Quantitative X-ray diffraction results from drill hole WP-4 in weight percent.

[All samples normalized to 100 percent. Pre-normalization totals are recorded in samples run with zincite standard, otherwise samples were run without an internal standard. See Appendix A for key to lithology and alteration codes. Lower values for degree of fit suggest more accurate analyses with values less than 0.1 considered ideal. Mineral percentages are blank where absent in the sample and therefore not analyzed]

Sample number	WP4 90-100	WP4 100-110	WP4 120-130	WP4 130-140
Lithology	1	1	2	2
Alteration	5	5	5	5a
		Non-clays		
Quartz	57.8	52.0	49.4	49.0
Potassium Feldspar				
Albite				
Plagioclase				
Amphibole				
Biotite				
Pyroxene				
Titanite	1.2	0.4		
Magnetite				
Anatase	0.0	0.0		
Rutile	0.7	0.7		0.8
Calcite				
Laumontite				
Hematite	0.0	0.0		
Maghemite				
Goethite	1.3	1.6		
Anhydrite				
Gypsum				
Jarosite	2.9	5.2	1.4	1.1
Pyrite	0.3	0.3	4.2	6.1
		Clays		
Illite/Fine Muscovite	35.0	35.9	43.6	38.6
Smectite				
Kaolinite	0.8	3.8	1.4	4.3
Pyrophyllite				
Chlorite				
Total clays	**35.8**	**39.7**	**45.0**	**42.9**
Full pattern region degree of fit	0.1085	0.0965	0.0961	0.1188
Clay region degree of fit	0.0731	0.0783	0.0812	0.0691
Pre-normalization total	98.6	106.1	101.8	102.2

Table B5. Quantitative X-ray diffraction results from drill hole WP-4 in weight percent.—Continued

[All samples normalized to 100 percent. Pre-normalization totals are recorded in samples run with zincite standard, otherwise samples were run without an internal standard. See Appendix A for key to lithology and alteration codes. Lower values for degree of fit suggest more accurate analyses with values less than 0.1 considered ideal. Mineral percentages are blank where absent in the sample and therefore not analyzed]

Sample number	WP4 160-170	WP4 200-210	WP4 210-220	WP4 230-240
Lithology	1	1	1	1
Alteration	5a	5	5	4a
		Non-clays		
Quartz	46.8	49.5	46.7	40.2
Potassium Feldspar				4.2
Albite				3.6
Plagioclase				
Amphibole				
Biotite				
Pyroxene				
Titanite				
Magnetite				
Anatase				
Rutile	0.7	0.8	0.8	1.4
Calcite				
Laumontite				
Hematite				
Maghemite				
Goethite				
Anhydrite				
Gypsum				
Jarosite	0.9	0.3	0.4	0.6
Pyrite	11.5	11.7	11.0	8.8
		Clays		
Illite/Fine Muscovite	35.7	35.4	38.0	20.9
Smectite				
Kaolinite	4.5	1.1	1.1	3.4
Pyrophyllite				
Chlorite		1.0	2.0	16.8
Total clays	**40.1**	**37.6**	**41.1**	**41.2**
Full Pattern region degree of fit	0.1169	0.1072	0.1172	0.0992
Clay region degree of fit	0.0647	0.0547	0.0647	0.0667
Pre-normalization total	97.8	95.9	101.6	96.4

Table B5. Quantitative X-ray diffraction results from drill hole WP-4 in weight percent.—Continued

[All samples normalized to 100 percent. Pre-normalization totals are recorded in samples run with zincite standard, otherwise samples were run without an internal standard. See Appendix A for key to lithology and alteration codes. Lower values for degree of fit suggest more accurate analyses with values less than 0.1 considered ideal. Mineral percentages are blank where absent in the sample and therefore not analyzed]

Sample number	WP4 280-290	WP4 320-330	WP4 350-360	WP4 380-390
Lithology	1	1	1	1
Alteration	5a	5a	5a	5a
		Non-clays		
Quartz	51.6	45.1	50.3	50.6
Potassium Feldspar				
Albite				
Plagioclase				
Amphibole				
Biotite				
Pyroxene				
Titanite				
Magnetite	0.0	0.0	0.0	0.0
Anatase				
Rutile	0.5	0.8	0.7	1.0
Calcite				
Laumontite				
Hematite				
Maghemite				
Goethite				
Anhydrite				
Gypsum	0.9			
Jarosite	0.0	0.0	0.0	0.7
Pyrite	8.8	10.0	9.3	9.3
		Clays		
Illite/Fine Muscovite	34.4	37.0	37.4	34.4
Smectite				
Kaolinite	2.5	5.8	2.3	4.0
Pyrophyllite				
Chlorite	1.2	1.4		
Total clays	**38.2**	**44.1**	**39.7**	**38.4**
Full pattern region degree of fit	0.1331	0.1220	0.1301	0.1070
Clay region degree of fit	0.0602	0.0625	0.0677	0.0778
Pre-normalization total	102.3	103.5	104.7	97.0

Table B5. Quantitative X-ray diffraction results from drill hole WP-4 in weight percent.—Continued

[All samples normalized to 100 percent. Pre-normalization totals are recorded in samples run with zincite standard, otherwise samples were run without an internal standard. See Appendix A for key to lithology and alteration codes. Lower values for degree of fit suggest more accurate analyses with values less than 0.1 considered ideal. Mineral percentages are blank where absent in the sample and therefore not analyzed]

Sample number	WP4 418-427	WP4 445-454	WP4 462-471	WP4 488-497
Lithology	1	1	1	1
Alteration	5b	5b	5b	5b
		Non-clays		
Quartz	46.5	53.5	45.2	50.5
Potassium Feldspar		0.1		
Albite				
Plagioclase				
Amphibole				
Biotite				
Pyroxene				
Titanite				
Magnetite	0.0	0.2	0.0	0.0
Anatase				
Rutile	1.0	0.7	1.1	0.9
Calcite				
Laumontite				
Hematite				
Maghemite				
Goethite				
Anhydrite				
Gypsum				
Jarosite	0.0	2.6	0.0	0.0
Pyrite	8.3	7.5	7.8	7.7
		Clays		
Illite/Fine Muscovite	37.8	34.3	33.5	31.7
Smectite				
Kaolinite	5.3	1.1	10.6	9.2
Pyrophyllite				
Chlorite	1.0		1.8	
Total clays	**44.1**	**35.4**	**45.9**	**40.9**
Full pattern region degree of fit	0.1030	0.1339	0.0957	0.0978
Clay region degree of fit	0.0747	0.0764	0.0706	0.0616
Pre-normalization total	101.3	99.9	97.9	97.0

Table B5. Quantitative X-ray diffraction results from drill hole WP-4 in weight percent.—Continued

[All samples normalized to 100 percent. Pre-normalization totals are recorded in samples run with zincite standard, otherwise samples were run without an internal standard. See Appendix A for key to lithology and alteration codes. Lower values for degree of fit suggest more accurate analyses with values less than 0.1 considered ideal. Mineral percentages are blank where absent in the sample and therefore not analyzed]

Sample number	WP4 506-515	WP4 534-543	WP4 588-597	WP4 597-606
Lithology	1	1	1	1
Alteration	5b	5b	5	5b
		Non-clays		
Quartz	50.3	45.7	45.9	45.8
Potassium Feldspar			0.2	1.3
Albite				
Plagioclase				
Amphibole				
Biotite				
Pyroxene				
Titanite			0.8	0.7
Magnetite	0.0	0.1	0.0	0.0
Anatase			0.0	0.0
Rutile	0.8	0.9	0.5	0.8
Calcite				
Laumontite				
Hematite			0.0	
Maghemite			3.1	
Goethite			0.4	1.0
Anhydrite				
Gypsum				
Jarosite	0.0	0.1	0.3	0.7
Pyrite	7.6	10.4	12.4	9.1
		Clays		
Illite/Fine Muscovite	32.7	34.7	35.0	32.7
Smectite				
Kaolinite	8.6	8.2	1.4	7.9
Pyrophyllite				
Chlorite				
Total clays	**41.3**	**42.9**	**36.4**	**40.6**
Full pattern region degree of fit	0.1007	0.1021	0.1066	0.1193
Clay region degree of fit	0.0612	0.0651	0.0687	0.0645
Pre-normalization total	98.3	96.0	101.0	95.6

Table B5. Quantitative X-ray diffraction results from drill hole WP-4 in weight percent.—Continued

[All samples normalized to 100 percent. Pre-normalization totals are recorded in samples run with zincite standard, otherwise samples were run without an internal standard. See Appendix A for key to lithology and alteration codes. Lower values for degree of fit suggest more accurate analyses with values less than 0.1 considered ideal. Mineral percentages are blank where absent in the sample and therefore not analyzed]

Sample number	WP4 624-633	WP4 689-699	WP4 765-775	WP4 838-849
Lithology	1	1	1	1
Alteration	5b	5b	5b	5a
		Non-clays		
Quartz	45.5	44.8	44.1	47.7
Potassium Feldspar			0.0	1.0
Albite				
Plagioclase				
Amphibole				
Biotite				
Pyroxene				
Titanite	0.3	0.4	1.0	0.8
Magnetite	0.0	0.2	0.0	0.0
Anatase	0.0	0.1	0.0	0.0
Rutile	0.9	1.1	0.6	0.9
Calcite				
Laumontite				
Hematite			0.0	
Maghemite			3.0	
Goethite	0.8	1.2	0.2	0.4
Anhydrite				
Gypsum				
Jarosite	0.1	0.6	0.0	0.4
Pyrite	9.0	14.3	10.1	11.8
		Clays		
Illite/Fine Muscovite	31.4	32.4	36.3	34.6
Smectite				
Kaolinite	12.1	5.0	4.6	2.3
Pyrophyllite				
Chlorite				
Total clays	**43.4**	**37.4**	**40.9**	**36.8**
Full pattern region degree of fit	0.0976	0.0985	0.1461	0.1070
Clay region degree of fit	0.0837	0.0646	0.0804	0.0602
Pre-normalization total	93.8	96.8	107.0	91.9

Table B5. Quantitative X-ray diffraction results from drill hole WP-4 in weight percent.—Continued

[All samples normalized to 100 percent. Pre-normalization totals are recorded in samples run with zincite standard, otherwise samples were run without an internal standard. See Appendix A for key to lithology and alteration codes. Lower values for degree of fit suggest more accurate analyses with values less than 0.1 considered ideal. Mineral percentages are blank where absent in the sample and therefore not analyzed]

Sample number	WP4 882-893	WP4 924-936	WP4 947-59	WP4 970-981
Lithology	1	1	1	1
Alteration	5b	5b	4b	2b
		Non-clays		
Quartz	45.3	46.3	36.5	31.3
Potassium Feldspar		0.6	3.9	6.5
Albite			5.4	6.6
Plagioclase				
Amphibole				
Biotite			6.4	9.0
Pyroxene				
Titanite		0.8		
Magnetite	0.0	0.1	0.0	0.0
Anatase	0.0	0.0		
Rutile	1.0	0.8	0.3	0.1
Calcite				
Laumontite				
Hematite				
Maghemite			1.8	2.2
Goethite	0.1	0.2		
Anhydrite				
Gypsum				
Jarosite	0.6	0.3		
Pyrite	12.1	10.5	5.9	5.9
		Clays		
Illite/Fine Muscovite	31.8	32.1	29.9	25.6
Smectite				2.1
Kaolinite	9.1	8.4	6.1	8.9
Pyrophyllite				
Chlorite			3.8	1.8
Total clays	**40.9**	**40.4**	**39.9**	**38.4**
Full pattern region degree of fit	0.1166	0.0983	0.1017	0.1076
Clay region degree of fit	0.0735	0.0560	0.0757	0.0674
Pre-normalization total	99.0	98.0	101.4	98.7

Table B5. Quantitative X-ray diffraction results from drill hole WP-4 in weight percent.—Continued

[All samples normalized to 100 percent. Pre-normalization totals are recorded in samples run with zincite standard, otherwise samples were run without an internal standard. See Appendix A for key to lithology and alteration codes. Lower values for degree of fit suggest more accurate analyses with values less than 0.1 considered ideal. Mineral percentages are blank where absent in the sample and therefore not analyzed]

Sample number	WP4 992-1003	WP4 1048-1059	WP4 1059-1071	WP4 1093-1105
Lithology	1	1	1	1
Alteration	2b	2b	2a	2b
		Non-clays		
Quartz	35.5	34.6	28.2	29.7
Potassium Feldspar	7.1	8.4	13.1	9.9
Albite				0.0
Plagioclase	10.1	4.5	16.3	11.1
Amphibole				
Biotite	7.7	7.5	12.0	9.0
Pyroxene				
Titanite			0.1	
Magnetite	0.0	0.0	0.0	
Anatase			0.0	
Rutile	0.2	0.3	0.1	0.6
Calcite				
Laumontite				
Hematite			0.1	
Maghemite	1.8	1.7	2.0	
Goethite			1.0	
Anhydrite				
Gypsum				
Jarosite			0.3	
Pyrite	6.3	5.8	5.0	6.2
		Clays		
Illite/Fine Muscovite	23.6	21.0	14.9	21.1
Smectite		3.7		2.7
Kaolinite	7.7	10.7	4.5	8.2
Pyrophyllite				
Chlorite		1.9	2.4	1.4
Total clays	**31.3**	**37.3**	**21.7**	**33.5**
Full pattern region degree of fit	0.0738	0.0773	0.0834	0.1082
Clay region degree of fit	0.0652	0.0642	0.0515	0.0906
Pre-normalization total	99.4	103.7	96.7	105.7

Table B5. Quantitative X-ray diffraction results from drill hole WP-4 in weight percent.—Continued

[All samples normalized to 100 percent. Pre-normalization totals are recorded in samples run with zincite standard, otherwise samples were run without an internal standard. See Appendix A for key to lithology and alteration codes. Lower values for degree of fit suggest more accurate analyses with values less than 0.1 considered ideal. Mineral percentages are blank where absent in the sample and therefore not analyzed]

Sample number	WP4 1105-1116	WP4 1164-1174	WP4 1183-94	WP4 1206-19
Lithology	1	1	1	1
Alteration	4b	4b	2b	2b
		Non-clays		
Quartz	36.8	40.4	36.2	39.6
Potassium Feldspar	6.6	2.5	6.0	6.0
Albite	0.6	0.3	0.6	2.0
Plagioclase		2.1	5.4	1.4
Amphibole				
Biotite	7.3	5.3	11.3	9.8
Pyroxene				
Titanite				
Magnetite				
Anatase				
Rutile	0.6	1.0	0.4	1.3
Calcite				
Laumontite				
Hematite		0.6		
Maghemite				
Goethite				
Anhydrite				
Gypsum				
Jarosite		0.6		
Pyrite	6.0	7.2	8.2	6.3
		Clays		
Illite/Fine Muscovite	19.1	25.1	24.8	22.0
Smectite	2.1			
Kaolinite	20.2	14.9	7.2	9.4
Pyrophyllite				
Chlorite	0.7			2.2
Total clays	**42.1**	**40.0**	**32.0**	**33.6**
Full pattern region degree of fit	0.1188	0.1208	0.0951	0.1463
Clay region degree of fit	0.0894	0.0851	0.0648	0.0722
Pre-normalization total	99.9	97.9	91.5	94.2

Table B5. Quantitative X-ray diffraction results from drill hole WP-4 in weight percent.—Continued

[All samples normalized to 100 percent. Pre-normalization totals are recorded in samples run with zincite standard, otherwise samples were run without an internal standard. See Appendix A for key to lithology and alteration codes. Lower values for degree of fit suggest more accurate analyses with values less than 0.1 considered ideal. Mineral percentages are blank where absent in the sample and therefore not analyzed]

Sample number	WP4 1229-1240	WP4 1261-1272	WP4 1305-1315	WP4 1355-1365
Lithology	1	1	1	1
Alteration	4b	5b	5b	5
		Non-clays		
Quartz	42.0	48.6	47.9	51.1
Potassium Feldspar	2.6			1.7
Albite				
Plagioclase				
Amphibole				
Biotite				
Pyroxene				
Titanite				
Magnetite				
Anatase				
Rutile	0.9	0.7	0.9	0.9
Calcite				
Laumontite				
Hematite				
Maghemite				
Goethite				
Anhydrite				
Gypsum				
Jarosite		0.0	0.2	
Pyrite	7.1	8.3	9.3	9.5
		Clays		
Illite/Fine Muscovite	36.2	35.6	36.5	35.6
Smectite				
Kaolinite	11.1	6.7	5.1	1.3
Pyrophyllite				
Chlorite				
Total clays	**47.3**	**42.3**	**41.7**	**36.9**
Full pattern region degree of fit	0.0958	0.1392	0.1153	0.1054
Clay region degree of fit	0.0842	0.0807	0.0743	0.0640
Pre-normalization total	106.4	90.4	98.7	97.9

Table B5. Quantitative X-ray diffraction results from drill hole WP-4 in weight percent.—Continued

[All samples normalized to 100 percent. Pre-normalization totals are recorded in samples run with zincite standard, otherwise samples were run without an internal standard. See Appendix A for key to lithology and alteration codes. Lower values for degree of fit suggest more accurate analyses with values less than 0.1 considered ideal. Mineral percentages are blank where absent in the sample and therefore not analyzed]

Sample number	WP4 1385-95	WP4 1406-1418	WP4 1449-1459	WP4 1470-1482
Lithology	1	1	1	1
Alteration	5	5b	5b	4b
		Non-clays		
Quartz	50.5	46.6	49.2	41.0
Potassium Feldspar		1.0	0.7	3.2
Albite				0.0
Plagioclase				0.5
Amphibole				
Biotite				2.5
Pyroxene				
Titanite				
Magnetite				
Anatase				
Rutile	0.8	0.8	0.7	0.4
Calcite				
Laumontite				
Hematite				
Maghemite				
Goethite				
Anhydrite				
Gypsum				
Jarosite	0.6			
Pyrite	10.5	7.1	9.3	5.8
		Clays		
Illite/Fine Muscovite	34.2	32.6	34.0	27.1
Smectite				
Kaolinite	1.5	11.8	5.9	11.7
Pyrophyllite	2.0			
Chlorite				7.7
Total clays	**37.7**	**44.4**	**39.9**	**46.5**
Full pattern region degree of fit	0.0958	0.1373	0.0955	0.1064
Clay region degree of fit	0.0687	0.0897	0.0665	0.0742
Pre-normalization total	98.5	104.6	93.8	107.0

Table B5. Quantitative X-ray diffraction results from drill hole WP-4 in weight percent.—Continued

[All samples normalized to 100 percent. Pre-normalization totals are recorded in samples run with zincite standard, otherwise samples were run without an internal standard. See Appendix A for key to lithology and alteration codes. Lower values for degree of fit suggest more accurate analyses with values less than 0.1 considered ideal. Mineral percentages are blank where absent in the sample and therefore not analyzed]

Sample number	WP4 1513-1523	WP4 1532-1543	WP4 1555-1566	WP4 1596-1607
Lithology	1	1	1	1
Alteration	5b	5b	5b	5b
		Non-clays		
Quartz	40.7	45.5	46.3	49.3
Potassium Feldspar	1.7	0.7	0.8	0.6
Albite	0.0	0.0	0.6	
Plagioclase	0.7	0.3	0.4	0.7
Amphibole				
Biotite	3.7	2.0	3.0	0.0
Pyroxene				
Titanite				1.3
Magnetite				0.0
Anatase				0.0
Rutile	0.4	0.6	0.5	0.6
Calcite				
Laumontite				
Hematite				0.6
Maghemite				0.7
Goethite				0.0
Anhydrite				
Gypsum				
Jarosite				0.0
Pyrite	7.3	6.8	8.2	11.3
		Clays		
Illite/Fine Muscovite	22.6	25.1	28.1	30.3
Smectite				
Kaolinite	22.9	19.0	12.1	4.7
Pyrophyllite				
Chlorite				0.0
Total clays	**45.5**	**44.1**	**40.2**	**35.0**
Full pattern region degree of fit	0.1420	0.1273	0.0995	0.1278
Clay region degree of fit	0.0966	0.0817	0.0666	0.0602
Pre-normalization total	100.0	101.4	100.5	96.8

Table B5. Quantitative X-ray diffraction results from drill hole WP-4 in weight percent.—Continued

[All samples normalized to 100 percent. Pre-normalization totals are recorded in samples run with zincite standard, otherwise samples were run without an internal standard. See Appendix A for key to lithology and alteration codes. Lower values for degree of fit suggest more accurate analyses with values less than 0.1 considered ideal. Mineral percentages are blank where absent in the sample and therefore not analyzed]

Sample number	WP4 1628-1638	WP4 1661-1672
Lithology	1	1
Alteration	4b	2b
	Non-clays	
Quartz	39.9	31.1
Potassium Feldspar	1.9	7.4
Albite		
Plagioclase	0.1	14.9
Amphibole		
Biotite	7.4	9.4
Pyroxene		
Titanite	0.5	0.0
Magnetite	0.0	0.0
Anatase	0.0	0.0
Rutile	0.3	0.4
Calcite		
Laumontite		
Hematite	0.8	0.5
Maghemite	0.1	1.1
Goethite	0.7	0.5
Anhydrite		
Gypsum		
Jarosite	0.0	0.4
Pyrite	8.2	5.5
	Clays	
Illite/Fine Muscovite	28.7	15.4
Smectite	2.5	3.1
Kaolinite	3.3	7.7
Pyrophyllite		
Chlorite	5.5	2.6
Total clays	**40.1**	**28.8**
Full pattern region degree of fit	0.0910	0.0955
Clay region degree of fit	0.0643	0.0531
Pre-normalization total	98.8	100.5

Table B6. Quantitative X-ray diffraction results from drill hole HCBW1 in weight percent.

[All samples normalized to 100 percent. Pre-normalization totals are recorded in samples run with zincite standard, otherwise samples were run without an internal standard. See Appendix A for key to lithology and alteration codes. Lower values for degree of fit suggest more accurate analyses with values less than 0.1 considered ideal. Mineral percentages are blank where absent in the sample and therefore not analyzed]

Sample number	HCBW1 47	HCBW1 49	HCBW1 98
Lithology	7	7	7
Alteration	31	31	33
		Non-clays	
Quartz	0.0	2.5	16.1
Potassium Feldspar			
Plagioclase (Andesine)	32.5	35.5	1.6
Albite		0.3	
Amphibole	39.3	28.0	0.7
Biotite	8.6	7.6	3.4
Pyroxene			
Titanite	0.0	0.0	3.3
Magnetite	7.1	3.4	0.0
Apatite		0.3	
Anatase		0.0	
Rutile		0.5	
Calcite		0.0	1.4
Epidote	0.9	1.3	12.2
Garnet (andradite)			5.4
Sillimanite			0.2
Anhydrite		0.3	
Gypsum	0.6	0.0	
Hematite			
Maghemite		0.5	0.5
Goethite		0.3	
Jarosite			
Pyrite	2.0	6.1	8.5
		Clays	
Illite/Fine Muscovite		1.8	5.3
Smectite			31.8
Kaolinite		6.4	7.3
Pyrophyllite			
Chlorite	9.1	5.2	2.2
Total clays	**9.1**	**13.4**	**46.7**
Full pattern region degree of fit	0.1276	0.1265	0.1411
Clay region degree of fit	0.0593		0.1001
Pre-normalization total	109.8	99.3	99.9

Table B7. Quantitative X-ray diffraction results from drill hole HCBW3 in weight percent.

[All samples normalized to 100 percent. Pre-normalization totals are recorded in samples run with zincite standard, otherwise samples were run without an internal standard. See Appendix A for key to lithology and alteration codes. Lower values for degree of fit suggest more accurate analyses with values less than 0.1 considered ideal. Mineral percentages are blank where absent in the sample and therefore not analyzed]

Sample number	HCBW3 29.2	HCBW3 47	HCBW3 48-49	HCBW3 58
Lithology	12	11	11	11
Alteration	12	9	4b	4
		Non-clays		
Quartz	58.3	88.3	36.6	46.7
Potassium Feldspar	3.0	0.0	3.7	0.6
Albite		0.0		6.9
Plagioclase	0.7	0.0	1.6	1.3
Amphibole				0.3
Biotite				0.6
Pyroxene				
Titanite	0.0		0.0	0.0
Magnetite	0.0	0.0	0.0	0.0
Anatase	0.2	0.0	0.0	0.0
Rutile	0.2	0.0	0.0	0.2
Apatite	0.6		0.8	0.2
Calcite		0.0		0.0
Ankerite				
Siderite		0.1		
Epidote				0.2
Garnet				
Sillimanite				
Hematite	0.0	0.0	0.0	0.2
Maghemite	5.8	0.5	4.3	1.0
Goethite	3.8	0.0	0.8	0.2
Anhydrite				0.0
Gypsum				0.0
Jarosite		0.0		1.4
Pyrite	0.2	0.1	3.5	0.0
		Clays		
Illite/Fine Muscovite	27.4	2.6	24.6	33.7
Smectite				0.0
Kaolinite		0.2	24.1	0.8
Pyrophyllite		8.2		
Chlorite				5.6
Total clays	**27.4**	**11.0**	**48.7**	**40.0**
Full pattern region degree of fit	0.1111	0.2191	0.1219	0.0877
Clay region degree of fit				
Pre-normalization total	108.8	103.2	109.4	105.7

Table B7. Quantitative X-ray diffraction results from drill hole HCBW3 in weight percent.—Continued

[All samples normalized to 100 percent. Pre-normalization totals are recorded in samples run with zincite standard, otherwise samples were run without an internal standard. See Appendix A for key to lithology and alteration codes. Lower values for degree of fit suggest more accurate analyses with values less than 0.1 considered ideal. Mineral percentages are blank where absent in the sample and therefore not analyzed]

Sample number	HCBW3 65	HCBW3 67	HCBW3 74	HCBW3 79
Lithology	11	11	11	11
Alteration	4	4	2b	2a
		Non-clays		
Quartz	55.6	61.0	20.8	43.6
Potassium Feldspar	0.8	0.7	3.8	0.3
Albite	3.1	1.4		9.5
Plagioclase	0.5	0.5		15.0
Amphibole	0.1	0.4		0.4
Biotite	0.4	0.4	9.6	0.6
Pyroxene				
Titanite	0.0	0.0		0.0
Magnetite	0.4	0.0		0.5
Anatase	0.0	0.0		0.0
Rutile	0.3	0.2		0.1
Apatite	0.0	0.1	2.5	0.1
Calcite	0.0	0.1	0.2	0.2
Ankerite				
Siderite				
Epidote	0.0	0.0		0.1
Garnet			1.0	
Sillimanite				
Hematite	0.4	0.7	0.3	0.3
Maghemite	1.7	1.4	2.7	1.3
Goethite	0.2	0.1	1.2	0.0
Anhydrite	0.0	0.0		0.0
Gypsum	0.0	0.0	0.3	0.0
Jarosite	0.1	0.0		0.1
Pyrite	2.3	2.3	4.7	0.8
		Clays		
Illite/Fine Muscovite	32.1	29.0	22.7	17.6
Smectite	0.0	0.0	2.9	0.0
Kaolinite	0.4	0.4	19.7	2.5
Pyrophyllite				
Chlorite	1.7	1.3	7.5	7.1
Total clays	**34.3**	**30.8**	**52.8**	**27.2**
Full pattern region degree of fit	0.0999	0.0920	0.1183	0.0808
Clay region degree of fit				
Pre-normalization total	112.0	110.6	113.2	107.9

Table B7. Quantitative X-ray diffraction results from drill hole HCBW3 in weight percent.—Continued

[All samples normalized to 100 percent. Pre-normalization totals are recorded in samples run with zincite standard, otherwise samples were run without an internal standard. See Appendix A for key to lithology and alteration codes. Lower values for degree of fit suggest more accurate analyses with values less than 0.1 considered ideal. Mineral percentages are blank where absent in the sample and therefore not analyzed]

Sample number	HCBW3 125	HCBW3 134.7	HC3 157A	HC3 157B
Lithology	11	11	11	11
Alteration	5	5b	2	2a
		Non-clays		
Quartz	56.3	58.0	33.8	40.5
Potassium Feldspar			2.9	0.4
Albite			0.3	0.0
Plagioclase				
Amphibole				
Biotite			28.1	17.7
Pyroxene				
Titanite	0.0	0.2		
Magnetite	0.3	0.3	0.0	0.2
Anatase	0.0	0.0	0.0	0.0
Rutile	0.8	0.3	0.0	0.0
Apatite				
Calcite	0.3	0.1		
Ankerite				
Siderite				
Epidote			2.2	2.2
Garnet				
Sillimanite				
Hematite				
Maghemite				
Goethite				
Anhydrite				
Gypsum				
Jarosite				
Pyrite	4.7	3.6	3.3	3.1
		Clays		
Illite/Fine Muscovite	37.6	32.5	17.0	25.5
Smectite				
Kaolinite		5.1		4.0
Pyrophyllite				
Chlorite			12.4	6.7
Total clays	**37.6**	**37.6**	**29.4**	**36.2**
Full pattern region degree of fit	0.1382	0.0880	0.1103	0.0906
Clay region degree of fit	0.0794	0.0610	0.0598	0.0481
Pre-normalization total	108.0	103.9	108.5	107.4

Table B7. Quantitative X-ray diffraction results from drill hole HCBW3 in weight percent.—Continued

[All samples normalized to 100 percent. Pre-normalization totals are recorded in samples run with zincite standard, otherwise samples were run without an internal standard. See Appendix A for key to lithology and alteration codes. Lower values for degree of fit suggest more accurate analyses with values less than 0.1 considered ideal. Mineral percentages are blank where absent in the sample and therefore not analyzed]

Sample number	HCBW3 167
Lithology	11
Alteration	5b
Non-clays	
Quartz	61.4
Potassium Feldspar	0.5
Albite	0.0
Plagioclase	0.7
Amphibole	
Biotite	
Pyroxene	
Titanite	0.0
Magnetite	0.0
Anatase	0.0
Rutile	0.0
Apatite	
Calcite	0.9
Ankerite	
Siderite	0.0
Epidote	
Garnet	
Sillimanite	
Hematite	
Maghemite	6.6
Goethite	0.0
Anhydrite	
Gypsum	
Jarosite	0.3
Pyrite	3.5
Clays	
Illite/Fine Muscovite	18.8
Smectite	
Kaolinite	7.5
Pyrophyllite	
Chlorite	
Total clays	26.3
Full pattern region degree of fit	0.1241
Clay region degree of fit	0.0828
Pre-normalization total	97.5

Table C1. Quantitative mineralogy by XRD showing alteration progression in dacite intrusions.

[See appendix for key to lithology and alteration assemblage. All samples normalized to 100 percent. Pre-normalization totals are recorded in samples run with zincite standard, otherwise samples were run without an internal standard. See Appendix A for key to lithology and alteration codes. Lower values for degree of fit suggest more accurate analyses with values less than 0.1 considered ideal. Mineral percentages are blank where absent in the sample and therefore not analyzed. All samples from outcrop except those with wp1 prefix, which were from footage intervals in drill hole WP1]

Sample number	PM4	PX40	MDBR01	WP1-1100
Lithology	1	1	1	1
Alteration	0	0	1	1b
Albite	5.0	8.9	11.2	2.2
Amphibole	2.0	1.4		0.2
Anatase	0.0	0.0		0.0
Anhydrite	0.2	0.0		
Apatite	1.6	1.7	0.8	
Biotite	4.3	4.9	0.0	5.1
Calcite	0.5	0.2		0.6
Chlorite	1.8	4.8	5.4	8.2
Epidote	0.4	0.6		
Garnet				
Goethite	0.0	0.1		0.2
Gypsum	0.5	0.0		
Hematite	0.0	0.0		0.3
Illite/Fine Muscovite	2.4	5.4	5.8	10.7
Jarosite	0.3	0.3	0.0	0.5
Kaolinite	0.5	0.9	0.8	4.2
K-spar	21.4	18.2	27.0	14.6
Maghemite	6.0	3.0		3.7
Magnetite	2.5	1.4	1.2	0.5
Plagioclase	30.6	27.5	20.1	20.8
Pyrite	0.0	0.6	0.8	1.7
Pyrophyllite				
Pyroxene	1.0	0.0		
Quartz	16.1	17.2	26.3	23.9
Rutile	0.0	0.1	0.6	0.3
Siderite	0.1	0.2		
Sillimanite				
Smectite	2.5	2.6		1.7
Titanite	0.4	0.0		0.7
Full pattern region degree of fit	0.1144	0.1036	0.0883	0.1054
Clay region degree of fit			0.0562	0.0634
Pre-normalization total	114.2	117.7	105.8	112.4

Table C1. Quantitative mineralogy by XRD showing alteration progression in dacite intrusions.—Continued

[See appendix for key to lithology and alteration assemblage. All samples normalized to 100 percent. Pre-normalization totals are recorded in samples run with zincite standard, otherwise samples were run without an internal standard. See Appendix A for key to lithology and alteration codes. Lower values for degree of fit suggest more accurate analyses with values less than 0.1 considered ideal. Mineral percentages are blank where absent in the sample and therefore not analyzed. All samples from outcrop except those with wp1 prefix, which were from footage intervals in drill hole WP1]

Sample number	WP2 1146-56	WP1-1108	MDBR0202	WP4 90-100
Lithology	1	1	1	1
Alteration	2	2b	4	5
Albite	11.6	11.7	1.0	
Amphibole			0.8	
Anatase	0.0	0.0	0.0	0.0
Anhydrite			0.0	
Apatite			0.0	
Biotite	2.6	3.4	0.6	
Calcite	1.0		0.1	
Chlorite	2.6	6.1	1.0	
Epidote	0.7		0.0	
Garnet				
Goethite	0.0	0.6	0.1	1.3
Gypsum	0.0		1.0	
Hematite			0.0	0.0
Illite/Fine Muscovite	20.5	14.8	35.0	35.0
Jarosite	0.3	0.2	2.1	2.9
Kaolinite	0.9	8.9	2.4	0.8
K-spar	10.3	13.7	2.4	
Maghemite	0.0	1.0	0.0	
Magnetite	0.0	0.0	0.1	
Plagioclase	11.4	4.9	0.2	
Pyrite	4.5	1.9	0.0	0.3
Pyrophyllite				
Pyroxene		0.7		
Quartz	31.1	26.6	50.1	57.8
Rutile	0.3	0.3	0.7	0.7
Siderite				
Sillimanite			0.4	
Smectite	2.0	5.3	1.9	
Titanite	0.0	0.0	0.2	1.2
Full attern region degree of fit	0.1008	0.0862	0.1402	0.1085
Clay region degree of fit		0.0609		0.0731
Pre-normalization total	102.3	93.5	98.3	98.6

Table C1. Quantitative mineralogy by XRD showing alteration progression in dacite intrusions.—Continued

[See appendix for key to lithology and alteration assemblage. All samples normalized to 100 percent. Pre-normalization totals are recorded in samples run with zincite standard, otherwise samples were run without an internal standard. See Appendix A for key to lithology and alteration codes. Lower values for degree of fit suggest more accurate analyses with values less than 0.1 considered ideal. Mineral percentages are blank where absent in the sample and therefore not analyzed. All samples from outcrop except those with wp1 prefix, which were from footage intervals in drill hole WP1]

Sample number	WP1-1173	WP4 350-360	WP4 445-454
Lithology	1	1	1
Alteration	5	5a	5b
Albite			
Amphibole			
Anatase	0.0		
Anhydrite			
Apatite			
Biotite			
Calcite			
Chlorite			
Epidote			
Garnet			
Goethite	0.5		
Gypsum			
Hematite	0.4		
Illite/Fine Muscovite	35.8	37.4	34.3
Jarosite	1.0	0.0	2.6
Kaolinite	1.4	2.3	1.1
K-spar	1.0		0.1
Maghemite	3.4		
Magnetite	0.0	0.0	0.2
Plagioclase			
Pyrite	13.5	9.3	7.5
Pyrophyllite			
Pyroxene			
Quartz	42.1	50.3	53.5
Rutile	0.8	0.7	0.7
Siderite			
Sillimanite			
Smectite			
Titanite	0.0		
Full pattern region degree of fit	0.1350	0.1301	0.1339
Clay region degree of fit	0.0641	0.0677	0.0764
Pre-normalization total	97.4	104.7	99.9

Table C2. Quantitative mineralogy by XRD showing alteration progression in biotite-feldspar-quartz gneiss.

[See appendix for key to lithology and alteration assemblage. All samples normalized to 100 percent. Pre-normalization totals are recorded in samples run with zincite standard, otherwise samples were run without an internal standard. See Appendix A for key to lithology and alteration codes. Lower values for degree of fit suggest more accurate analyses with values <0.1 considered ideal. Mineral percentages are blank where absent in the sample and therefore not analyzed. All samples from outcrop except those with wp1 prefix, which were from footage intervals in drill hole WP1]

Sample number	JSC0602	JSC6A02	MDBR0302	JSC6C02
Lithology	9	9	9	9
Alteration	1	1	4	5
Albite	8.2	11.9	16.1	0.0
Amphibole	0.0	0.0	0.0	1.0
Anatase			0.0	
Anhydrite			0.0	
Apatite	0.1	0.1	0.1	0.0
Biotite	2.3	5.3	0.3	0.7
Calcite	0.0	0.0	0.0	0.0
Chlorite	6.7	3.1	0.5	0.8
Epidote	0.0	0.0	0.0	0.0
Garnet				
Goethite	0.1	0.0	0.8	0.5
Gypsum	0.8	1.0	0.3	0.2
Hematite	0.0	0.0	0.0	0.2
Illite/Fine Muscovite	18.7	7.5	40.2	44.9
Jarosite	0.2	0.9	0.4	2.1
Kaolinite	1.0	0.4	0.0	0.0
K-spar	3.7	4.8	0.5	1.6
Maghemite	0.0	0.0	0.2	0.6
Magnetite	0.0	0.1	0.0	0.0
Plagioclase	14.9	27.5	6.9	0.0
Pyrite	0.0	0.0	0.0	0.0
Pyrophyllite	0.0	0.0		0.0
Pyroxene	0.0	0.0		0.7
Quartz	42.8	36.2	31.8	46.5
Rutile			0.1	
Siderite				
Sillimanite	0.3	0.7	0.7	0.0
Smectite	0.0	0.0	1.0	0.0
Titanite	0.0	0.7	0.2	0.3
Full pattern region degree of fit	0.1244	0.1555	0.1479	0.1331
Clay region degree of fit				
Pre-normalization total				

Table C2. Quantitative mineralogy by XRD showing alteration progression in biotite-feldspar-quartz gneiss.—Continued

[See appendix for key to lithology and alteration assemblage. All samples normalized to 100 percent. Pre-normalization totals are recorded in samples run with zincite standard, otherwise samples were run without an internal standard. See Appendix A for key to lithology and alteration codes. Lower values for degree of fit suggest more accurate analyses with values <0.1 considered ideal. Mineral percentages are blank where absent in the sample and therefore not analyzed. All samples from outcrop except those with wp1 prefix, which were from footage intervals in drill hole WP1]

Sample number	WP1-49	105WDB4A	WP1-276
Lithology	9	9	9
Alteration	5	5a	5d
Albite			
Amphibole			
Anatase			0.0
Anhydrite			
Apatite			
Biotite			
Calcite			
Chlorite			8.9
Epidote			
Garnet			
Goethite	3.0		
Gypsum			
Hematite	0.2		
Illite/Fine Muscovite	33.0	31.6	23.9
Jarosite		7.2	0.0
Kaolinite		5.2	20.8
K-spar			
Maghemite		2.9	
Magnetite	0.0		0.7
Plagioclase			
Pyrite	0.3	0.3	3.7
Pyrophyllite			
Pyroxene			
Quartz	62.6	50.7	40.5
Rutile	0.8	2.2	1.6
Siderite			
Sillimanite			
Smectite			
Titanite	0.1		
Full pattern region degree of fit	0.1046	0.0864	0.0975
Clay region degree of fit	0.0709	0.0624	0.0792
Pre-normalization total	100.4	106.9	99.1

Table C3. Quantitative mineralogy by XRD showing alteration progression in biotite-sillimanite-quartz gneiss and augen gneiss from outcrop (JSC prefix) and drill hole WP3.

[See appendix for key to lithology and alteration assemblage. All samples normalized to 100 percent. Pre-normalization totals are recorded in samples run with zincite standard, otherwise samples were run without an internal standard. Lower values for degree of fit suggest more accurate analyses with values less than 0.1 considered ideal. Mineral percentages are blank where absent in the sample and therefore not analyzed. All samples from outcrop except those with wp1 prefix, which were from footage intervals in drill hole WP1]

Sample number	JSC19	JSC1902	JSC17A02	JSC12A02
Lithology	4	4	4	4
Alteration	1	1	2	5
Albite	0.6	1.4	6.4	0.0
Amphibole		0.0		
Anatase			1.0	0.0
Anhydrite			0.6	0.4
Apatite		0.0	0.0	0.0
Biotite	13.1	4.9	0.0	0.0
Calcite		0.0	0.0	0.0
Chlorite	13.5	4.9	1.5	0.0
Epidote		1.0	0.0	0.0
Garnet				
Goethite		0.1	0.0	0.0
Gypsum		0.5	0.5	0.1
Hematite		0.0	0.0	0.0
Illite/Fine Muscovite	25.9	12.7	18.2	35.6
Jarosite		0.0	0.5	0.6
Kaolinite		0.0	1.4	0.0
K-spar	1.6	1.1	17.3	0.0
Maghemite	2.0	0.5	0.0	0.0
Magnetite	0.0	0.3	0.0	0.0
Plagioclase		1.1	12.6	0.0
Pyrite		0.0	0.0	0.0
Pyrophyllite		0.0	0.0	0.0
Pyroxene		0.0		
Quartz	23.2	58.0	34.1	63.1
Rutile			0.9	0.2
Siderite				
Sillimanite	20.1	13.2	5.0	0.0
Smectite		0.0		
Titanite	0.0	0.2	0.0	0.0
Full pattern region degree of fit	0.1168	0.1789	0.1393	0.1834
Clay region degree of fit	0.0798			
Pre-normalization total	103.2			

Table C3. Quantitative mineralogy by XRD showing alteration progression in biotite-sillimanite-quartz gneiss and augen gneiss from outcrop (JSC prefix) and drill hole WP3.—Continued

[See appendix for key to lithology and alteration assemblage. All samples normalized to 100 percent. Pre-normalization totals are recorded in samples run with zincite standard, otherwise samples were run without an internal standard. Lower values for degree of fit suggest more accurate analyses with values less than 0.1 considered ideal. Mineral percentages are blank where absent in the sample and therefore not analyzed. All samples from outcrop except those with wp1 prefix, which were from footage intervals in drill hole WP1]

Sample number	WP3 314-324	WP3 94 -104
Lithology	4	4
Alteration	5	9
Albite	0.0	
Amphibole	0.0	
Anatase	0.0	
Anhydrite		
Apatite		
Biotite		
Calcite		
Chlorite		
Epidote		
Garnet		
Goethite		
Gypsum		
Hematite		
Illite/Fine Muscovite	37.4	20.5
Jarosite		9.3
Kaolinite		
K-spar	0.0	1.9
Maghemite		
Magnetite		
Plagioclase		
Pyrite	9.9	0.5
Pyrophyllite		6.6
Pyroxene		
Quartz	51.0	60.3
Rutile	1.0	0.8
Siderite		
Sillimanite		
Smectite		
Titanite		
Full pattern region degree of fit	0.1137	0.1027
Clay region degree of fit	0.1024	0.0712
Pre-normalization total	105.8	101.1
Norm total		

Table C4. Quantitative mineralogy by XRD showing alteration progression in amphibolite in drill holes WP3 and HCBW1.

[See appendix for key to lithology and alteration assemblage. All samples normalized to 100 percent. Pre-normalization totals are recorded in samples run with zincite standard, otherwise samples were run without an internal standard. Lower values for degree of fit suggest more accurate analyses with values less than 0.1 considered ideal. Mineral percentages are blank where absent in the sample and therefore not analyzed. All samples from outcrop except those with wp1 prefix, which were from footage intervals in drill hole WP1]

Sample number	HCBW1 47	WP3 1181-1191	WP3 999-1011	HCBW1 98
Lithology	7	7	7	7
Alteration	8	8	6	7
Albite			0.0	
Amphibole	39.3	28.5	0.0	0.7
Anatase			0.0	
Anhydrite				
Apatite				
Biotite	8.6	6.7	4.8	3.4
Calcite				1.4
Chlorite	9.1	10.3	15.0	2.2
Epidote	0.9		2.1	12.2
Garnet				5.4
Goethite				
Gypsum	0.6			
Hematite				
Illite/Fine Muscovite			4.6	5.3
Jarosite			0.0	
Kaolinite			0.0	7.3
K-spar			0.0	
Maghemite				0.5
Magnetite	7.1	5.6	3.4	0.0
Plagioclase	32.5	33.6	38.6	1.6
Pyrite	2.0	7.1	8.9	8.5
Pyrophyllite			0.0	
Pyroxene				
Quartz	0.0	9.7	8.0	16.1
Rutile		0.9	1.6	
Siderite				
Sillimanite				0.2
Smectite			2.0	31.8
Titanite	0.0		0.0	3.3
Full Pattern region degree of fit	0.1276	0.1313	0.0949	0.1411
Clay region degree of fit	0.0593	0.0974	0.0657	0.1001
Pre-normalization total	109.8	100.4	95.0	99.9
Norm total				

Table C5. Quantitative mineralogy by XRD showing alteration progression in feldspar-biotite-quartz granofels and gneiss in drill hole HCBW3.

[See appendix for key to lithology and alteration assemblage. All samples normalized to 100 percent. Pre-normalization totals are recorded in samples run with zincite standard, otherwise samples were run without an internal standard. Lower values for degree of fit suggest more accurate analyses with values less than 0.1 considered ideal. Mineral percentages are blank where absent in the sample and therefore not analyzed. All samples from outcrop except those with wp1 prefix, which were from footage intervals in drill hole WP1]

Sample number	HCBW3 157A	HCBW3 157B	HCBW3 74	HCBW3 58
Lithology	11	11	11	11
Alteration	2	2a	2b	4
Albite	0.3	0.0		6.9
Amphibole				0.3
Anatase	0.0	0.0		0.0
Anhydrite				0.0
Apatite			2.5	0.2
Biotite	28.1	17.7	9.6	0.6
Calcite			0.2	0.0
Chlorite	12.4	6.7	7.5	5.6
Epidote	2.2	2.2		0.2
Garnet			1.0	
Goethite			1.2	0.2
Gypsum			0.3	0.0
Hematite			0.3	0.2
Illite/Fine Muscovite	17.0	25.5	22.7	33.7
Jarosite				1.4
Kaolinite		4.0	19.7	0.8
K-spar	2.9	0.4	2.7	0.6
Maghemite			2.7	1.0
Magnetite	0.0	0.2		0.0
Plagioclase				1.3
Pyrite	3.3	3.1	4.5	0.0
Pyrophyllite				
Pyroxene				
Quartz	33.8	40.5	20.8	46.7
Rutile	0.0	0.0		0.2
Siderite				
Sillimanite				
Smectite			2.9	0.0
Titanite				0.0
Full pattern region degree of fit	0.1103	0.0906	0.1183	0.0877
Clay region degree of fit	0.0598	0.0481		
Pre-normalization total	108.5	107.4	113.2	105.7
Norm total				

Table C5. Quantitative mineralogy by XRD showing alteration progression in feldspar-biotite-quartz granofels and gneiss in drill hole HCBW3.—Continued

[See appendix for key to lithology and alteration assemblage. All samples normalized to 100 percent. Pre-normalization totals are recorded in samples run with zincite standard, otherwise samples were run without an internal standard. Lower values for degree of fit suggest more accurate analyses with values less than 0.1 considered ideal. Mineral percentages are blank where absent in the sample and therefore not analyzed. All samples from outcrop except those with wp1 prefix, which were from footage intervals in drill hole WP1]

Sample number	HCBW3 125	HCBW3 134.7
Lithology	11	11
Alteration	5	5b
Albite		
Amphibole		
Anatase	0.0	0.0
Anhydrite		
Apatite		
Biotite		
Calcite	0.3	0.1
Chlorite		
Epidote		
Garnet		
Goethite		
Gypsum		
Hematite		
Illite/Fine Muscovite	37.6	32.5
Jarosite		
Kaolinite		5.1
K-spar		
Maghemite		
Magnetite	0.3	0.3
Plagioclase		
Pyrite	4.7	3.6
Pyrophyllite		
Pyroxene		
Quartz	56.3	58.0
Rutile	0.8	0.3
Siderite		
Sillimanite		
Smectite		
Titanite	0.0	0.2
Full pattern region degree of fit	0.1382	0.0880
Clay region degree of fit	0.0794	0.0610
Pre-normalization total	108.0	103.9
Norm total		

Table D1. Feldspar compositions from footage intervals in drill holes HCBW1, WP1, and WP3 in weight percent oxide determined by electron probe analyses.

[Data were normalized to 8 oxygen equivalents to calculate a structural formula]

Sample	HCBW1 81.5'-c4-2	HCBW1 81.5'-c4-3	HC181.5'-c4-6	WP1-1225'-c4a-4b-1	WP1-1225'-c4a-4b-3	WP3-1222'-c4-2	WP3-1222'-c4-4	WP3-1222'-c4-6
SiO_2	60.3	61.8	61.9	65.2	65.1	55.6	55.6	55.2
Al_2O_3	25.1	23.9	23.5	18.5	19.1	28.0	28.2	28.0
FeO	0.37	0.54	0.94	0.11	0.12	0.34	0.39	0.28
CaO	6.85	5.14	5.06	bdl	0.34	9.98	10.3	10.5
Na_2O	7.84	8.04	7.54	1.03	4.05	5.93	5.58	5.53
K_2O	0.12	0.14	0.16	14.9	10.4	0.05	0.11	0.17
BaO	n.a.	n.a.	n.a.	n.a.	n.a.	n.a.	n.a.	n.a.
Total	**100.6**	**99.5**	**99.1**	**99.8**	**99.0**	**99.8**	**100.2**	**99.7**
Structural formula to 8 oxygen equivalents								
Si	2.675	2.752	2.766	3.001	2.976	2.506	2.501	2.497
Al	1.313	1.253	1.239	1.006	1.029	1.487	1.495	1.494
Fe(ii)	0.014	0.020	0.035	0.004	0.005	0.013	0.015	0.011
Ca	0.326	0.245	0.242	0.000	0.017	0.482	0.496	0.506
Na	0.674	0.695	0.653	0.092	0.359	0.518	0.486	0.485
K	0.007	0.008	0.009	0.876	0.604	0.003	0.006	0.010
Ba	0.000	0.000	0.000	0.000	0.000	0.000	0.000	0.000
Total	**5.009**	**4.973**	**4.945**	**4.980**	**4.990**	**5.011**	**4.998**	**5.003**
Endmembers								
Anorthite	32	26	27	0	2	48	50	51
Albite	67	73	72	10	37	52	49	48
Orthoclase	1	1	1	90	62	0	1	1

Table D2. Amphibole compositions from footage intervals in drill hole HCBW1 in weight percent oxide determined by electron probe analyses.

[Data were normalized to 23 oxygen equivalents following the recommendations of Leake and others (1997)]

Sample	HC181.5'-c4-1	HC181.5'-c5-1	HC181.5'-c5-2	HC181.5'-c5-3
SiO_2	42.5	42.8	43.2	44.3
TiO_2	1.06	1.03	1.40	1.72
Al_2O_3	12.8	11.9	11.0	9.98
Cr_2O_3	n.a.	n.a.	n.a.	n.a.
FeO	13.2	13.4	14.0	12.3
MnO	0.27	0.18	0.27	0.25
MgO	12.8	13.5	13.5	13.9
CaO	11.7	11.8	11.8	11.8
Na_2O	2.40	2.31	2.08	1.70
K_2O	0.31	0.39	0.48	0.50
F	0.43	0.28	0.16	0.18
Cl	bdl	0.21	0.28	0.29
O=F,Cl	0.19	0.16	0.13	0.14
Total	**97.4**	**97.5**	**98.0**	**96.8**
Structural formula to 23 oxygen equivalents				
Si	6.260	6.285	6.321	6.531
Al (IV)	1.740	1.715	1.679	1.469
Sum T	8.000	8.000	8.000	8.000
Al (VI)	0.479	0.337	0.224	0.265
Ti	0.117	0.114	0.154	0.191
Fe^{3+}	0.446	0.571	0.632	0.383
Cr	0.000	0.000	0.000	0.000
Mg	2.813	2.949	2.947	3.064
Fe^{2+}	1.145	1.029	1.043	1.097
Mn	0.000	0.000	0.000	0.000
Sum C	5.000	5.000	5.000	5.000
Mg	0.000	0.000	0.000	0.000
Fe^{2+}	0.038	0.045	0.039	0.031
Mn	0.033	0.022	0.033	0.031
Ca	1.847	1.857	1.845	1.868
Na	0.081	0.076	0.082	0.070
Sum B	2.000	2.000	2.000	2.000
Na	0.605	0.582	0.507	0.414
K	0.059	0.073	0.090	0.095
Sum A	0.663	0.655	0.598	0.509
Total	**15.663**	**15.655**	**15.598**	**15.509**
Name	**pargasite**	**magnesio-hastingsite**	**magnesio-hastingsite**	**edenite**

Table D2. Amphibole compositions from footage intervals in drill hole HCBW1 in weight percent oxide determined by electron probe analyses.—Continued

[Data were normalized to 23 oxygen equivalents following the recommendations of Leake and others (1997)]

Sample	WP3-1222'-c4-1	WP3-1222'-c4-3	WP3-1222'-c4-5
SiO_2	46.6	47.1	46.8
TiO_2	0.86	0.95	0.97
Al_2O_3	8.85	8.26	8.51
Cr_2O_3	n.a.	n.a.	n.a.
FeO	12.9	12.6	12.4
MnO	0.25	0.26	0.29
MgO	14.4	14.9	14.6
CaO	11.7	11.8	11.9
Na_2O	1.32	1.19	1.20
K_2O	0.53	0.57	0.54
F	0.28	0.28	0.34
Cl	bdl	bdl	0.13
O=F,Cl	0.13	0.14	0.17
Total	**97.6**	**97.8**	**97.5**
Structural formula to 23 oxygen equivalents			
Si	6.767	6.810	6.799
Al (IV)	1.233	1.190	1.201
Sum T	8.000	8.000	8.000
Al (VI)	0.281	0.218	0.258
Ti	0.094	0.103	0.106
Fe^{3+}	0.489	0.512	0.445
Cr	0.000	0.000	0.000
Mg	3.108	3.205	3.165
Fe^{2+}	1.029	0.962	1.026
Mn	0.000	0.000	0.000
Sum C	5.000	5.000	5.000
Mg	0.000	0.000	0.000
Fe^{2+}	0.054	0.049	0.032
Mn	0.031	0.032	0.036
Ca	1.819	1.827	1.855
Na	0.097	0.092	0.078
Sum B	2.000	2.000	2.000
Na	0.274	0.242	0.262
K	0.098	0.105	0.101
Sum A	0.372	0.346	0.362
Total	**15.372**	**15.346**	**15.362**
Name	**magnesio-hornblende**	**magnesio-hornblende**	**magnesio-hornblende**

Table D3. Compositional data for chorite that replaced biotite. Analyses in weight percent oxide as determined by electron probe analyses.

[Data were normalized to 28 oxygen equivalents. WEBCHL analyses from chlorite after biotite in outcrops of biotite-rich gneiss. Other samples from chlorite that replaced primary biotite in footage intervals from drill hole WP1]

Sample	WEBCHLc1-1	WEBCHLc1-l2	WEBCHLc1-3	WEBCHLc1-4	WEBCHLc1-5	WEBCHLc2-1	WEBCHLc2-l2	WEBCHLc2-3
SiO_2	29.8	30.0	29.0	30.7	29.4	30.3	28.4	29.8
TiO_2	0.18	0.07	0.07	0.06	0.07	0.23	0.00	0.16
Al_2O_3	20.7	20.3	21.3	19.3	21.1	21.9	21.8	21.3
FeO	14.2	14.2	15.2	13.5	14.6	14.6	15.1	15.2
MnO	0.81	0.34	0.86	0.48	0.70	0.60	0.57	0.94
MgO	21.3	22.2	21.7	22.8	21.7	19.9	20.4	19.8
CaO	0.03	0.03	0.06	0.06	0.03	0.07	0.02	0.02
Na_2O	0.05	0.08	0.04	0.08	0.02	0.07	0.03	0.04
K^2O	0.06	0.05	0.01	0.05	0.03	0.04	0.02	0.09
Cl	0.01	0.00	0.01	0.00	0.01	0.00	0.00	0.02
F	0.54	0.54	0.57	0.68	0.63	0.29	0.41	0.53
Total	**87.7**	**87.8**	**88.8**	**87.8**	**88.2**	**87.9**	**86.7**	**87.9**
O=F,Cl	0.23	0.23	0.24	0.29	0.26	0.12	0.17	0.23
Total	**87.4**	**87.5**	**88.5**	**87.5**	**88.0**	**87.8**	**86.5**	**87.6**
Structural formula to 28 oxygen equivalents								
Si	5.920	5.943	5.725	6.070	5.822	5.966	5.728	5.925
Al(IV)	2.080	2.057	2.275	1.930	2.178	2.034	2.272	2.075
Sum T	8.000	8.000	8.000	8.000	8.000	8.000	8.000	8.000
Al(VI)	2.769	2.676	2.689	2.574	2.740	3.050	2.906	2.924
Ti	0.026	0.010	0.011	0.009	0.011	0.033	0.000	0.025
Fe(ii)	2.360	2.347	2.510	2.236	2.422	2.405	2.547	2.525
Mn	0.136	0.057	0.144	0.080	0.118	0.101	0.097	0.159
Mg	6.314	6.562	6.406	6.737	6.402	5.836	6.118	5.892
Sum C	11.605	11.651	11.759	11.636	11.692	11.425	11.669	11.524
Ca	0.006	0.007	0.013	0.012	0.007	0.015	0.005	0.004
Na	0.018	0.032	0.015	0.029	0.008	0.026	0.011	0.016
K	0.015	0.013	0.002	0.013	0.007	0.010	0.005	0.024
SUM I	0.039	0.052	0.030	0.054	0.023	0.051	0.021	0.044
Cl	0.002	0.000	0.003	0.000	0.002	0.000	0.001	0.005
F	0.340	0.339	0.354	0.425	0.392	0.178	0.258	0.332
Total	**19.645**	**19.703**	**19.789**	**19.690**	**19.715**	**19.476**	**19.690**	**19.568**

Table D3. Compositional data for chorite that replaced biotite. Analyses in weight percent oxide as determined by electron probe analyses.—Continued

[Data were normalized to 28 oxygen equivalents. WEBCHL analyses from chlorite after biotite in outcrops of biotite-rich gneiss. Other samples from chlorite that replaced primary biotite in footage intervals from drill hole WP1]

Sample	WEBCHLc2-l4	WEBCHLc2-l5	WP1-1225'-c1-1	WP1-1225'-c4a-1	WP1-1225'-c4a-2	WP1-1225'-c4a-3	WP1-1289'-c1-10	WP1-1289'-c1-2
SiO_2	30.3	29.2	27.6	27.1	27.0	27.5	27.9	27.9
TiO_2	0.01	0.14	0.14	0.08	0.02	0.04	0.17	0.13
Al_2O_3	20.6	21.2	19.0	20.5	19.9	20.0	20.1	20.1
FeO	14.9	14.8	23.2	21.2	22.0	22.3	21.0	21.6
MnO	0.48	0.63	0.32	0.35	0.35	0.33	0.13	0.08
MgO	20.8	20.7	17.6	17.8	17.6	17.7	18.1	18.3
CaO	0.03	0.08	0.04	0.00	0.06	0.03	0.04	0.03
Na2O	0.10	0.01	0.01	0.00	0.00	0.00	0.02	0.01
K2O	0.06	0.01	0.30	0.10	0.07	0.26	0.27	0.18
Cl	0.01	0.01	0.03	0.01	0.08	0.04	0.02	0.00
F	0.49	0.60	0.10	0.13	0.12	0.15	0.28	0.23
Total	**87.7**	**87.4**	**88.4**	**87.3**	**87.2**	**88.3**	**88.0**	**88.5**
O=F,Cl	0.21	0.25	0.05	0.06	0.07	0.07	0.12	0.10
Total	**87.5**	**87.1**	**88.3**	**87.3**	**87.1**	**88.3**	**87.9**	**88.4**
Structural formula to 28 oxygen equivalents								
Si	6.016	5.840	5.711	5.607	5.624	5.667	5.730	5.705
Al(IV)	1.984	2.160	2.289	2.393	2.376	2.333	2.270	2.295
Sum T	8.000	8.000	8.000	8.000	8.000	8.000	8.000	8.000
Al(VI)	2.835	2.829	2.354	2.617	2.516	2.517	2.584	2.538
Ti	0.001	0.021	0.022	0.013	0.003	0.007	0.027	0.021
Fe(ii)	2.473	2.482	4.015	3.671	3.837	3.847	3.609	3.696
Mn	0.081	0.107	0.057	0.061	0.061	0.058	0.023	0.014
Mg	6.149	6.184	5.442	5.496	5.470	5.424	5.521	5.559
Sum C	11.539	11.623	11.890	11.859	11.888	11.854	11.763	11.828
Ca	0.006	0.018	0.010	0.000	0.014	0.006	0.009	0.006
Na	0.037	0.002	0.003	0.001	0.002	0.001	0.009	0.003
K	0.016	0.001	0.079	0.027	0.018	0.067	0.071	0.046
SUM I	0.059	0.021	0.091	0.029	0.033	0.074	0.090	0.054
Cl	0.003	0.005	0.009	0.004	0.029	0.013	0.008	0.001
F	0.306	0.377	0.066	0.085	0.077	0.095	0.184	0.147
Total	**19.598**	**19.644**	**19.982**	**19.887**	**19.922**	**19.928**	**19.853**	**19.882**

Table D3. Compositional data for chorite that replaced biotite. Analyses in weight percent oxide as determined by electron probe analyses.—Continued

[Data were normalized to 28 oxygen equivalents. WEBCHL analyses from chlorite after biotite in outcrops of biotite-rich gneiss. Other samples from chlorite that replaced primary biotite in footage intervals from drill hole WP1]

Sample	WP1-1289'-c1-4	WP1-1289'-c1-6	WP1-1289'-c1-8	WP1-1289'-c2-2	WP1-1289'-c2-3	WP1-1289'-c2-6	WP1-1289'-c5-1	WP1-1289'-c5-2
SiO_2	28.1	27.9	28.0	27.4	29.1	28.1	27.8	27.5
TiO_2	0.34	0.04	0.10	0.12	0.46	0.00	0.01	0.09
Al_2O_3	19.8	19.9	19.9	20.1	18.7	20.1	19.4	19.5
FeO	20.8	20.5	21.0	20.0	19.7	20.2	20.1	19.8
MnO	0.06	0.10	0.10	0.16	0.09	0.12	0.12	0.10
MgO	18.5	18.7	18.7	18.4	17.6	16.8	18.3	19.0
CaO	0.04	0.01	0.02	0.02	0.02	0.04	0.02	0.02
Na_2O	0.01	0.01	0.01	0.00	0.05	0.00	0.02	0.00
K_2O	0.21	0.07	0.15	0.49	0.66	0.02	0.17	0.10
Cl	0.02	0.01	0.01	0.01	0.03	0.02	0.01	0.01
F	0.24	0.16	0.37	0.47	0.35	0.25	0.21	0.17
Total	**88.1**	**87.4**	**88.3**	**87.2**	**86.8**	**85.7**	**86.2**	**86.2**
O=F,Cl	0.10	0.07	0.16	0.20	0.16	0.11	0.09	0.07
Total	**88.0**	**87.4**	**88.2**	**87.0**	**86.6**	**85.6**	**86.1**	**86.2**
Structural formula to 28 oxygen equivalents								
Si	5.741	5.739	5.728	5.680	6.016	5.884	5.799	5.716
Al(IV)	2.259	2.261	2.272	2.320	1.984	2.116	2.201	2.284
Sum T	8.000	8.000	8.000	8.000	8.000	8.000	8.000	8.000
Al(VI)	2.524	2.557	2.518	2.586	2.584	2.842	2.557	2.498
Ti	0.052	0.006	0.015	0.019	0.072	0.000	0.002	0.014
Fe(ii)	3.560	3.519	3.582	3.469	3.418	3.529	3.510	3.450
Mn	0.011	0.018	0.017	0.028	0.016	0.021	0.022	0.018
Mg	5.629	5.731	5.704	5.675	5.430	5.229	5.697	5.880
Sum C	11.775	11.831	11.835	11.776	11.520	11.622	11.787	11.861
Ca	0.008	0.003	0.004	0.005	0.005	0.009	0.004	0.004
Na	0.003	0.005	0.004	0.000	0.022	0.001	0.008	0.002
K	0.054	0.018	0.039	0.130	0.175	0.006	0.046	0.025
SUM I	0.065	0.026	0.047	0.135	0.201	0.016	0.057	0.031
Cl	0.006	0.002	0.002	0.004	0.011	0.007	0.005	0.002
F	0.153	0.106	0.241	0.305	0.231	0.167	0.135	0.109
Total	**19.841**	**19.857**	**19.883**	**19.911**	**19.721**	**19.637**	**19.845**	**19.891**

Table D3. Compositional data for chorite that replaced biotite. Analyses in weight percent oxide as determined by electron probe analyses.—Continued

[Data were normalized to 28 oxygen equivalents. WEBCHL analyses from chlorite after biotite in outcrops of biotite-rich gneiss. Other samples from chlorite that replaced primary biotite in footage intervals from drill hole WP1]

Sample	WP1-1289'-c5-3	WP1-1289'-c6-1	WP1-1289'-c6-2	WP1-1289'-c6-3	WP1-1289'-c7-4	WP1-1289'-c7-5	WP1-1372'-c1-'1	WP1-1372'-c1-'2
SiO_2	27.6	27.5	28.9	28.0	27.9	27.3	25.9	26.7
TiO_2	0.28	0.07	0.19	0.07	0.14	0.35	0.03	0.05
Al_2O_3	19.7	20.1	19.7	19.8	20.8	20.1	20.9	21.3
FeO	19.9	20.3	19.8	19.5	17.8	19.2	22.2	21.6
MnO	0.09	0.14	0.13	0.10	0.18	0.13	0.54	0.54
MgO	18.7	18.7	18.4	19.2	20.2	18.9	17.0	17.5
CaO	0.02	0.04	0.04	0.05	0.04	0.04	0.03	0.20
Na_2O	0.01	0.00	0.01	0.00	0.00	0.01	0.00	0.00
K_2O	0.08	0.05	0.75	0.10	0.43	0.21	0.02	0.01
Cl	0.01	0.00	0.02	0.01	0.02	0.03	0.01	0.00
F	0.28	0.25	0.51	0.35	0.37	0.21	0.00	0.14
Total	**86.6**	**87.3**	**88.5**	**87.1**	**87.9**	**86.5**	**86.7**	**88.0**
O=F,Cl	0.12	0.11	0.22	0.15	0.16	0.09	0.00	0.06
Total	**86.5**	**87.2**	**88.2**	**87.0**	**87.7**	**86.5**	**86.7**	**88.0**
Structural formula to 28 oxygen equivalents								
Si	5.718	5.673	5.881	5.752	5.644	5.653	5.449	5.502
Al(IV)	2.282	2.327	2.119	2.248	2.356	2.347	2.551	2.498
Sum T	8.000	8.000	8.000	8.000	8.000	8.000	8.000	8.000
Al(VI)	2.525	2.566	2.603	2.553	2.607	2.560	2.623	2.680
Ti	0.043	0.011	0.029	0.011	0.022	0.055	0.005	0.007
Fe(ii)	3.445	3.499	3.372	3.345	3.021	3.316	3.897	3.710
Mn	0.016	0.025	0.022	0.017	0.031	0.023	0.095	0.093
Mg	5.789	5.754	5.592	5.887	6.104	5.841	5.326	5.366
Sum C	11.818	11.855	11.617	11.812	11.785	11.795	11.946	11.857
Ca	0.004	0.008	0.009	0.010	0.009	0.008	0.008	0.043
Na	0.002	0.000	0.003	0.000	0.000	0.004	0.000	0.000
K	0.022	0.013	0.195	0.027	0.111	0.056	0.005	0.003
SUM I	0.028	0.021	0.206	0.037	0.119	0.068	0.013	0.046
Cl	0.004	0.000	0.008	0.002	0.008	0.011	0.005	0.000
F	0.185	0.166	0.328	0.224	0.238	0.137	0.000	0.088
Total	**19.846**	**19.876**	**19.824**	**19.849**	**19.904**	**19.863**	**19.959**	**19.903**

Table D3. Compositional data for chorite that replaced biotite. Analyses in weight percent oxide as determined by electron probe analyses.—Continued

[Data were normalized to 28 oxygen equivalents. WEBCHL analyses from chlorite after biotite in outcrops of biotite-rich gneiss. Other samples from chlorite that replaced primary biotite in footage intervals from drill hole WP1]

Sample	WP1-1372'-c1-3	WP1-1372'-c1-'4	WP1-1372'-c1-'5	WP1-1372'-c2a-7	WP1-1372'-c2a-8	WP1-1372'-c2a-9	WP1-1372'-c2b-3	WP1-1372'-c2b-4
SiO2	44.2	26.1	27.0	27.1	27.6	26.8	26.7	26.7
TiO2	0.12	0.02	0.07	0.10	0.04	0.09	0.08	0.06
Al2O3	30.2	21.5	20.7	20.9	20.9	21.3	20.4	20.4
FeO	6.4	22.4	22.2	20.6	21.8	21.7	22.5	22.5
MnO	0.05	0.46	0.45	0.63	0.67	0.46	0.73	0.32
MgO	3.4	17.2	17.6	16.4	16.5	17.6	16.6	17.3
CaO	0.08	0.02	0.02	0.06	0.06	0.02	0.05	0.00
Na2O	0.23	0.00	0.02	0.01	0.00	0.01	0.01	0.00
K2O	8.91	0.02	0.01	0.02	0.04	0.02	0.03	0.00
Cl	0.02	0.01	0.01	0.02	0.01	0.00	0.02	0.01
F	0.11	0.09	0.26	0.16	0.15	0.00	0.13	0.39
Total	**93.7**	**87.9**	**88.3**	**86.1**	**87.7**	**88.0**	**87.3**	**87.7**
O=F,Cl	0.05	0.04	0.11	0.07	0.07	0.00	0.06	0.17
Total	**93.7**	**87.8**	**88.2**	**86.0**	**87.6**	**88.0**	**87.2**	**87.5**
Structural formula to 28 oxygen equivalents								
Si	7.819	5.416	5.563	5.678	5.698	5.517	5.580	5.563
Al(IV)	0.181	2.584	2.437	2.322	2.302	2.483	2.420	2.437
Sum T	8.000	8.000	8.000	8.000	8.000	8.000	8.000	8.000
Al(VI)	6.100	2.657	2.586	2.838	2.779	2.672	2.614	2.574
Ti	0.016	0.004	0.011	0.015	0.006	0.013	0.013	0.010
Fe(ii)	0.943	3.889	3.830	3.614	3.757	3.736	3.925	3.918
Mn	0.007	0.081	0.079	0.112	0.118	0.079	0.129	0.057
Mg	0.898	5.322	5.398	5.125	5.077	5.383	5.187	5.361
Sum C	7.963	11.953	11.904	11.705	11.736	11.884	11.869	11.920
Ca	0.015	0.004	0.005	0.013	0.013	0.004	0.011	0.000
Na	0.079	0.000	0.006	0.004	0.000	0.003	0.006	0.000
K	2.010	0.005	0.002	0.006	0.010	0.004	0.007	0.000
SUM I	2.104	0.008	0.013	0.023	0.023	0.012	0.023	0.000
Cl	0.005	0.003	0.003	0.009	0.005	0.001	0.008	0.004
F	0.062	0.058	0.166	0.106	0.096	0.000	0.086	0.254
Total	**18.067**	**19.961**	**19.917**	**19.727**	**19.759**	**19.896**	**19.892**	**19.920**

Table D3. Compositional data for chorite that replaced biotite. Analyses in weight percent oxide as determined by electron probe analyses.—Continued

[Data were normalized to 28 oxygen equivalents. WEBCHL analyses from chlorite after biotite in outcrops of biotite-rich gneiss. Other samples from chlorite that replaced primary biotite in footage intervals from drill hole WP1]

Sample	WP1-1372'-c2b-5	WP1-1869'-c1-1	WP1-1869'-c1-2	WP1-1869'-c1-3	WP1-1869'-c1-5	WP1-1869'-c2-1	WP1-1869'-c2-2	WP1-1869'-c2-3
SiO_2	27.0	26.8	27.1	26.8	27.3	27.4	27.2	26.9
TiO_2	0.05	0.13	0.09	0.04	0.09	0.12	0.07	0.12
Al_2O_3	20.6	20.2	20.4	20.0	20.4	20.2	20.9	20.8
FeO	22.2	23.7	22.7	22.3	22.7	23.0	23.1	22.0
MnO	0.50	0.15	0.16	0.16	0.16	0.11	0.19	0.20
MgO	17.4	16.5	17.1	17.3	17.8	17.3	17.7	18.0
CaO	0.03	0.03	0.06	0.02	0.00	0.06	0.02	0.01
Na_2O	0.02	0.02	0.00	0.00	0.00	0.01	0.00	0.01
K_2O	0.11	0.01	0.03	0.00	0.00	0.13	0.11	0.04
Cl	0.01	0.00	0.00	0.01	0.01	0.02	0.01	0.01
F	0.38	0.30	0.27	0.32	0.38	0.40	0.38	0.24
Total	**88.3**	**87.9**	**88.0**	**86.9**	**88.8**	**88.7**	**89.7**	**88.2**
O=F,Cl	0.16	0.13	0.12	0.14	0.16	0.17	0.16	0.10
Total	**88.1**	**87.7**	**87.9**	**86.8**	**88.6**	**88.5**	**89.5**	**88.1**
Structural formula to 28 oxygen equivalents								
Si	5.582	5.589	5.620	5.623	5.604	5.640	5.545	5.530
Al(IV)	2.418	2.411	2.380	2.377	2.396	2.360	2.455	2.470
Sum T	8.000	8.000	8.000	8.000	8.000	8.000	8.000	8.000
Al(VI)	2.587	2.567	2.597	2.555	2.532	2.550	2.567	2.570
Ti	0.008	0.021	0.013	0.006	0.014	0.018	0.010	0.019
Fe(ii)	3.838	4.141	3.931	3.917	3.900	3.963	3.934	3.785
Mn	0.088	0.027	0.028	0.029	0.027	0.020	0.033	0.035
Mg	5.359	5.132	5.293	5.392	5.443	5.302	5.370	5.510
Sum C	11.880	11.888	11.861	11.900	11.917	11.852	11.914	11.919
Ca	0.007	0.006	0.013	0.004	0.000	0.013	0.004	0.003
Na	0.007	0.009	0.002	0.000	0.000	0.002	0.000	0.005
K	0.028	0.004	0.007	0.000	0.000	0.033	0.029	0.011
SUM I	0.042	0.019	0.021	0.004	0.000	0.049	0.033	0.019
Cl	0.005	0.001	0.001	0.002	0.002	0.008	0.004	0.002
F	0.250	0.200	0.179	0.213	0.247	0.259	0.243	0.155
Total	**19.922**	**19.907**	**19.882**	**19.904**	**19.917**	**19.901**	**19.947**	**19.938**

Table D3. Compositional data for chorite that replaced biotite. Analyses in weight percent oxide as determined by electron probe analyses.—Continued

[Data were normalized to 28 oxygen equivalents. WEBCHL analyses from chlorite after biotite in outcrops of biotite-rich gneiss. Other samples from chlorite that replaced primary biotite in footage intervals from drill hole WP1]

Sample	WP1-1869'-c2-4	WP1-1869'-c2-5
SiO_2	26.7	28.1
TiO_2	0.11	0.11
Al_2O_3	21.6	19.9
FeO	22.4	23.1
MnO	0.20	0.01
MgO	17.6	16.8
CaO	0.02	0.07
Na_2O	0.00	0.00
K_2O	0.15	0.19
Cl	0.02	0.01
F	0.07	0.43
Total	**88.8**	**88.8**
O=F,Cl	0.03	0.18
Total	**88.8**	**88.6**
Structural formula to 28 oxygen equivalents		
Si	5.452	5.776
Al(IV)	2.548	2.224
Sum T	8.000	8.000
Al(VI)	2.645	2.607
Ti	0.017	0.017
Fe(ii)	3.833	3.979
Mn	0.034	0.002
Mg	5.376	5.143
Sum C	11.906	11.749
Ca	0.004	0.016
Na	0.001	0.000
K	0.038	0.050
SUM I	0.044	0.066
Cl	0.008	0.003
F	0.042	0.280
Total	**19.950**	**19.815**

Table D4. Compositional data for late-stage chlorite from footage intervals in drill hole WP1.

[Analyses in weight percent oxide as determined by electron probe analyses. Data were normalized to 28 oxygen equivalents]

Sample	WP1-451'-c1-7	WP1-451'-c1-8	WP1-451'-c2-1	WP1-451'-c2-2	WP1-451'-c2-3	WP1-451'-c2-4	WP1-451'-c2-5
SiO_2	27.7	28.0	27.5	27.8	26.9	33.6	39.0
TiO_2	0.00	0.01	0.02	0.03	0.04	0.03	0.12
Al_2O_3	25.5	26.2	24.4	25.4	24.8	27.8	30.6
FeO	6.5	6.2	7.3	9.2	9.3	7.3	5.2
MnO	0.06	0.12	0.09	0.17	0.18	0.15	0.10
MgO	25.7	25.5	24.5	23.6	24.4	16.6	10.6
CaO	0.03	0.03	0.06	0.03	0.02	0.03	0.01
Na_2O	0.00	0.00	0.05	0.02	0.03	0.14	0.27
K_2O	0.00	0.02	0.04	0.19	0.03	3.03	4.69
Cl	0.01	0.02	0.05	0.03	0.02	0.02	0.03
F	0.34	0.28	0.26	0.27	0.29	0.24	0.20
Total	**85.8**	**86.5**	**84.2**	**86.6**	**86.0**	**88.9**	**90.9**
O=F,Cl	0.15	0.12	0.12	0.12	0.13	0.10	0.09
Total	**85.7**	**86.3**	**84.1**	**86.5**	**85.8**	**88.8**	**90.8**
Structural formula to 28 oxygen equivalents							
Si	5.376	5.386	5.457	5.415	5.297	6.293	7.003
Al(IV)	2.624	2.614	2.543	2.585	2.703	1.707	0.997
Sum T	8.000	8.000	8.000	8.000	8.000	8.000	8.000
Al(VI)	3.213	3.312	3.175	3.247	3.056	4.434	5.485
Ti	0.000	0.001	0.003	0.004	0.006	0.004	0.016
Fe(ii)	1.052	0.998	1.204	1.495	1.538	1.137	0.788
Mn	0.010	0.019	0.015	0.027	0.029	0.023	0.015
Mg	7.422	7.307	7.247	6.853	7.172	4.637	2.844
Sum C	11.697	11.638	11.645	11.626	11.801	10.235	9.149
Ca	0.005	0.006	0.012	0.006	0.004	0.006	0.002
Na	0.000	0.001	0.020	0.009	0.011	0.051	0.095
K	0.000	0.005	0.011	0.048	0.008	0.724	1.075
SUM I	0.006	0.012	0.043	0.063	0.023	0.781	1.172
Cl	0.005	0.006	0.016	0.008	0.008	0.007	0.008
F	0.211	0.172	0.163	0.167	0.181	0.140	0.115
Total	**19.703**	**19.650**	**19.688**	**19.689**	**19.824**	**19.016**	**18.321**

Table D4. Compositional data for late-stage chlorite from footage intervals in drill hole WP1.—Continued

[Analyses in weight percent oxide as determined by electron probe analyses. Data were normalized to 28 oxygen equivalents]

Sample	WP1-451'-c1-1	WP1-451'-c1-2	WP1-451'-c1-3	WP1-451'-c1-4	WP1-451'-c1-5	WP1-451'-c1-6
SiO2	26.8	27.8	26.1	27.1	26.2	26.6
TiO2	0	0	0	0.01	0	0
Al2O3	24.7	25.3	24.5	23.7	24	24
FeO	12.3	5.6	13.6	12.6	13.4	12.8
MnO	0.26	0.09	0.29	0.21	0.27	0.28
MgO	22.6	26.6	21.8	22.4	21.8	22.2
CaO	0	0.01	0	0.01	0	0.04
Na2O	0.01	0.02	0.01	0.03	0.01	0.04
K2O	0.01	0.01	0.02	0.02	0.01	0.06
Cl	0.01	0.01	0.01	0.01	0.01	0.03
F	0.06	0.32	0.11	0.12	0.06	0
Total	**86.7**	**85.8**	**86.5**	**86.2**	**85.8**	**86.1**
O=F,Cl	0.03	0.13	0.05	0.05	0.03	0.01
Total	**86.6**	**85.6**	**86.5**	**86.2**	**85.7**	**86.1**
Structural formula to 28 oxygens						
Si	5.303	5.381	5.227	5.404	5.294	5.334
Al(IV)	2.697	2.619	2.773	2.596	2.706	2.666
Sum T	8	8	8	8	8	8
Al(VI)	3.066	3.14	3.018	2.983	2.988	2.988
Ti	0	0	0	0.002	0	0
Fe(ii)	2.036	0.909	2.281	2.109	2.253	2.149
Mn	0.043	0.014	0.05	0.036	0.046	0.048
Mg	6.665	7.668	6.523	6.662	6.567	6.627
Sum C	11.81	11.731	11.872	11.792	11.854	11.812
Ca	0	0.002	0	0.003	0	0.008
Na	0.003	0.007	0.005	0.013	0.004	0.014
K	0.003	0.002	0.004	0.004	0.002	0.016
SUM I	0.006	0.011	0.009	0.02	0.006	0.037
Cl	0.004	0.003	0.002	0.002	0.004	0.011
F	0.035	0.193	0.07	0.078	0.038	0
Total	**19.817**	**19.742**	**19.881**	**19.812**	**19.86**	**19.848**

Table D5. Biotite compositions in weight percent oxide determined by electron probe analyses.

[Data were normalized to 22 oxygen equivalents. Biotite from footage intervals in drill holes HCBW1, WP1, and WP3. Analyses from primary, altered or oxidized primary, and secondary biotites. The fluorine index was calculated using the methods described in Munoz (1984)]

Sample	HCBW1 81.5'-c4-4	HCBW1 81.5'-c4-5	WP1-1289'-c1-1	WP1-1289'-c1-3	WP1-1289'-c1-5	WP1-1289'-c2-1
Description	**Primary altered**	**Primary altered**	**Primary**	**Primary**	**Primary**	**Primary**
SiO_2	39.7	40.1	37.5	37.3	36.9	38.4
TiO_2	0.87	0.72	4.21	4.43	3.59	2.81
Al_2O_3	15.1	14.5	14.6	14.0	15.5	14.1
FeO	13.9	13.6	16.7	15.7	17.0	14.7
MnO	0.12	0.12	0.09	0.20	0.19	0.10
MgO	14.7	16.4	12.4	14.2	12.5	14.1
CaO	0.55	0.07	0.00	0.01	0.01	0.03
Na_2O	0.07	0.07	0.12	0.18	0.11	0.09
K_2O	8.60	9.31	9.41	9.26	9.18	8.99
Cl	0.15	0.15	0.30	0.29	0.30	0.34
F	0.96	1.08	0.71	0.65	0.43	0.87
Total	**94.7**	**96.2**	**96.0**	**96.1**	**95.7**	**94.6**
O=F,Cl	0.44	0.49	0.37	0.34	0.25	0.44
Total	**94.2**	**95.7**	**95.7**	**95.8**	**95.5**	**94.2**
Structural formula to 22 oxygens						
Si	5.631	5.691	5.313	5.287	5.238	5.449
Al(IV)	2.369	2.309	2.447	2.337	2.587	2.363
Al(VI)	0.150	0.121	0.000	0.000	0.000	0.000
Ti	0.093	0.077	0.449	0.472	0.383	0.300
Fe(ii)	1.647	1.614	1.976	1.858	2.015	1.744
Mn	0.014	0.014	0.010	0.024	0.023	0.012
Mg	3.104	3.463	2.629	3.001	2.649	2.980
Ca	0.083	0.011	0.000	0.002	0.001	0.004
Na	0.020	0.019	0.033	0.048	0.031	0.026
K	1.557	1.685	1.703	1.675	1.661	1.626
Cl	0.037	0.037	0.076	0.074	0.077	0.086
F	0.449	0.499	0.334	0.307	0.206	0.413
OH	3.514	3.463	3.590	3.619	3.717	3.501
IV(F)	2.0	2.0	2.0	2.1	2.2	2.0
IV(Cl)	-4.2	-4.3	-4.4	-4.5	-4.4	-4.6
IV(F/Cl)	6.2	6.3	6.5	6.6	6.7	6.6
Fluorine Index (FI)	4.9	4.9	4.7	4.3	3.8	4.8

Table D5. Biotite compositions in weight percent oxide determined by electron probe analyses.—Continued

[Data were normalized to 22 oxygen equivalents. Biotite from footage intervals in drill holes HCBW1, WP1, and WP3. Analyses from primary, altered or oxidized primary, and secondary biotites. The fluorine index was calculated using the methods described in Munoz (1984)]

Sample	WP1-1289'-c2-4	WP1-1289'-c2-5	WP1-1289'-c5-4	WP1-1289'-c5-5	WP1-1289'-c5-6	WP1-1289'-c6-4
Description	**Primary**	**Primary**	**Primary**	**Primary**	**Primary**	**Primary**
SiO_2	38.4	37.7	37.0	36.8	37.0	37.6
TiO_2	4.00	3.82	4.25	4.38	4.89	3.27
Al_2O_3	13.2	13.8	14.5	13.7	14.2	15.0
FeO	15.1	15.4	15.1	15.6	15.0	16.4
MnO	0.10	0.16	0.17	0.12	0.13	0.12
MgO	13.2	13.9	13.3	13.1	13.6	13.3
CaO	0.00	0.00	0.06	0.08	0.01	0.00
Na_2O	0.18	0.13	0.16	0.13	0.20	0.10
K_2O	8.97	9.03	9.01	8.80	9.08	9.38
Cl	0.29	0.30	0.33	0.33	0.29	0.32
F	0.68	0.53	0.57	0.68	0.48	0.78
Total	**94.1**	**94.7**	**94.5**	**93.7**	**94.9**	**96.3**
O=F,Cl	0.35	0.29	0.31	0.36	0.27	0.40
Total	**93.7**	**94.4**	**94.2**	**93.3**	**94.7**	**95.9**
Structural formula to 22 oxygen equivalents						
Si	5.445	5.344	5.243	5.214	5.251	5.335
Al(IV)	2.203	2.303	2.430	2.285	2.375	2.512
Al(VI)	0.000	0.000	0.000	0.000	0.000	0.000
Ti	0.426	0.407	0.453	0.467	0.521	0.349
Fe(ii)	1.793	1.825	1.789	1.851	1.783	1.947
Mn	0.012	0.019	0.020	0.015	0.016	0.014
Mg	2.788	2.943	2.818	2.776	2.873	2.802
Ca	0.000	0.000	0.009	0.013	0.001	0.000
Na	0.049	0.037	0.045	0.035	0.056	0.028
K	1.624	1.634	1.630	1.592	1.643	1.698
Cl	0.074	0.078	0.083	0.085	0.074	0.080
F	0.325	0.252	0.272	0.326	0.229	0.366
OH	3.601	3.670	3.645	3.589	3.697	3.553
IV(F)	2.1	2.2	2.2	2.1	2.3	2.0
IV(Cl)	-4.5	-4.5	-4.5	-4.5	-4.5	-4.5
IV(F/Cl)	6.6	6.8	6.7	6.6	6.8	6.5
Fluorine Index (FI)	4.4	3.9	4.1	4.5	3.7	4.8

Table D5. Biotite compositions in weight percent oxide determined by electron probe analyses.—Continued

[Data were normalized to 22 oxygen equivalents. Biotite from footage intervals in drill holes HCBW1, WP1, and WP3. Analyses from primary, altered or oxidized primary, and secondary biotites. The fluorine index was calculated using the methods described in Munoz (1984)]

Sample	WP1-1289'-c6-5	WP1-1289'-c6-6	WP1-1289'-c1-7	WP1-1289'-c1-9	WP1-1289'-c1-11	WP1-1289'-c7-1
Description	**Primary**	**Primary**	**Primary oxidized**	**Primary oxidized**	**Primary oxidized**	**Primary oxidized**
SiO_2	37.5	37.5	37.6	37.3	37.2	37.3
TiO_2	4.86	4.09	4.47	4.13	3.97	4.48
Al_2O_3	14.1	14.3	14.0	14.2	14.2	14.8
FeO	16.2	16.2	16.9	16.1	16.4	16.1
MnO	0.15	0.17	0.16	0.10	0.17	0.11
MgO	12.6	13.2	13.3	12.9	12.9	13.1
CaO	0.00	0.00	0.00	0.00	0.00	0.00
Na_2O	0.14	0.17	0.14	0.13	0.16	0.13
K_2O	9.40	9.32	9.47	9.47	9.21	9.46
Cl	0.29	0.29	0.29	0.29	0.29	0.32
F	0.46	0.68	0.51	0.62	0.80	0.63
Total	**95.7**	**95.8**	**96.8**	**95.2**	**95.2**	**96.5**
O=F,Cl	0.26	0.35	0.28	0.32	0.40	0.34
Total	**95.4**	**95.5**	**96.5**	**94.8**	**94.8**	**96.1**
Structural formula to 22 oxygen equivalents						
Si	5.312	5.314	5.330	5.285	5.273	5.294
Al(IV)	2.360	2.382	2.335	2.373	2.367	2.477
Al(VI)	0.000	0.000	0.000	0.000	0.000	0.000
Ti	0.519	0.436	0.477	0.440	0.424	0.478
Fe(ii)	1.924	1.916	2.001	1.909	1.946	1.906
Mn	0.018	0.021	0.019	0.012	0.020	0.013
Mg	2.656	2.800	2.820	2.723	2.721	2.776
Ca	0.000	0.000	0.000	0.000	0.000	0.000
Na	0.039	0.048	0.037	0.036	0.044	0.037
K	1.701	1.686	1.713	1.714	1.666	1.712
Cl	0.074	0.074	0.073	0.073	0.073	0.081
F	0.216	0.321	0.239	0.294	0.382	0.296
OH	3.709	3.605	3.688	3.633	3.544	3.623
IV(F)	2.3	2.1	2.2	2.1	2.0	2.1
IV(Cl)	-4.4	-4.5	-4.4	-4.4	-4.5	-4.5
IV(F/Cl)	6.7	6.6	6.6	6.6	6.4	6.6
Fluorine Index (FI)	3.8	4.5	3.9	4.3	4.8	4.3

Table D5. Biotite compositions in weight percent oxide determined by electron probe analyses.—Continued

[Data were normalized to 22 oxygen equivalents. Biotite from footage intervals in drill holes HCBW1, WP1, and WP3. Analyses from primary, altered or oxidized primary, and secondary biotites. The fluorine index was calculated using the methods described in Munoz (1984)]

Sample	WP1-1289'-c7-2	WP1-1289'-c7-3	WP1-1225'-c1-2	WP1-1225'-c1-3	WP1-1225'-c1-4	WP1-1225'-c2-1
Description	**Primary oxidized**	**Primary oxidized**	**Secondary**	**Secondary**	**Secondary**	**Secondary**
SiO_2	37.4	37.2	36.5	36.9	37.1	37.1
TiO_2	4.30	4.22	2.90	3.05	3.39	2.80
Al_2O_3	13.9	14.1	16.0	16.0	16.0	15.7
FeO	15.6	16.0	17.9	15.3	15.4	18.3
MnO	0.18	0.14	0.21	0.17	0.24	0.21
MgO	14.5	13.5	11.9	13.5	14.2	12.3
CaO	0.01	0.00	0.00	0.00	0.00	0.00
Na_2O	0.20	0.19	0.08	0.12	0.26	0.15
K_2O	9.18	9.27	9.78	9.69	9.31	9.40
Cl	0.27	0.30	0.30	0.28	0.26	0.32
F	0.71	0.69	0.55	0.65	0.65	0.46
Total	**96.2**	**95.6**	**96.1**	**95.6**	**96.8**	**96.7**
O=F,Cl	0.36	0.36	0.30	0.34	0.33	0.27
Total	**95.8**	**95.2**	**95.8**	**95.3**	**96.5**	**96.5**
Structural formula to 22 oxygen equivalents						
Si	5.309	5.272	5.173	5.234	5.255	5.263
Al(IV)	2.323	2.354	2.683	2.674	2.677	2.618
Al(VI)	0.000	0.000	0.000	0.000	0.000	0.000
Ti	0.459	0.450	0.309	0.325	0.361	0.299
Fe(ii)	1.845	1.896	2.118	1.812	1.830	2.171
Mn	0.022	0.017	0.026	0.020	0.029	0.025
Mg	3.059	2.861	2.513	2.856	3.002	2.600
Ca	0.001	0.000	0.000	0.000	0.000	0.000
Na	0.054	0.051	0.022	0.033	0.070	0.042
K	1.662	1.676	1.770	1.753	1.684	1.701
Cl	0.068	0.076	0.076	0.070	0.064	0.082
F	0.335	0.329	0.261	0.309	0.305	0.216
OH	3.597	3.595	3.663	3.621	3.631	3.702
IV(F)	2.1	2.1	2.1	2.1	2.1	2.2
IV(Cl)	-4.5	-4.5	-4.4	-4.5	-4.5	-4.4
IV(F/Cl)	6.6	6.6	6.5	6.6	6.6	6.6
Fluorine Index (FI)	4.4	4.5	4.4	4.4	4.3	4.0

Table D5. Biotite compositions in weight percent oxide determined by electron probe analyses.—Continued

[Data were normalized to 22 oxygen equivalents. Biotite from footage intervals in drill holes HCBW1, WP1, and WP3. Analyses from primary, altered or oxidized primary, and secondary biotites. The fluorine index was calculated using the methods described in Munoz (1984)]

Sample	WP1-1225'-c2-2	WP1-1225'-c2-3	WP1-1225'-c3-1	WP1-1225'-c3-2	WP1-1225'-c3-3	WP3-1222'-c3-1
Description	**Secondary**	**Secondary**	**Secondary**	**Secondary**	**Secondary**	**Secondary**
SiO_2	36.2	36.8	36.3	36.5	37.0	40.1
TiO_2	3.00	2.97	3.04	2.95	2.71	1.48
Al_2O_3	16.2	16.0	16.1	15.9	15.9	14.7
FeO	16.6	16.3	16.7	16.3	16.8	10.3
MnO	0.21	0.23	0.23	0.22	0.25	0.10
MgO	12.9	13.1	12.9	13.3	12.9	18.6
CaO	0.00	0.00	0.00	0.00	0.00	0.05
Na_2O	0.26	0.22	0.17	0.22	0.20	0.12
K_2O	9.44	9.32	9.36	9.51	9.45	8.85
Cl	0.29	0.26	0.26	0.28	0.31	0.14
F	0.56	0.62	0.44	0.51	0.63	0.32
Total	**95.7**	**95.8**	**95.5**	**95.7**	**96.1**	**94.7**
O=F,Cl	0.30	0.32	0.24	0.28	0.34	0.16
Total	**95.4**	**95.5**	**95.2**	**95.4**	**95.8**	**94.6**
Structural formula to 22 oxygen equivalents						
Si	5.134	5.222	5.150	5.170	5.247	5.681
Al(IV)	2.709	2.672	2.692	2.656	2.655	2.319
Al(VI)	0.000	0.000	0.000	0.000	0.000	0.142
Ti	0.319	0.316	0.324	0.315	0.289	0.158
Fe(ii)	1.971	1.929	1.984	1.933	1.989	1.222
Mn	0.025	0.028	0.027	0.026	0.030	0.012
Mg	2.725	2.780	2.719	2.820	2.735	3.932
Ca	0.000	0.000	0.000	0.000	0.001	0.007
Na	0.071	0.062	0.046	0.061	0.055	0.033
K	1.708	1.686	1.694	1.721	1.709	1.601
Cl	0.074	0.066	0.066	0.071	0.077	0.034
F	0.265	0.294	0.208	0.244	0.300	0.145
OH	3.661	3.640	3.725	3.685	3.623	3.821
IV(F)	2.1	2.1	2.3	2.2	2.1	2.6
IV(Cl)	-4.4	-4.4	-4.4	-4.4	-4.5	-4.4
IV(F/Cl)	6.6	6.5	6.6	6.6	6.5	7.0
Fluorine Index (FI)	4.2	4.4	3.8	4.0	4.5	2.2

Table D5. Biotite compositions in weight percent oxide determined by electron probe analyses.—Continued

[Data were normalized to 22 oxygen equivalents. Biotite from footage intervals in drill holes HCBW1, WP1, and WP3. Analyses from primary, altered or oxidized primary, and secondary biotites. The fluorine index was calculated using the methods described in Munoz (1984)]

Sample	WP3-1222'-c3-2	WP3-1222'-c3-3	WP3-1222'-c5-1	WP3-1222'-c5-4	WP3-1222'-c3-4	WP1-1372'-c3-1
Description	**Secondary**	**Secondary**	**Secondary**	**Secondary**	**Secondary**	**Secondary mass**
SiO_2	40.7	46.1	40.9	40.9	40.4	35.3
TiO_2	0.96	0.98	1.21	1.64	1.51	2.77
Al_2O_3	14.9	13.2	14.1	14.5	13.9	17.5
FeO	10.3	9.3	10.5	10.8	10.3	18.3
MnO	0.12	0.06	0.09	0.11	0.11	0.18
MgO	18.5	16.1	19.7	18.9	19.3	12.0
CaO	0.07	0.14	0.05	0.08	0.12	0.00
Na_2O	0.10	0.13	0.12	0.17	0.23	0.13
K_2O	8.63	8.36	8.07	7.93	7.36	9.90
Cl	0.08	0.07	0.12	0.16	0.13	0.25
F	0.62	0.14	0.68	0.43	0.27	0.60
Total	**95.1**	**94.5**	**95.5**	**95.6**	**93.6**	**96.9**
O=F,Cl	0.28	0.07	0.31	0.22	0.14	0.31
Total	**94.8**	**94.5**	**95.2**	**95.4**	**93.5**	**96.6**
Structural formula to 22 oxygen equivalents						
Si	5.776	6.535	5.803	5.799	5.730	5.007
Al(IV)	2.224	1.465	2.197	2.201	2.270	2.919
Al(VI)	0.273	0.738	0.154	0.216	0.048	0.000
Ti	0.102	0.105	0.129	0.175	0.161	0.296
Fe(ii)	1.225	1.097	1.245	1.279	1.222	2.174
Mn	0.014	0.008	0.011	0.013	0.014	0.022
Mg	3.919	3.415	4.158	4.006	4.089	2.539
Ca	0.010	0.021	0.008	0.012	0.019	0.000
Na	0.027	0.037	0.032	0.045	0.063	0.035
K	1.562	1.512	1.460	1.435	1.331	1.791
Cl	0.020	0.016	0.028	0.039	0.032	0.063
F	0.281	0.061	0.309	0.195	0.126	0.286
OH	3.699	3.923	3.663	3.766	3.843	3.651
IV(F)	2.3	3.0	2.3	2.5	2.7	2.0
IV(Cl)	-4.1	-3.9	-4.3	-4.4	-4.4	-4.3
IV(F/Cl)	6.4	6.9	6.6	6.9	7.1	6.3
Fluorine Index (FI)	3.5	0.8	3.6	2.8	1.9	4.6

Table D5. Biotite compositions in weight percent oxide determined by electron probe analyses.—Continued

[Data were normalized to 22 oxygen equivalents. Biotite from footage intervals in drill holes HCBW1, WP1, and WP3. Analyses from primary, altered or oxidized primary, and secondary biotites. The fluorine index was calculated using the methods described in Munoz (1984)]

Sample	WP1-1372-c3-2	WP1-1372-c3-3	WP1-1372-c3-4	WP1-1372-c3-5	WP1-1372-c3-6	WP1-1372-c2b-1
Description	**secondary mass**	**secondary mass**	**secondary mass**	**secondary mass**	**secondary mass**	**secondary mass?**
SiO_2	35.6	36.4	35.7	37.0	35.9	37.6
TiO_2	2.88	2.80	2.93	3.17	2.85	3.59
Al_2O_3	17.2	16.3	16.7	16.0	17.1	14.5
FeO	17.3	17.9	18.0	14.3	14.4	14.9
MnO	0.16	0.13	0.14	0.20	0.17	0.17
MgO	12.6	12.1	12.0	14.3	14.0	14.0
CaO	0.00	0.02	0.00	0.01	0.00	0.00
Na_2O	0.20	0.13	0.15	0.25	0.28	0.24
K_2O	9.68	9.59	9.67	9.42	9.05	8.89
Cl	0.24	0.25	0.25	0.25	0.23	0.27
F	0.61	0.78	0.62	0.87	0.87	0.96
Total	**96.5**	**96.5**	**96.2**	**95.7**	**94.8**	**95.1**
O=F,Cl	0.31	0.38	0.32	0.42	0.42	0.47
Total	**96.2**	**96.1**	**95.8**	**95.3**	**94.4**	**94.6**
			Structural formula to 22 oxygen equivalents			
Si	5.055	5.162	5.063	5.248	5.094	5.327
Al(IV)	2.871	2.729	2.790	2.672	2.857	2.419
Al(VI)	0.000	0.000	0.000	0.000	0.000	0.000
Ti	0.308	0.299	0.312	0.338	0.304	0.383
Fe(ii)	2.050	2.126	2.139	1.691	1.707	1.771
Mn	0.019	0.016	0.016	0.024	0.020	0.021
Mg	2.669	2.569	2.535	3.029	2.961	2.959
Ca	0.000	0.002	0.000	0.002	0.000	0.000
Na	0.056	0.035	0.041	0.068	0.077	0.066
K	1.751	1.735	1.750	1.705	1.637	1.607
Cl	0.062	0.063	0.065	0.062	0.057	0.069
F	0.286	0.370	0.294	0.408	0.411	0.455
OH	3.652	3.567	3.641	3.530	3.531	3.476
IV(F)	2.1	1.9	2.0	2.0	2.0	2.0
IV(Cl)	-4.3	-4.3	-4.3	-4.5	-4.4	-4.5
IV(F/Cl)	6.4	6.3	6.3	6.5	6.4	6.5
Fluorine Index (FI)	4.5	5.0	4.6	4.7	4.8	5.0

Table D5. Biotite compositions in weight percent oxide determined by electron probe analyses.—Continued

[Data were normalized to 22 oxygen equivalents. Biotite from footage intervals in drill holes HCBW1, WP1, and WP3. Analyses from primary, altered or oxidized primary, and secondary biotites. The fluorine index was calculated using the methods described in Munoz (1984)]

Sample	WP1-1372'-c2b-2	WP3-1222'-c6-1	WP3-1222'-c6-2	WP3-1222'-c6-3
Description	**Secondary?**	**Secondary?**	**Secondary?**	**Secondary?**
SiO_2	37.1	41.6	41.0	40.4
TiO_2	3.16	1.04	0.92	0.95
Al_2O_3	15.1	14.7	17.1	16.6
FeO	15.2	10.2	8.8	10.2
MnO	0.19	0.06	0.09	0.10
MgO	13.6	19.4	16.4	17.5
CaO	0.00	0.15	0.22	0.20
Na_2O	0.21	0.34	0.23	0.26
K_2O	9.23	8.72	7.82	8.02
Cl	0.28	0.06	0.05	0.10
F	0.81	0.57	0.27	0.44
Total	**94.8**	**96.9**	**92.9**	**94.8**
O=F,Cl	0.40	0.25	0.13	0.21
Total	**94.4**	**96.7**	**92.8**	**94.6**
Structural formula to 22 oxygen equivalents				
Si	5.255	5.903	5.812	5.733
Al(IV)	2.524	2.097	2.188	2.267
Al(VI)	0.000	0.366	0.668	0.509
Ti	0.337	0.111	0.098	0.101
Fe(ii)	1.797	1.209	1.049	1.212
Mn	0.022	0.007	0.011	0.012
Mg	2.873	4.105	3.466	3.697
Ca	0.000	0.023	0.034	0.030
Na	0.057	0.093	0.062	0.072
K	1.670	1.578	1.414	1.452
Cl	0.071	0.015	0.012	0.024
F	0.384	0.254	0.125	0.202
OH	3.545	3.731	3.863	3.774
IV(F)	2.0	2.4	2.6	2.4
IV(Cl)	-4.5	-4.0	-3.8	-4.1
IV(F/Cl)	6.5	6.4	6.4	6.6
Fluorine Index (FI)	4.7	3.3	2.3	3.1

Table D6. Sericite (fine-grained muscovite) compositions from footage intervals in drill holes WP1 and WP2 in weight percent oxide determined by electron probe analyses.

[Data were normalized to 22 oxygen equivalents]

Sample	WP1-451'-c2-6	WP1-451'-c2-7	WP1-451'-c3-1	WP1-451'-c3-2	WP1-451'-c3-3	WP1-451'-c3-4
SiO_2	47.1	47.1	46.1	46.6	45.7	47.6
TiO_2	0.13	0.29	0.16	0.41	0.25	0.20
Al_2O_3	33.5	35.5	34.2	34.7	32.3	34.4
FeO	2.63	2.57	2.48	2.42	3.23	1.43
MnO	0.00	0.00	0.01	0.00	0.00	0.02
MgO	1.13	0.79	0.69	0.72	1.25	1.32
CaO	0.00	0.01	0.00	0.00	0.03	0.01
Na_2O	0.44	0.54	0.53	0.52	0.45	0.44
K_2O	9.69	9.86	10.02	9.95	9.89	9.50
Cl	0.01	0.01	0.02	0.01	0.03	0.02
F	0.18	0.03	0.00	0.00	0.10	0.09
Total	**94.8**	**96.6**	**94.2**	**95.4**	**93.2**	**95.1**
O=F,Cl	0.08	0.01	0.00	0.00	0.05	0.04
Total	**94.7**	**96.6**	**94.2**	**95.4**	**93.2**	**95.0**
Structural formula to 22 oxygen equivalents						
Si	6.317	6.185	6.221	6.208	6.276	6.310
Al (IV)	1.683	1.815	1.779	1.792	1.724	1.690
Al (VI)	3.604	3.678	3.668	3.658	3.501	3.682
Ti	0.013	0.028	0.016	0.041	0.026	0.020
Fe(ii)	0.295	0.282	0.280	0.270	0.371	0.159
Mn	0.000	0.000	0.001	0.000	0.000	0.002
Mg	0.226	0.154	0.139	0.143	0.256	0.260
Ca	0.000	0.001	0.000	0.000	0.004	0.001
Na	0.115	0.137	0.140	0.135	0.120	0.112
K	1.657	1.654	1.727	1.691	1.732	1.606
Cl	0.003	0.002	0.004	0.002	0.006	0.003
F	0.076	0.012	0.000	0.000	0.043	0.038
OH	3.921	3.986	3.996	3.998	3.951	3.959

Table D6. Sericite (fine-grained muscovite) compositions from footage intervals in drill holes WP1 and WP2 in weight percent oxide determined by electron probe analyses.—Continued

[Data were normalized to 22 oxygen equivalents]

Sample	WP1-451'-c3-3	WP1-451'-c3-4	WP1-451'-c3-5	WP1-1869'-c1-4
SiO_2	45.7	47.6	45.8	49.3
TiO_2	0.25	0.2	0.25	0.55
Al_2O_3	32.3	34.4	33.4	29.0
FeO	3.23	1.43	3.27	4.10
MnO	0	0.02	0.00	0.02
MgO	1.25	1.32	1.54	2.62
CaO	0.03	0.01	0.01	0.03
Na_2O	0.45	0.44	0.49	0.07
K_2O	9.89	9.5	10.16	10.20
Cl	0.03	0.02	0.02	0.02
F	0.1	0.09	0.00	0.68
Total	**93.2**	**95.1**	**94.9**	**96.6**
O=F,Cl	0.05	0.04	0.00	0.29
Total	**93.2**	**95**	**94.9**	**96.3**
Structural formula to 22 oxygen equivalents				
Si	6.276	6.31	6.176	6.586
Al (IV)	1.724	1.69	1.824	1.414
Al (VI)	3.501	3.682	3.494	3.154
Ti	0.026	0.02	0.025	0.055
Fe(ii)	0.371	0.159	0.369	0.458
Mn	0	0.002	0.000	0.003
Mg	0.256	0.26	0.310	0.521
Ca	0.004	0.001	0.001	0.004
Na	0.12	0.112	0.128	0.018
K	1.732	1.606	1.749	1.738
Cl	0.006	0.003	0.004	0.005
F	0.043	0.038	0.000	0.288
OH	3.951	3.959	3.996	3.707

Table D6. Sericite (fine-grained muscovite) compositions from footage intervals in drill holes WP1 and WP2 in weight percent oxide determined by electron probe analyses.—Continued

[Data were normalized to 22 oxygen equivalents]

Sample	WP1-1372'-c1-6	WP1-1372'-c1-7	WP1-1372'-c2a-1	WP1-1372'-c2a-2
SiO_2	45.2	45.8	45.2	46.1
TiO_2	0.07	0.03	0.42	0.15
Al_2O_3	32.3	33.0	31.1	33.4
FeO	3.94	4.06	4.71	3.66
MnO	0.00	0.02	0.03	0.03
MgO	1.97	2.15	2.13	1.51
CaO	0.02	0.02	0.03	0.02
Na_2O	0.26	0.23	0.29	0.27
K_2O	10.12	10.34	10.10	9.83
Cl	0.02	0.02	0.02	0.02
F	0.07	0.15	0.24	0.14
Total	**94.1**	**95.8**	**94.2**	**95.1**
$O=F_2Cl$	0.03	0.07	0.11	0.06
Total	**94.0**	**95.8**	**94.1**	**95.0**
Structural formula to 22 oxygen equivalents				
Si	6.191	6.161	6.218	6.211
Al (IV)	1.809	1.839	1.782	1.789
Al (VI)	3.408	3.399	3.260	3.508
Ti	0.007	0.003	0.044	0.015
Fe(ii)	0.451	0.457	0.542	0.412
Mn	0.000	0.003	0.004	0.003
Mg	0.402	0.431	0.437	0.303
Ca	0.003	0.003	0.004	0.003
Na	0.070	0.060	0.078	0.072
K	1.767	1.776	1.774	1.689
Cl	0.005	0.004	0.004	0.005
F	0.030	0.065	0.104	0.060
OH	3.966	3.931	3.891	3.935

Table D6. Sericite (fine-grained muscovite) compositions from footage intervals in drill holes WP1 and WP2 in weight percent oxide determined by electron probe analyses.—Continued

[Data were normalized to 22 oxygen equivalents]

Sample	WP1-1372'-c2a-3	WP2-1289'-a3	WP2-1289'-a4	WP2-1289'-a5	WP2-1289'-b1
SiO_2	46.3	49.6	51.7	46.9	49.4
TiO_2	0.38	0.01	0.00	0.01	0.17
Al_2O_3	31.3	31.5	32.3	29.8	36.3
FeO	4.07	2.25	2.30	2.51	1.48
MnO	0.05	0.00	0.00	0.01	0.00
MgO	1.95	1.93	1.87	2.03	0.81
CaO	0.06	0.13	0.01	0.07	0.00
Na_2O	0.23	0.09	0.05	0.05	0.29
K_2O	9.42	10.40	10.45	10.58	9.89
Cl	0.02	0.03	0.00	0.03	0.01
F	0.06	0.28	0.35	0.14	0.05
Total	**93.8**	**96.2**	**99.0**	**92.1**	**98.4**
O=F,Cl	0.03	0.13	0.15	0.06	0.02
Total	**93.8**	**96.1**	**98.8**	**92.0**	**98.4**
Structural formula to 22 oxygen equivalents					
Si	6.318	6.556	6.613	6.507	6.311
Al (IV)	1.682	1.444	1.387	1.493	1.689
Al (VI)	3.356	3.455	3.486	3.383	3.772
Ti	0.039	0.001	0.000	0.001	0.017
Fe(ii)	0.464	0.248	0.247	0.291	0.158
Mn	0.006	0.000	0.000	0.001	0.000
Mg	0.396	0.380	0.357	0.419	0.153
Ca	0.009	0.018	0.001	0.010	0.000
Na	0.062	0.023	0.012	0.014	0.072
K	1.641	1.752	1.706	1.874	1.610
Cl	0.004	0.006	0.000	0.007	0.002
F	0.028	0.118	0.140	0.061	0.020
OH	3.968	3.875	3.859	3.932	3.979

Table D6. Sericite (fine-grained muscovite) compositions from footage intervals in drill holes WP1 and WP2 in weight percent oxide determined by electron probe analyses.—Continued

[Data were normalized to 22 oxygen equivalents]

Sample	WP2-1289'-b3	WP2-1289'-b4	WP1-1869-c1-4
SiO_2	46.5	46.7	49.3
TiO_2	0.14	0.06	0.55
Al_2O_3	34.4	36.4	29.0
FeO	1.83	1.18	4.10
MnO	0.01	0.01	0.02
MgO	0.99	0.87	2.62
CaO	0.00	0.01	0.03
Na_2O	0.29	0.37	0.07
K_2O	10.01	9.80	10.20
Cl	0.03	0.01	0.02
F	0.00	0.05	0.68
Total	**94.2**	**95.5**	**96.6**
O=F,Cl	0.01	0.02	0.29
Total	**94.1**	**95.4**	**96.3**
Structural formula to 22 oxygen equivalents			
Si	6.251	6.164	6.586
Al (IV)	1.749	1.836	1.414
Al (VI)	3.695	3.820	3.154
Ti	0.014	0.006	0.055
Fe(ii)	0.206	0.130	0.458
Mn	0.001	0.001	0.003
Mg	0.198	0.170	0.521
Ca	0.000	0.001	0.004
Na	0.075	0.095	0.018
K	1.716	1.649	1.738
Cl	0.006	0.002	0.005
F	0.000	0.022	0.288
OH	3.994	3.976	3.707

Table D7. Smectite compositions in weight percent oxide determined by electron probe analyses.

[Samples analyzed from drill holes WP1 and WP3. Data were normalized to 22 oxygen equivalents]

Sample	WP1-1372'-c2a-4	WP1-1372'-c2a-5	WP1-1372'-c2a-6	WP3-1222'-c1-3	WP3-1222'-c1-4	WP3-1222'-c2-4	WP3-1222'-c5-3
SiO_2	57.87	55.76	56.24	52.19	53.15	57.32	54.95
TiO_2	0.01	0.00	0.03	0.25	0.01	0.04	0.00
Al_2O_3	18.52	17.45	17.59	22.80	22.81	21.79	18.61
FeO	5.98	6.29	7.22	5.67	4.81	4.42	9.10
MnO	0.02	0.04	0.07	0.01	0.03	0.00	0.02
MgO	2.40	2.27	2.61	4.04	2.26	3.14	2.87
CaO	1.15	1.11	1.24	0.57	0.43	0.53	0.80
Na_2O	0.07	0.08	0.05	0.49	0.47	0.51	0.68
K_2O	0.16	0.18	0.19	0.88	0.76	0.87	1.43
Cl	0.43	0.32	0.43	0.00	0.02	0.02	0.00
F	0.08	0.17	0.21	0.08	0.11	0.08	0.19
Total	**86.69**	**83.67**	**85.87**	**86.98**	**84.86**	**88.71**	**88.64**
O=F,Cl	0.13	0.14	0.18	0.03	0.05	0.04	0.08
Total	**86.56**	**83.53**	**85.69**	**86.95**	**84.80**	**88.67**	**88.56**
Structural formula to 22 oxygen equivalents							
Si	8.01	8.03	7.96	7.29	7.52	7.73	7.69
Al	0.00	0.00	0.04	0.71	0.48	0.27	0.31
Sum Tetrahedral	8.01	8.03	8.00	8.00	8.00	8.00	8.00
Al	3.02	2.96	2.89	3.04	3.33	3.19	2.76
Ti	0.00	0.00	0.00	0.03	0.00	0.00	0.00
Fe(ii)	0.69	0.76	0.85	0.66	0.57	0.50	1.07
Mn	0.00	0.01	0.01	0.00	0.00	0.00	0.00
Mg	0.50	0.49	0.55	0.84	0.48	0.63	0.60
Sum Octahedral	4.22	4.21	4.31	4.58	4.37	4.32	4.43
Ca	0.17	0.17	0.19	0.09	0.07	0.08	0.12
Na	0.02	0.02	0.01	0.13	0.13	0.13	0.18
K	0.03	0.03	0.03	0.16	0.14	0.15	0.26
Sum Interlayer	0.22	0.23	0.24	0.38	0.33	0.36	0.56
Cl	0.10	0.08	0.10	0.00	0.01	0.00	0.00
F	0.03	0.08	0.09	0.03	0.05	0.03	0.08
Total	**12.45**	**12.47**	**12.54**	**12.95**	**12.71**	**12.68**	**12.99**